Multiple layers of inhibition in the direction coding circuit in mouse retina

by

K. Alex Hoggarth
BSc, Dalhousie University, 2012

A Thesis Submitted in Partial Fulfillment
of the Requirements for the Degree of

MASTER OF SCIENCE

in the Department of Biology (Neuroscience)

Supervisory Committee

Multiple layers of inhibition in the direction coding circuit in mouse retina

by

K. Alex Hoggarth
BSc, Dalhousie University, 2012

Supervisory Committee

Dr. Gautam B. Awatramani, Department of Biology
Supervisor

Dr. Robert L. Chow, Department of Biology
Departmental Member

Abstract

Supervisory Committee
Dr. Gautam B. Awatramani, Department of Biology
Supervisor
Dr. Robert L. Chow, Department of Biology
Departmental Member

Local and global forms of inhibition control directionally selective ganglion cells (DSGCs) in the mammalian retina. Specifically, local inhibition arising from GABAergic starburst amacrine cells (SACs) strongly contributes to direction selectivity. In this thesis, I demonstrate that increasing ambient illumination leads to the recruitment of GABAergic wide-field amacrine cells (WACs) endowing the DS circuit with an additional feature: size selectivity. Using a combination of electrophysiology, pharmacology and light/electron microscopy, I demonstrate that WACs predominantly contact presynaptic bipolar cells, which drive direct excitation and feed-forward inhibition (through SACs) to DSGCs, therefore maintaining the appropriate balance of inhibition/excitation required for generating DS. This circuit arrangement permits high-fidelity direction coding over a range of ambient light levels, over which size selectivity is adjusted. Together, these results provide novel insights into the anatomical and functional arrangement of multiple inhibitory interneurons within a single computational module in the retina.

Table of Contents

List of Figures

Acknowledgments

I wish to thank the contributions (incomplete and in no particular order) of Stu Trenholm, Kara Ronellenfitch, Amanda McLaughlin, Rishi Vasandani, Tom McKellar, Patrick Reeson, Sammy Weiser Novak, Jose Gomez, David Schwab, Kevin Briggman, Ariel Sullivan, Aastha Nanda, Santhosh Sethrumanujam, and Varsha Jain.

Dedication

I would like to dedicate this thesis to my brothers - David, Peter and Johnathan. They were right.

1. Introduction

Throughout the nervous system, inhibition expands computational abilities of neuronal circuits. Inhibitory interneurons modulate the responses of their downstream target neurons. Depending on the neural system, inhibitory neurons can modulate neuronal gain, limit spike number, control spike bursting or spike timing, and drive synchronization or desynchronization (Mitchell and Silver, 2003, Ackert et al., 2006, Silver, 2010, Breton and Stuart, 2012, Ryan et al., 2012). The multitude of roles and computations these diverse neurons perform make the properties of inhibitory interneurons an important topic of study. An emerging and recent topic of study is the intersection of multiple inhibitory interneurons within individual circuits, and how their activity may be coordinated to accomplish parallel tasks. In order to fully understand the role of inhibition in neuronal circuits, it is first necessary to understand their response properties and anatomical wiring.

The mouse retina is a good model system for studying inhibitory interneurons (Masland, 2001). The diversity of inhibitory interneurons of the retina is better understood than in many areas of the CNS (MacNeil and Masland, 1998). In the retina, greater than 35 types of specialized inhibitory interneurons have been discovered and described (MacNeil and Masland, 1998; Masland, 2012). In this thesis, I will investigate the roles of two types of inhibitory cells in a single CNS circuit, and how their anatomical wiring and biophysical properties enable simultaneous distinct computations in a commonly regulated relay neuron. I aim to describe the coordination of these two amacrine cells, specifically how the stimulus-specific activity of individual amacrine cell populations endows this circuit with the ability to independently detect multiple

characteristics of visual stimuli. Additionally, I will describe how this dual innervation elegantly leads to the ability to specifically and selectively alter only certain types of visual responses to account for changing environmental conditions.

In this introduction, I outline the functional plan of the retina and the neural circuitry which allows for extraction of information from the visual scene. Subsequently, I describe the neural basis for two types of stimulus specificity – namely size and direction coding. Finally, I introduce the challenges presented to the retina during changing light conditions and how this is addressed by adaptation to light.

1.1 Retinal Structure and Function

The retina is a complex system of neural circuits, which parses and decodes components of the visual scene before sending information to the brain. The retina does not function as a simple light detector; rather it performs complex computations which shape the higher sensory functions of the visual system, passing a continuous stream of information via the optic nerve to higher order visual centers in the brain. This is accomplished by the anatomically and functionally layered structure of the retina, which iteratively extracts information at each of two major synaptic layers. Information about the brightness and colour of a scene is extracted first, followed by more contextual and computationally difficult information, such as the presence of motion, edges, object size, and orientation (Masland, 2001, Kolb, 2003). As signals travel from photoreceptors to ganglion cells, these parallel streams of information are split into ~30 different populations of ganglion cells. Ganglion cells can be categorized by morphology, physiological responses, or genetic markers (Sumbul et al., 2014, Li et al., 2015, Sanes and Masland, 2015). The computational tasks that each ganglion cell population can

perform relies on the types of other retinal neurons which form synaptic connections with either the ganglion cell itself or synapse onto other cells which influence ganglion cell responses (here this will collectively be referred to as a "circuit"). It is therefore an important task in retinal physiology to determine which types of cells and specific connections make up each ganglion cell circuit. A somewhat recent estimate predicts that approximately half of the synaptic connections in the retina are known, leaving the remaining wiring to be discovered (Kolb, 2003). This thesis will confirm the presence of an additional interneuron in a well-studied ganglion cell circuit, and address the novel wiring of multiple independent inhibitory neurons within this circuit.

Light driven information flows in a feedforward pathway through the retina from photoreceptors to bipolar cells, and finally to ganglion cells (see Figure 1 for a schematic of retinal organization). Excitation from bipolar cells drives ganglion cells to fire action potentials, which are transmitted via the optic nerve to higher visual centres in the brain. These bipolar cell signals are modified within the retina prior to being passed to the ganglion cells, allowing the retina to serve as the primary computational center for visual perception. This active signal modification takes place at two major synapses in the retina. First, signals from photoreceptors are modified by two subtypes of horizontal cells, which act at the photoreceptor-bipolar cell synaptic layer in the outer retina (Kolb, 1974). The photoreceptor-bipolar cell synaptic connections, along with lateral connections from horizontal cells, form the outer plexiform layer (OPL). These signals are passed through two pathways, split between the two major classifications of bipolar cells - the sign reversing ON bipolar cells (which depolarize in response to light) , and the sign conserving OFF bipolar cells (which hyperpolarize in response to light, following

the photoreceptor response) (Nelson and Kolb, 1983, Kolb, 2003). There are 10 total bipolar cell subtypes, each of which projects to a specific sub-lamina in the inner plexiform layer (IPL), with ON BCs projecting more proximal to the ganglion cell layer and OFF BCs projecting distally (Famiglietti and Kolb, 1976). Downstream from bipolar cells, a large diversity (>30 subtypes) of amacrine cells further shape the visual signals as they are integrated by retinal ganglion cells (MacNeil and Masland, 1998). Amacrine cells form connections at the bipolar cell-ganglion cell synaptic layer, synapsing either onto ganglion cells, or on the bipolar cell terminals which excite the ganglion cells, or onto other amacrine cells. Each population of ganglion cells is specialized to extract specific visual information. The multiple types of amacrine cells which participate in a given ganglion cell circuit determine the properties of visual stimuli to which the ganglion cells will preferentially respond. It is predicted that 2-3 types of amacrine cells participate in shaping the response of each ganglion cell circuit (Masland, 2012). Their diversity, connectivity, and biophysical properties (activation) define the study of amacrine cell properties. It is an important goal in the study of the retinal circuitry to determine which amacrine cells are involved in the computations of each ganglion cell circuit, which stimuli drive activation of each amacrine cell, and under which conditions each type of amacrine cell is active.

Amacrine cells can be broadly classified as narrow-field, medium-field or wide-field, depending on the area over the retina that is covered by their dendritic fields (MacNeil and Masland, 1998). Of these types, narrow- and medium-field are best studied and classified, while the diversity, activity, and the role in shaping visual responses of the wide-field amacrine cells are less defined (Lin and Masland, 2006, Pérez De Sevilla

Müller et al., 2007). One of the major accomplishments of this thesis work is to incorporate a class of wide-field amacrine cells into the well-studied directionally selective (DS) circuit, which has previously only be considered to be recipient to one type of medium-field amacrine cell – the starburst amacrine cell (SAC). The DS circuitry is outlined in Figure 1. The following section will describe the DS circuit.

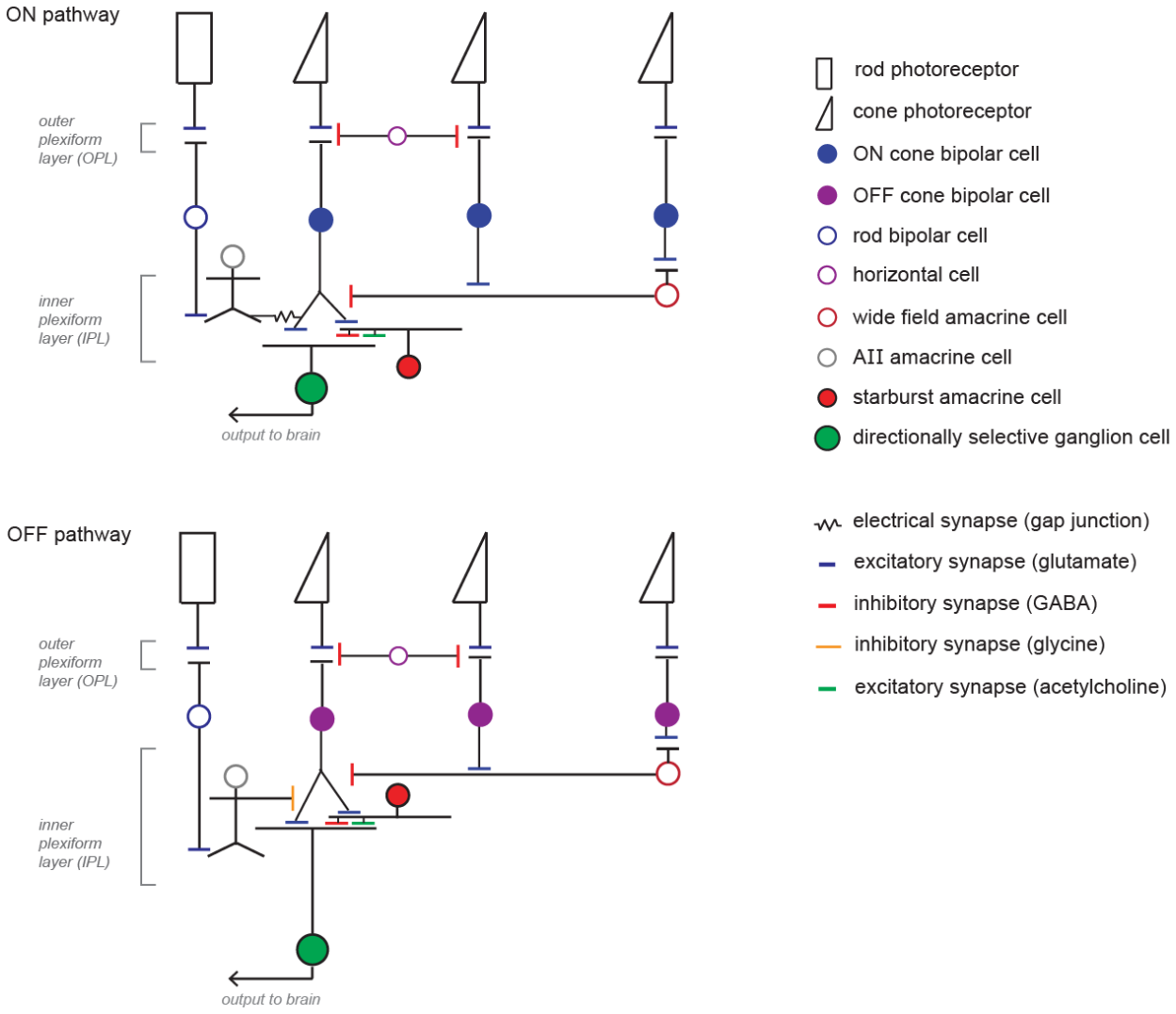

Figure 1: The directionally selective circuit of the retina, including a presynaptic wide-field amacrine cell

In dim light, vision is mediated by the rod pathway, while in bright light conditions, the cone pathway dominates. Signals are separated into ON (top) and OFF (bottom) parallel pathways at the photoreceptor to bipolar cell synapse. In response to light onset, rod and cone photoreceptors hyperpolarize, reducing glutamate release. This signal is translated to a depolarization by ON cone bipolar cells and rod bipolar cells via sign-inverting mGluR6 receptors. Depolarizing photoreceptor responses at light offset lead to depolarizations in OFF cone bipolar cells via AMPA/kainite receptors. The bipolar cells driving DSGC and SAC responses may be different types than those driving WACs. Rod bipolar cells synapse onto the intermediate AII amacrine cells, which are electrically coupled to ON cone bipolar cell terminals. AII amacrine cells also provide glycinergic inhibition to OFF bipolar cell terminals, allowing for rod-driven OFF signals via disinhibition. The inhibitory interneurons of the outer retina are the horizontal cells, which act at the photoreceptor-bipolar cell synapse. In the inner retina, amacrine cells act at on bipolar cells and ganglion cells. Starburst amacrine cells (SACs) provide directional inhibition to directionally selective ganglion cells (DSGCs). Putative wide-field amacrine cells provide inhibition to the bipolar cells driving DSGCs and SACs.

1.2 Direction Selectivity

Information pertaining to motion in the visual field is relayed to the brain by functionally specialized directionally selective ganglion cells (Barlow and Levick, 1965, Borst and Euler, 2011, Vaney et al., 2012). Direction selectivity (DS) refers to the phenomenon by which populations of ganglion cells (direction selective ganglion cells; DSGCs) respond by firing action potentials at a high quantity and rate in response to light moving in one direction (deemed the preferred direction), and at a low rate or not at all in response to light moving in the opposite (null) direction (Barlow and Levick, 1965). The presence of motion in a scene drives a response in one of the four types of ON-OFF DSGCs, which code for motion in each of the four cardinal directions, described on the retina relative to anatomical direction as nasal, dorsal, temporal, and ventral (Oyster and Barlow, 1967). In addition (while not studied here) there are also 3 types of ON DSGCs whose preferred directions align with the orientation of the semicircular canals in the inner ear (Oyster et al., 1972, Dhande et al., 2013). Directionally selective ganglion cells

represent one of the best studied circuits in the mammalian brain. The extraction of direction is an interesting problem for a number of reasons. First, the outputs from the photoreceptors in these scenarios may be measurably identical except for the direction of their sequence of activation, necessitating a precise neural circuit for differentiation. Second, motion detection represents a neural computation that exists at an early sensory level (before light information leaves the eye), meaning any mechanisms that encode a direction preference must do so quickly, and with limited input. Third, directionally selective activity is a highly conserved phenomenon across species, having been described in both vertebrates and invertebrates (Thorson, 1964, Barlow and Levick, 1965), and involving numerous mechanisms (Borst and Euler, 2011), hinting at a complex evolutionary history. In this thesis, I will focus on the well-studied DS circuit of the mouse retina.

The major mechanism for direction selectivity in the mouse retina is an asymmetric inhibitory synaptic input mediated by the starburst amacrine cell (SAC). SACs are amacrine cells which display a characteristic radial morphology, giving rise to the "starburst" nomenclature (Famiglietti, 1983, Miller and Bloomfield, 1983, Yoshida et al., 2001). SACs release both GABA and acetylcholine (which drives DS during low contrast stimuli; Sethuramanujam et al., 2016) via synapses on dendrites of DSGCs in both the ON and OFF layers of the IPL, through mirror symmetric populations of ON and OFF SACs (Famiglietti, 1983, O'Malley et al., 1992). SACs are non-spiking neurons (Bloomfield, 1992, Peters and Masland, 1996), and provide local inhibition over small subunits, significantly smaller than the dimensions of the SAC (Grzywacz et al., 1994). SACs display a pattern of synaptic specificity that leads to direction selectivity, inhibiting

DSGCs preferentially in response to null direction stimuli (Taylor and Vaney, 2002, Taylor and Smith, 2012). Functionally, this means that the differential excitation and inhibition leads to a direction preference, as large inhibition occurs concurrent (slightly earlier) with excitation for null stimuli, inhibiting the DSGC from firing, and an equal excitation occurs slightly before minimal inhibition for preferred stimuli, allowing maximum firing (Figure 2; Taylor and Vaney, 2002). Additionally, this inhibition has classically been attributed to a spatial offset of SACs, where more SACs connecting on the null side (defined as the direction from which null direction stimuli approach) of the receptive field generate a direction preference (Fried et al., 2005). However, recently it was shown that specific wiring of SACs to DSGCs underlies direction selectivity, with only SAC dendrites extending/pointing in the null direction of a particular population of SACs synapsing with those DSGC populations (Briggman et al., 2011). These SAC dendrites are more strongly activated during centrifugal (soma to dendrite) motion (Euler et al., 2002). Together, this leads to an intrinsic directionality of individual SAC dendrites, which project to specific populations of DGSCs, resulting in directional GABA release onto DSGCs. DS has been shown to critically rely on SACs, as laser ablation of SACs or pharmacological blockade of GABA results in a loss of DS (Caldwell et al., 1978, Yoshida et al., 2001, Taylor and Vaney, 2002), except in circumstances where one population of DSGCs can generate a DS preference postsynaptically (Trenholm et al., 2011). Previous literature indicated that DS can be sharpened by an asymmetry in excitatory (glutamatergic) transmission from bipolar cells to DSGCs (Taylor and Vaney, 2002, but see Poleg-Polsky and Diamond, 2011). However, more recent optical imaging studies have shown that both glutamate release as well as Ca^{2+} dynamics in the

presynaptic bipolar cell terminals innervating DSGCs are non-directional (Yonehara et al., 2013, Park et al., 2014). Importantly, this suggests that directional inhibition from SACs is exclusively directed to DSGCs, and does not feedback to presynaptic bipolar cells.

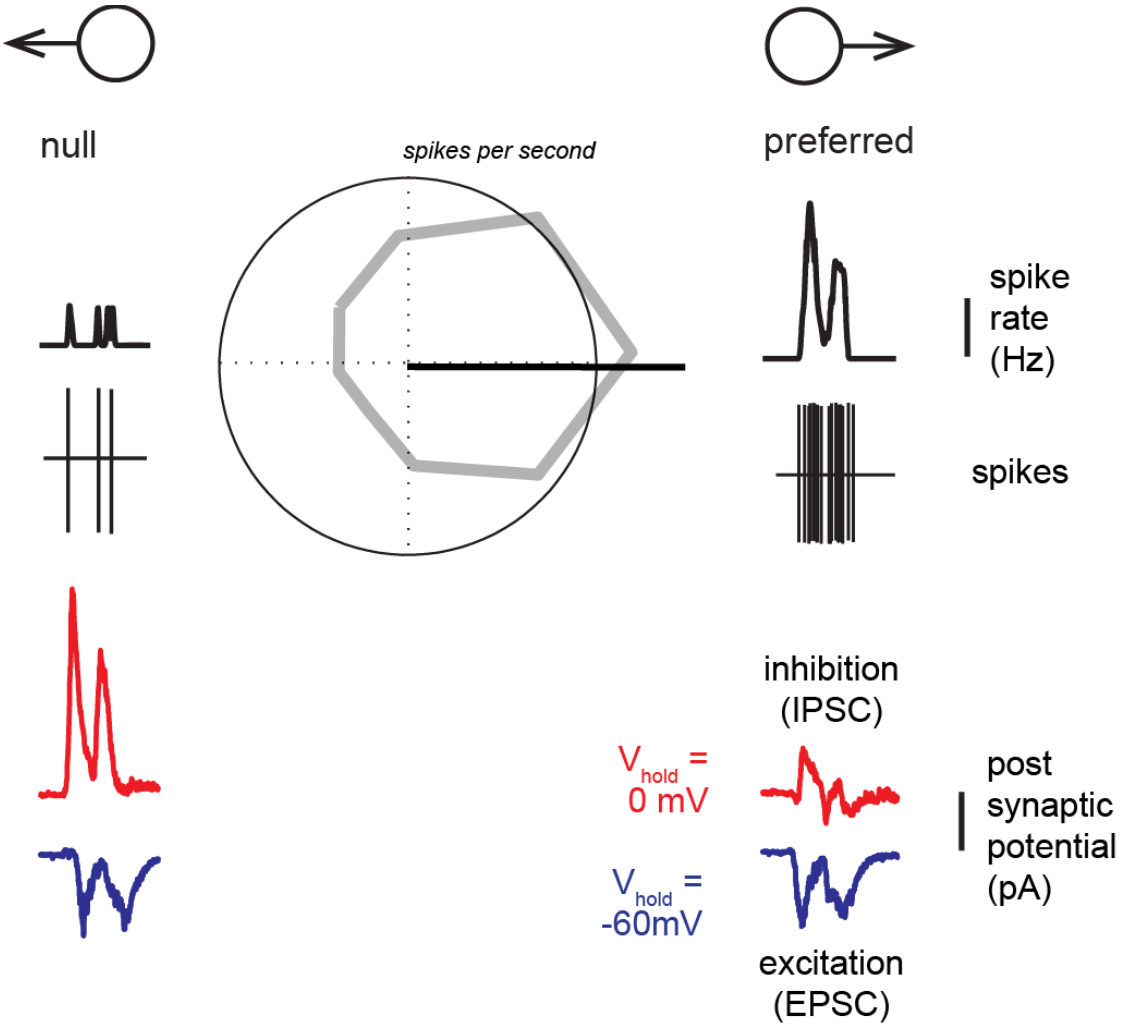

Figure 2: Directionally selective inhibition drives DS responses

Assymetric inhibition leads to a reduced response in the null direction in ON-OFF DSGCs. Spiking responses are reported as either spike rate or spike number. Spike rate is illustrated by filtering the light evoked spike train using a convolution with a Gaussian kernel with a fixed width, $\sigma = 25$ ms, and measured in spikes per second (Hz). DS responses are illustrated on a polar plot (middle), where responses are plotted with increasing distance from the origin as responses increase (grey). The vector sum of the

responses is illustrated in black. Post-synaptic currents drive spiking responses are measured in voltage clamp. Holding the cell at 0 mV, the reversal potential for excitation, isolates inhibitory currents (IPSCs; red), while holding at -60 mV, the reversal for inhibition, isolates excitatory currents (EPSCs; blue). Null direction stimuli drives larger IPSCs, shunting spiking.

As light moves across the visual field, retinal signals are separated both temporally (as photoreceptors are sequentially activated) and spatially (as the pattern of activation moves across the retina). Spatial information also exists pertaining to the size of the object. The direction of moving objects is reliably detected by the DSGCs using the previously described mechanism – local, asymmetric GABAergic inhibition via direct synapses with SACs (Yoshida et al., 2001, Borst and Euler, 2011, Vaney et al., 2012). However less is known about how DSGCs respond to other characteristics of visual stimuli (He and Levick, 2000, Grzywacz and Amthor, 2007, Nowak et al., 2011). In fact, to date, it is unknown whether the well-studied SAC-DSGC synapse drives responses that are selective to spatial or temporal (or otherwise) properties of the stimulus (also known as the "tuning" of the circuit). Determining whether this tuning is computed by SACs, or elsewhere, is a major goal of this thesis (Wyatt and Daw, 1975, Chiao and Masland, 2003). Spatial tuning in other ganglion cell types is known to rely on wide-field amacrine cells (Cook and McReynolds, 1998). Recently several studies have hinted that other non-SAC amacrine cells may participate in stimulus tuning of DSGCs. However these studies relied only on indirect evidence (Stasheff and Masland, 2002, Chiao and Masland, 2003, Fried et al., 2005, Rivlin-Etzion et al., 2012). The possibility of multiple amacrine cells acting with coordinated activity to accomplish specific computations is only just

beginning to be proposed as a strategy for coding in the retina (Roska et al., 2000, Venkataramani et al., 2014).

DSGCs intrinsically deal with stimuli with a temporal and spatial component (ie motion), therefore they must execute simultaneous computations (van Hateren, 1990, Krekelberg and van Wezel, 2013). A confound exists however, as spatial tuning may be influenced by the temporal characteristics of the stimuli, as is seen in other populations of ganglion cells (Frishman et al., 1987). Additionally, if direction coding is influenced by other stimuli properties, this could affect the core computation of the DSGC, which would be expected to interfere with important visual functions. Therefore, it is an important goal to determine 1) the spatio-temporal tuning profile of the DSGC, 2) whether these characteristics are independent (separable), and 3) which circuit elements are responsible for different tuning properties. A major goal of this thesis work will be to parse out the contributions of distinct amacrine cells on shaping this spatiotemporal selectivity, and their roles on tuning the DS responses to different characteristics of moving objects.

1.3 Center-Surround Receptive Field Organization

Galileo's study of celestial bodies led to the first observations of a visual phenomenon which is now attributed to the retinal circuitry (Piccolino and Wade, 2008). He observed that the edges of the moon appeared to be sharper and brighter than their surroundings. Knowing that smooth spheres would not appear this way, he correctly concluded that an active process in his own visual system must lead to this experience. The physicist Ernst Mach later described these edge effects (now known as Mach bands),

where the contrast at the intersection between two areas of differing contrast is enhanced (Mach, 1865, Ratliff, 1965). This phenomenon leads to enhanced edge detection in visual processing of natural scenes. The neurological basis of this enhanced edge detection is lateral inhibition in the retina, as first described by Hartline's Nobel Prize winning work in limulus (Hartline and Ratliff, 1957). Ganglion cell receptive fields are organized into a center and a surround, where light in the center increases ganglion cell firing, while light in the surround has an antagonistic effect (Figure 2). ON and OFF cells have antagonistic surrounds, such that increased brightness in the surround inhibits ON cells, while decreased brightness in the surround inhibits OFF cells (Kuffler, 1953, Wiesel, 1959). When this receptive field lays on the border between two areas of different contrast, the excitatory region is optimally stimulated, while the inhibitory region is only partially recruited, leading to the edge enhancement observed by Galileo. More importantly for this thesis, these center-surround receptive fields lead to ganglion cell responses which have a preference for stimulus size. As the size of an object increases, it recruits more of the lateral inhibitory surround, decreasing the ganglion cell's response.

Lateral inhibition in the retina can arise from multiple possible sources - horizontal cells, amacrine cells, or a combination of both can contribute to the inhibitory surround (Flores-Herr et al., 2001). Horizontal cells in the outer retina are known to feed back onto photoreceptors in the outer retina using either pH modulation to affect presynaptic calcium channels or GABAergic inhibition (Hartline and Ratliff, 1957, Kolb, 1974, Mangel, 1991, Hirasawa, 2003, Vessey et al., 2005). Surround inhibition may also be conferred by a class of wide-field amacrine cells (WACs) in the inner retina (Olveczky et al., 2003, Zaghloul et al., 2007, Farrow et al., 2013). The processes (neurites) of WACs

span large distances, and their inhibition relies on spiking activity driven by voltage-gated Na^+ channels (Cook and McReynolds, 1998, Demb et al., 1999, Taylor, 1999, Protti et al., 2014). Notably, since horizontal cells hyperpolarize in response to light, they can be excluded as using voltage-gated Na^+ channels as a mechanism for relaying inhibition, contrary to the spiking activity of WACs. Therefore, previous studies have used the sodium channel blocker tetrodotoxin (TTX) to selectively block inhibition from WACs, without perturbing horizontal cell mediated inhibition (Taylor, 1999). While surround inhibition and spatial selectivity have been previously observed in DSGCs, the relative contribution of horizontal cells and WACs in contributing to the surround inhibition of DSGCs is not yet known (Wyatt and Daw, 1975, Chiao and Masland, 2003). Potential benefits to WAC-mediated inhibition are the WAC's ability to adjust its activity in response to ambient light levels, which allows for switching inhibition to best suit the environment (Farrow et al., 2013), as well as the ability to take advantage of bipolar cell output in the inner retina leading to non-linear inhibitory properties, which leads to complex receptive field properties such as object motion detection (Takeshita and Gollisch, 2014). However, if WACs participate in the DS circuit, changes in WAC activity levels may be expected to alter the balance between excitation and inhibition, undermining directional selectivity. Alternatively, horizontal cells which have been shown to control DSGC responses (Mangel, 1991) could potentially mediate wide-field inhibition by modulating photoreceptor-to-bipolar cell synapses in the outer retina. One of the major goals of this thesis will be to determine the source of surround inhibition to DSGCs.

There are multiple ways in which the inhibitory surround can integrate light stimulus in order to supress ganglion cell activity (Enroth-Cugell and Jakiela, 1980, Enroth-Cugell et al., 1983, Passaglia et al., 2001). The nature of the receptive field surround grants insight into the way the ganglion cell circuit will respond to different types of stimuli. The types of surround can be classified as classical or extra-classical: where classical receptive fields interact linearly with the receptive field centre, while extra-classical receptive fields are made up of non-linear subunits (Hochstein and Shapley, 1976a, Zaghloul et al., 2007, Takeshita and Gollisch, 2014). Non-linear computations endow retinal circuits with many unique features such as contrast gain control (Solomon et al., 2002), spatial selectivity (Barlow and Levick, 1965, He and Levick, 2000, Solomon et al., 2002), object motion sensitivity (Olveczky et al., 2003) and possibly other functions (Roska and Werblin, 2003). Receptive field strategies of linear versus non-linear summation of light were first described in the excitatory regions of ganglion cells of the cat (Enroth-Cugell and Robson, 1966, Hochstein and Shapley, 1976a). Cells in the inner retina (either amacrine or ganglion) use multiple independently activated subunits to comprise the receptive field, each sampling input at a distinct region, and then summing this activity to represent many points in space (Figure 3). Linear summation of this input can be thought of as representing the output of a single bipolar cell, as the mean contrast in the receptive field increases, as does the cell's response (Enroth-Cugell and Robson, 1966, Demb et al., 2001). However, this poses a problem during vision of more complex stimuli, where a spatial structure may exist in which the mean contrast of all features may be similar to the background and would not drive a response if the light was linearly summed over space (Figure 3C). In these cases,

non-linear summation is required for a response to be generated. This is commonly done by having the receptive field comprised of many non-linear subunits, each sampling input at a distinct region, and then summing this activity to represent many points in space (Figure 3 B,C). A common stimulus for testing for non-linear summation (and thus the presence of subunits) is a sine wave grating, with contrast-reversing gratings being classically used (Enroth-Cugell et al., 1983, Demb et al., 1999). Gratings allow for modulation of the spatial frequency (wavelength) and the contrast (amplitude), without changing the total average light present in the stimuli (Figure 3A). Linear receptive fields will not respond to a contrast reversal, but receptive fields comprised of non-linear subunits will respond at twice the frequency of the stimulus, provided the spatial frequency of the grating is larger than the width of a single subunit (Hochstein and Shapley, 1976b, Enroth-Cugell et al., 1983). Above this spatial frequency (smaller bars), the neuron will be insensitive to changes. Multiple cell types use non-linear subunits to drive activation, in cases where their computation relies on activation of an individual subunit (or only a partial fraction of the subunits) to be activated above their threshold, leading to sensitivity for textured motion, differential motion, approaching motion, and other functions (for review of computations/circuits which use non-linear subunits see Gollisch and Meister, 2010). If non-linear subunits comprise the suppressive surround, it follows that inhibition will be present when light is detected in the surround, independent of the spatial structure of the stimulus (Enroth-Cugell and Jakiela, 1980, Passaglia et al., 2001, Troy et al., 2005). This non-classical interaction with the center allows for input with any spatial distribution present in the surround to reliably drive inhibition to the ganglion cell. WAC activity has been shown to rely on such subunit structure in other

retinal circuits (Baccus et al., 2008, Passaglia et al., 2009). DSGC inhibitory surrounds have been also shown to exhibit some properties of receptive fields comprised of subunits, leading to the hypothesis that WACs drive the inhibitory surround to DSGCs (Chiao and Masland, 2003). However, the output properties of the WACs in the DS circuit have not been directly tested, nor have the physiological basis for each subunit.

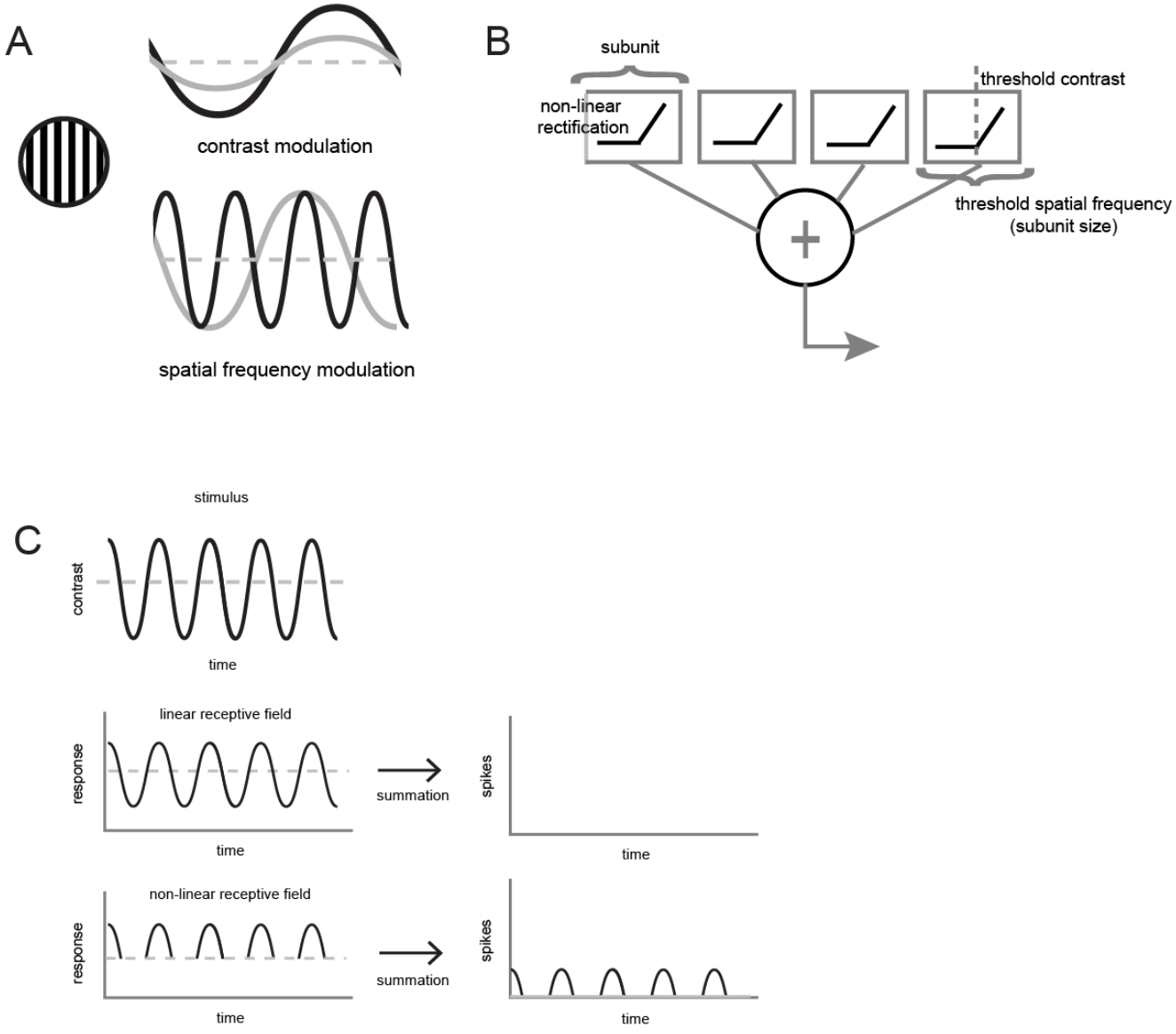

Figure 3: Non-linear receptive field schematic

A. Sine wave stimuli (inset) can be modulated using contrast (top) or spatial frequency (bottom), each conserving the total amount of light presented around the mean (dotted lines). The x axis represents space, and the y axis represents contrast.

B. Schematic of a receptive field comprised of non-linear subunits. Each subunit (rectangles) detects a threshold contrast within its own receptive field (the size of which represents the threshold spatial frequency). Increasing spatial frequency (narrowing bars) above the subunit width will result in equal light on average to each subunit, resulting in no further increase in response. Responses are summed from each subunit to drive postsynaptic responses.

C. Hypothetical responses from a non-linear and linear receptive field. A linear receptive field (middle) follows the stimulus (top), while a non-linear receptive field (bottom) shows positive rectification. Summation of these responses (right) leads to no net firing in the linear receptive field, while the non-linear receptive field shows spiking that follows the stimulus. These responses would be consistent independent of spatial frequency above the subunit threshold size (as in **B**).

1.4 Modulation by Ambient Light Levels

The visual system is tasked with coding visual stimuli in the presence of constantly changing environmental light conditions. Over the course of a single day, the visual system is presented with a billion-fold range of light intensities. The range of background (ambient) light that the retina is exposed to is vastly larger than the dynamic range of any single type of photoreceptor (Rieke and Rudd, 2009). The retina must therefore change its function to account for the large range of light intensities, in order to function both in dim environments, where light is limited, and bright daylight, where photons are plentiful (Morgan and Boelen, 1996). The first step for probing differential visual functions in different environmental light conditions is to assess the consequences of the separate retinal coding strategies that are present in dim versus bright light.

The most significant change in the retina's light detection strategy across this range of brightness is the separation of signals into two different circuits, beginning at the level of rod and cone photoreceptors (see Figure 1 for basic schematic of rod and cone

circuitry). Rods are used for dim vision (scotopic), while cones are used for bright vision (photopic). Each of these two types of photoreceptor exhibits different intrinsic light sensitivities, which allows for visual function over a large range of background light levels, ranging from a detection threshold of single photons in low light to a barrage of billions of photons in bright daylight scenes (Hecht et al., 1942). Moreover, rod and cone signals are subsequently separated further downstream in the retina into two distinct neural circuits, allowing for differences in retinal functionality across light levels. In bright light, signals travel from cone photoreceptors, through cone bipolar cells to ganglion cells (Figure 1). In dim light, information traverses the retina via a separate pathway. Photons are sparse, and therefore light collection requires multiple levels of signal convergence. The more sensitive rod photoreceptors synapse with specialized rod bipolar cells, which collect light from multiple rod photoreceptors (Schwartz and Rieke, 2013). Rod photoreceptor information is transmitted through rod bipolar cells, which subsequently synapse onto the specialized AII amacrine cells. AII amacrine cells are gap junction coupled to cone bipolar cell terminals (Famiglietti and Kolb, 1975). In this way, the rod signals are routed through the cone pathway, through the common cone bipolar terminal-ganglion cell glutamatergic synapse to ganglion cells. AII amacrine cells also provide glycinergic inhibition to OFF bipolar cell terminals, allowing for rod-driven OFF signals via disinhibition. This fundamental change in the way light information is routed through the retina can have effects on downstream signalling.

One important adaptational strategy is the retina's ability to functionally 'switch' inhibition from the periphery. From the earliest recordings of optic nerve impulses, it was observed that the center-surround receptive field organization undergoes a critical change

based on the ambient light level present in the environment (Barlow et al., 1957). In bright light conditions, the recruitment of center-surround receptive fields leads to an increase in visual acuity, which was found to be conspicuously absent under dim light conditions (Figure 4). Spatial acuity in behavioural and psychophysical experiments was also found to be absent in dim light conditions in humans and mice (van Nes et al., 1967, Umino et al., 2008, Farrow et al., 2013) The specific mechanisms of reducing surround inhibition in dim light remain to be fully investigated (Farrow et al., 2013, Demb and Singer, 2015). As a functional consequence of this adaptation, it was hypothesized that during conditions of low illumination, it would be advantageous to trade-off visual acuity for increased sensitivity (Barlow et al., 1957, Peichl and Wassle, 1983). Downregulation of inhibition accomplishes this by allowing weak stimuli anywhere in the receptive field to drive responses, without being silenced by coincident inhibition. However, due to the numerous complex computational roles of inhibition in the retina, silencing inhibition may be expected to negatively impact visual tasks which require active inhibitory activity, such as direction selectivity. In the following work, I investigated whether light-driven inactivation of inhibition impacted the DS circuit and whether this change was limited to spatial tuning exclusively or if light-driven changes in inhibition also affected direction coding.

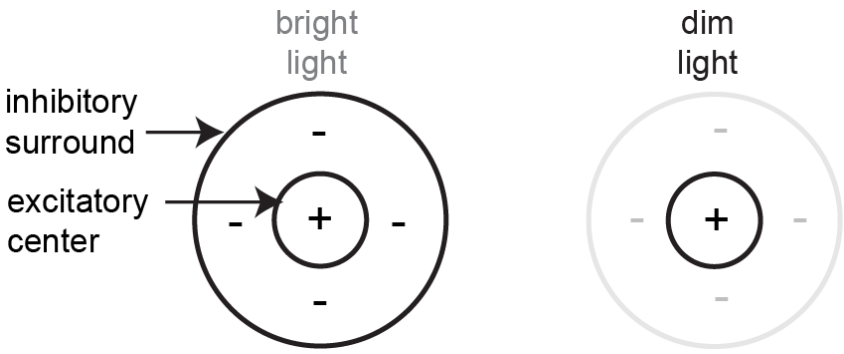

Figure 4: Ambient light alters receptive field function

In bright light, retinal ganglion cells exhibit receptive fields containing an excitatory center and an inhibitory surround. The presence of light in the surround reduces responses to center stimulation. In dim light, however, the inhibitory surround is reduced or absent.

1.5 Objectives

Whether WACs play a role in the DS circuit is not clear. While initial studies suggested that long range inhibition in the DS circuit is inextricably linked with DS inhibition itself (Wyatt and Daw, 1975), a number of more recent studies have provided indirect evidence that non-starburst amacrine cells participate in the DS circuit (Stasheff and Masland, 2002, Chiao and Masland, 2003, Fried et al., 2005, Rivlin-Etzion et al., 2012). The finding that WAC-mediated inhibition is highly dependent on ambient light levels (Farrow et al., 2013) made them unlikely candidates, since changes in WAC activity levels would be expected to alter the balance between excitation and inhibition and undermine directional selectivity. In this study, however, I present several lines of physiological, pharmacological and anatomical evidence to implicate a role for spiking GABAergic WACs in modulating the DS circuit. I show that through specific wiring to presynaptic elements of the DS circuit (bipolar cells), WACs are able to control spatial selectivity in a manner that strongly depends on ambient illumination. Further, they do so

without compromising the balance between inhibition and excitation required for direction coding.

2. Methods

2.1 Animals

The majority of the recordings from DSGCs were obtained from retina harvested from Hb9::eGFP mouse line in which superior coding DSGCs are selectively labelled (Trenholm et al., 2013). However, in a few experiments, DSGCs in non-transgenic C57/Blk6 mice were identified by their directional selective properties. Global inhibition in the unidentified DSGC population was indistinguishable from that observed in superior coding cells in the Hb9::eGFP retina (data not shown). WAC and SAC imaging and recording data were obtained in the ChAT-Cre:Ai9 mouse line, in which SACs are labelled. Mice were housed and maintained on a 12 hour light/dark cycle. All procedures were performed in accordance with the CCAC and approved by the University of Victoria's Animal Care Committee.

2.2 Retinal Preparation

Following a period of ~2 hour dark adaptation, mice were briefly anesthetized (inhalant isoflurane or injected euthanyl) and decapitated. During the removal of the eyes, a small incision was made to maintain orientation of the retina. Isolated retinae were laid photoreceptor side down on a 0.22 μm membrane nitrocellulose filter (Millipore, Bedford, MA, USA) with a pre-cut window, through which images were focused onto the retina. Visualization under IR illumination utilized a Spot RT3 CCD camera (Diagnostic Instruments, Inc., Sterling Heights, MI, USA) attached to an upright Olympus BX51 WI fluorescent microscope, equipped with either a 40 or 60 X water-immersion lens (Olympus Canada Inc., Markham, Ontario, Canada). Retinal preparations were

continuously bathed with Ringer's solution containing (in mM): 110 NaCl, 2.5 KCl, 1 $CaCl_2$, 1.6 $MgCl_2$, 10 dextrose, and 22 $NaHCO_3$; which was bubbled with carbogen (95% O_2: 5 % CO_2; pH 7.4). Experiments were performed near physiological temperatures (35-36 °C). All reagents were purchased from Sigma-Aldrich Canada Ltd. (Oakville, Ont. CA) unless otherwise noted.

2.3 Whole-cell patch clamp recordings

Extracellular spike recordings were made using ~5-10 MΩ electrodes filled with Ringer's solution. Whole-cell spike (current clamp) recordings were made using an electrode solution containing (in mM): 115 K^+ gluconate, 5 KCl, 1 $MgCl_2$, 10 EGTA, 10 HEPES, 4 ATP Mg_2, 0.5 GTP Na_3. The pH was adjusted to 7.4 with KOH. For voltage clamp recordings, electrodes contained (in mM): 112.5 $CsCH_3SO_3$, 9.7 KCl, 1 $MgCl_2$, 1.5 EGTA, 10 HEPES, 4 ATP Mg_2, and 0.5 GTP Na_3. The pH was adjusted to 7.4 with CsOH. Intracellular recordings were made using ~3-6 MΩ electrodes. The reversal potential for chloride (E_{Cl}) was calculated to be ~ -60 mV. Recordings were made with a Multiclamp 700B amplifier (Molecular Devices Inc, Sunnyvale, CA). Signals were digitized at 10 kHz (National Instruments A/D board) and acquired using custom software written in the LabVIEW environment. Spike activity was blocked with bath application of tetrodotoxin (TTX, Alomone Labs, Israel). GABA receptors were antagonized with picrotoxin (PTX) and (1,2,5,6-Tetrahydropyridin-4-yl)methylphosphinic acid (TPMPA). Excitatory responses were partially blocked using a low concentration (4 µM) of AMPA/kainite receptor antagonist 6-cyano-7-nitroquinoxaline-2,3-dione (CNQX).

2.4 Light Stimulus

Stimuli (spots and gratings) were generated with a DLP projector (Texas Instruments; refresh rate 75 HZ) controlled with custom software written by Dr. David Balya (Friedrich Meischer Institute, Switzerland) based on the Psychophysics toolbox extension for Matlab (Brainard, 1997). The ambient background intensity, measured with a calibrated spectrophotometer (USB2000, Ocean Optics), was reported as photoisomerizations per rod per second (R*/s; derived from the absorption spectrum of mouse photoreceptors; Lyubarsky et al., 1999). As most experiments (with the exception of experiments shown in Figure 1 and 2) utilized intensities expected to favour rod responses (less than 13 R*/s; Farrow et al., 2013; Grimes et al., 2014b), for simplicity, I report all intensity values using the R*/s convention. Neutral density filters were used to control the stimulus light intensity.

Light stimuli were focussed on the photoreceptor layer using the substage condenser. Spot stimuli ranged in size from 25 – 1000 μm, and were presented at full positive contrast (Michelson contrast = 0.94) on a black background unless otherwise specified. Drifting gratings stimuli (mostly sine wave gratings, but in some initial experiments square wave gratings were utilized) of 96 different spatio-temporal frequencies (spatial frequency (sf) = [0.0125, 0.025, 0.05, 0.1, 0.2, 0.4] cyc/deg; temporal frequency (tf) = [0.17, 0.25, 0.33, 0.467, 0.50, 0.67, 0.833, 1, 1.33, 1.67, 2, 2.67, 3.56, 5.33, 6.67, 8] cyc/s) were presented at full contrast on black or gray background. Each grating was presented for 5-10s. Responses were quantified by integrating the response to the grating over equal time intervals, measured after the initial transient response to the grating presentation (Supplementary Figure 8). Grating widths were converted to

cycles/degree of visual angle assuming 1 degree of visual angle corresponds to 30 μm on the mouse retina (Remtulla and Hallett, 1985).

2.5 Analysis of Physiological Data

Physiological data was analyzed using custom routines written in Matlab (Mathworks) or Igor (Wavemetrics). Spike numbers or peak spike rates were reported for extracellular or current clamp recording analysis. Spike rate was estimated by filtering the light evoked spike train using a convolution with a Gaussian kernel with a fixed width, $\sigma = 25$ ms. Responses were averaged over multiple trials (3-5). Either peak amplitude or integrated postsynaptic currents were used to quantify light-evoked synaptic current responses, but no qualitative differences were observed between these two methods. Cross-correlation statistics are reported as Pearson's R correlation coefficient. Statistical power is reported as the result of a Student's t-test, un-paired unless stated, with significance levels as reported. Data are presented as mean ± SEM.

Spatial selectivity was quantified using a spatial selective index (SSi), which was calculated as (C – S / C + S) where C is the amplitude of the maximum response (regardless of stimulus size) and S is the response to the largest stimulus. Similarly, a direction selectivity index (DSi) was quantified as (P – N / P + N), where P and N are responses recorded to images moving in the preferred and null direction, respectively. These indices range from -1 to 1, where 1 represents strongest suppression and 0 represents equal responses to preferred and non-preferred stimuli. A DSi of -1 represents strongest responses in the DSGC's null direction, and is a common value obtained for

inhibitory currents. Directional tuning widths were estimated using a Gaussian function (Nowak et al., 2011).

Similar to previous studies (Perrone and Thiele, 2001, Priebe et al., 2003, Gale and Murphy, 2014), responses (R (sf,tf)) were fit with a 2D Gaussian on a logarithmic scale, using the equation:

$$R(sf,tf) = A \times \exp\left[\frac{-1}{2(1-cor)^2} \times \left(\left(\frac{-log_2\left(\frac{sf}{sf_0}\right)}{sf_{width}}\right)^2 \times \left(\frac{-log_2\left(\frac{tf}{tf_0}\right)}{tf_{width}}\right)^2 - \left(\frac{2 \times cor \times log_2\left(\frac{sf}{sf_0}\right) \times log_2\left(\frac{tf}{tf_0}\right)}{sf_{width} \times tf_{width}}\right)\right)\right]$$

where A is the peak response, sf_0 and tf_0 are the spatial and temporal frequency locations of the peak, respectively, sf_{width} and tf_{width} are standard deviations of the spatial frequency and temporal frequency responses, respectively, and cor is the correlation co-efficient which relates to the dependence of spatial frequency responses to temporal frequency. To compare the degree to which tuning curves aligned with the velocity of the stimulus, the velocity tuning index (VTi) was calculated as

$$VTi = cor \times \left(\frac{tf_{width}}{sf_{width}}\right)$$

where an VTi of 1 indicates responses orientated along the diagonal (speed) axis, and an VTi of 0 indicates independent spatial and temporal frequency preferences. Goodness of fit was assessed using a Chi-square test.

3. Results

3.1 Wide-field inhibition but not DS inhibition is modulated by ambient light levels

In a recent study, an increase in ambient illumination was shown to lead to the recruitment of a class of WACs in select circuits, including those driving ON and OFF alpha-like ganglion cells (Farrow et al., 2013). However, whether other types of ganglion cells such as DSGCs are subject to ambient light-dependent forms of inhibition, or conversely whether other types of amacrine cells are modulated by ambient light is not clear. To test these possibilities, I examined the effects of ambient illumination on direction and size coding in DSGCs, which rely on local and wide-field inhibition, respectively. I used small moving spots or large stationary stimuli to bias the strength of different forms of inhibition.

I first compared the spiking responses of DSGCs to spots moving in 8 directions (velocity 1000 μm/s) under different ambient illuminations (Figure 5A,B). Motion in the 'preferred' direction evoked a robust spiking response, while motion in the opposite or 'null' direction did not (Figure 5A). Movement in other directions evoked responses of intermediate amplitudes (Figure 5B). Regardless of the ambient illumination, the relative amplitudes of responses evoked by spots moving in all directions remained constant (Figure 5B) resulting in a stable direction selectivity across all ambient light levels (as indicated by a stable direction selective index, DSi; where values near 1 indicate strong direction selectivity; Figure 5C). Thus, directional selectivity in ganglion cells appears to be independent of ambient illumination, as previously reported (Farrow et al., 2013).

Surround inhibition to the DS circuit, on the other hand, was strongly modulated by ambient illumination. To assess the strength of wide-field inhibition I examined the peak amplitude of responses evoked by a series of stationary spots of increasing sizes (ranging from 25 μm-1000 μm). Under dim ambient light levels (10^{-3} - 10^{-1} rod isomerizations s^{-1}, R*/s), spiking responses to flashed of light increased to the optimal stimulus size of 436 ± 59 μm (n = 11) and remained relatively constant thereafter (Figure 5D,E), indicating poor spatial selectivity (responses to large stimuli are similar to responses to optimal stimuli). The average spatial selectivity index (SSi, which is derived from responses to the optimal and largest size spots, where 0 indicates poor spatial selectivity and values near 1 indicate a strong selectivity; see Methods) under dim light conditions was 0.19 ± 0.03 (n = 11). Under brighter ambient illumination (10^{1} - 10^{4} R*/s; near cone threshold, henceforth referred to as the 'bright' condition), however, response amplitude increased more sharply with size up to an optimal spot diameter of 182 ± 20 μm (which was less than half of the optimal size measured under dim light conditions; n = 20; $p < 0.005$). Under these conditions, the optimal size closely matched the dendritic field size (Trenholm et al., 2011). More strikingly, when the size of the spot was increased beyond an optimal size, the response amplitudes declined sharply, indicating the engagement of a suppressive surround mechanism , henceforth referred to as a wide-field inhibition, due to the large stimulus size required to recruit it(Figure 5E). The SSi under bright conditions was 0.68 ± 0.06 (n = 21), significantly higher than observed under dim light conditions (Figure 5E,F; $p < 0.05$). When SSi was plotted against ambient intensity, SSI was constant to 1.5R*/s, however an abrupt transition was observed such that SSi increased from 0.18 ± 0.05 to 0.81 ± 0.08 over a 10 fold increase

in ambient light intensity (Figure 5F), but remained constant thereafter. The ‘switch’ like behaviour of wide-field inhibition is reminiscent of WAC-mediated surround inhibition to ON and OFF alpha-like ganglion cells and appears to occur at a similar light level (Farrow et al., 2013). Taken together, comparison of spiking activity to moving and stationary stimuli indicate that local and wide-field forms of inhibition are differentially regulated by ambient light, suggesting that they arise from separate sources. Importantly, recruitment of wide-field inhibition has no effect on directional computation in the DS circuit.

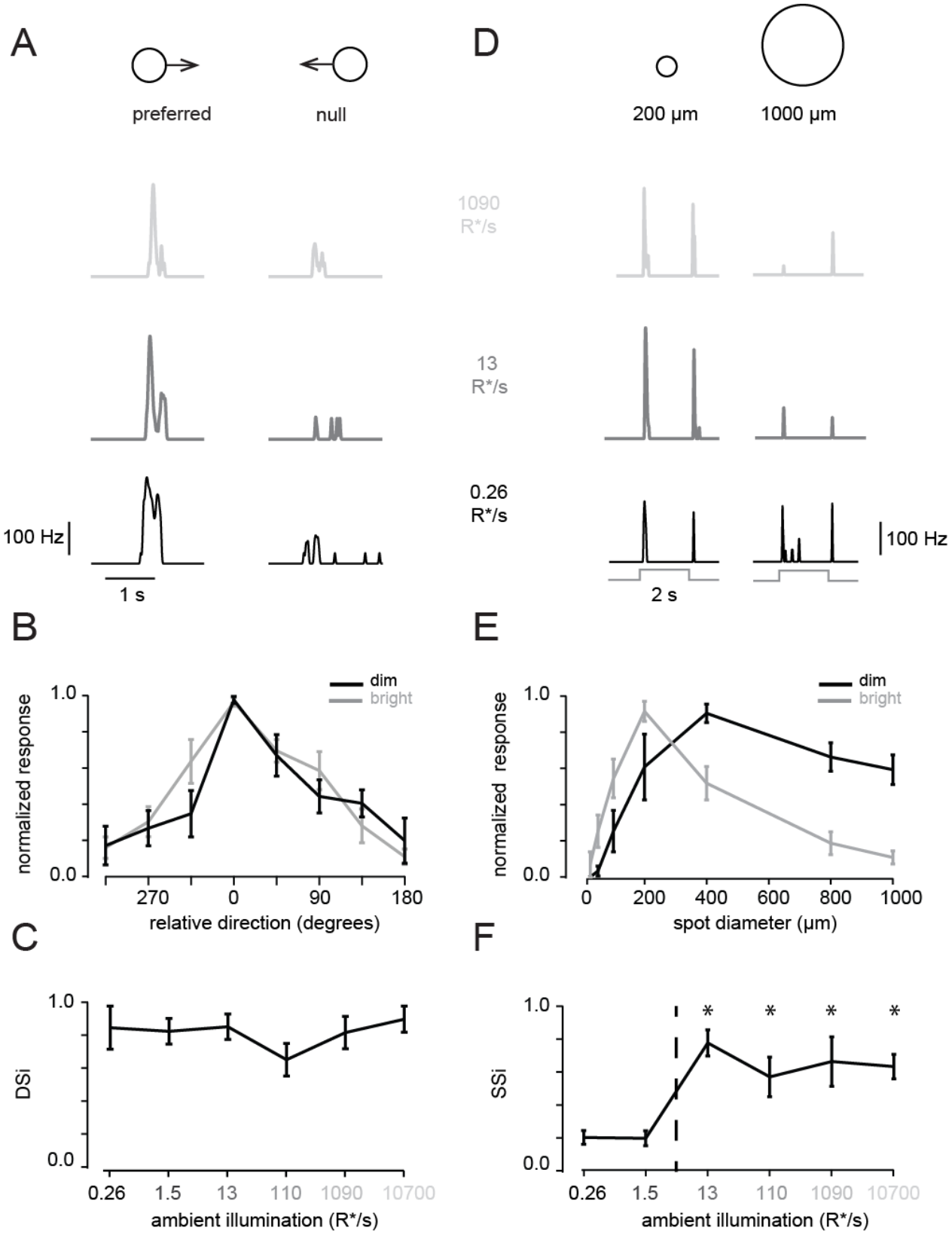

Figure 5: Multiple layers of inhibition to DSGCs are differentially modulated by light

A. Spiking responses measured in a DSGC, evoked by spots moving in the preferred or null direction (spot diameter 400 μm; speed ~ 1000 μm/s). The spike rate was estimated by filtering the light evoked spike trains using a convolution with a Gaussian kernel with a fixed width, $\sigma = 25$ ms. Responses to preferred and null direction stimuli were measured under different ambient illuminations (1090 R*/s, 13 R*/s or 0.26 R*/s, as indicated).

B. Normalized peak responses as a function of stimulus direction (preferred direction was set to 0 degrees) measured in dim (black traces; ~0.26 – 1.5 R*/s; n = 7) and bright conditions (gray traces; ~13-10^4 R*/s; n = 10).

C. The average directional selectivity index (DSi) is plotted as a function of ambient illumination (n = 3 to 5 cells for each light condition).

D. DSGC responses evoked by a 200 μm or 1000 μm diameter spot (centered over the soma; duration 2 seconds), under different ambient illuminations as in **A**.

E. The average normalized peak response to stationary spots measured under dim conditions (black traces; ~0.26 – 1.5 R*/s; n = 8) and bright conditions (gray traces; ~13-10^4 R*/s, n = 9), is plotted as a function of stimulus diameter.

F. The average spatial selectivity index (SSi) is plotted as a function of ambient illumination. All SSi values to the right of the dotted line (bright conditions) are significantly larger than values measured under dim conditions (left of the dotted line, asterisks represent $p < 0.05$; n = 5 to 6 cells for each condition).

3.2 Wide-field inhibition is mediated by a presynaptic mechanism

To investigate synaptic mechanisms underlying DS and wide-field inhibition under different ambient light conditions, I next measured inhibitory and excitatory postsynaptic currents (IPSCs and EPSCs, respectively) in voltage-clamped DSGCs in response to either stimuli moving along the preferred-null axis, or static stimuli of increasing size, respectively. Measurement of EPSCs evoked by moving spots along the preferred-null axis indicated that output from bipolar cells, on average, was not DS (Figure 6B,E). On the other hand, IPSCs measured in DSGCs were always larger in the null direction (Figure 6), compared to those evoked in the preferred direction, consistent

with previous studies (Taylor and Vaney, 2002). Importantly, inhibitory currents remained strongly directional across all ambient light conditions (Figure 6B,E; $p > 0.1$; Figure 7 shows inhibitory DSi at all light levels studied. Note that a negative DSi indicates inhibitory currents are stronger in the null direction). Thus, conventional directional inhibitory signals, likely mediated by SACs, appear to be operational at all ambient light levels.

When I examined the impact of wide-field inhibition on the local synaptic inputs to DSGCs, I found not only did it change with ambient light, but also found that wide-field inhibition was expressed almost exclusively at a presynaptic locus. In dim light conditions, the peak amplitude of both the inhibitory and excitatory responses to spots larger than an optimal size remained approximately constant (Figure 6C), indicating weak surround inhibition. In contrast, under bright ambient illumination, both inhibitory and excitatory responses decreased as the spot size was increased beyond the optimal size (Figure 6C). This resulted in a marked increase in SSi values for both excitation and inhibition under bright conditions compared to values measured under dim conditions (Figure 6E). This was consistent for both ON and OFF responses (Figure 6E). Furthermore, response profiles (and estimates of SSi) were similar whether the peak amplitude or integrated current was used to quantify the responses (Figure 8).

It is worth noting that the peak amplitude of excitatory currents evoked with optimal-sized stimuli were not significantly larger in bright vs. dim light conditions (ON EPSCs peak amplitude was 283 ± 32 pA in dim light, $n = 8$; 305 ± 27 pA in bright light, $n = 11$; $p = 0.6$), indicating that it was not simply changes in the magnitude of the responses that triggered surround inhibition. These data suggest a fundamental change in

the relationship between excitation and wide-field inhibition which is triggered by changes in background illumination.

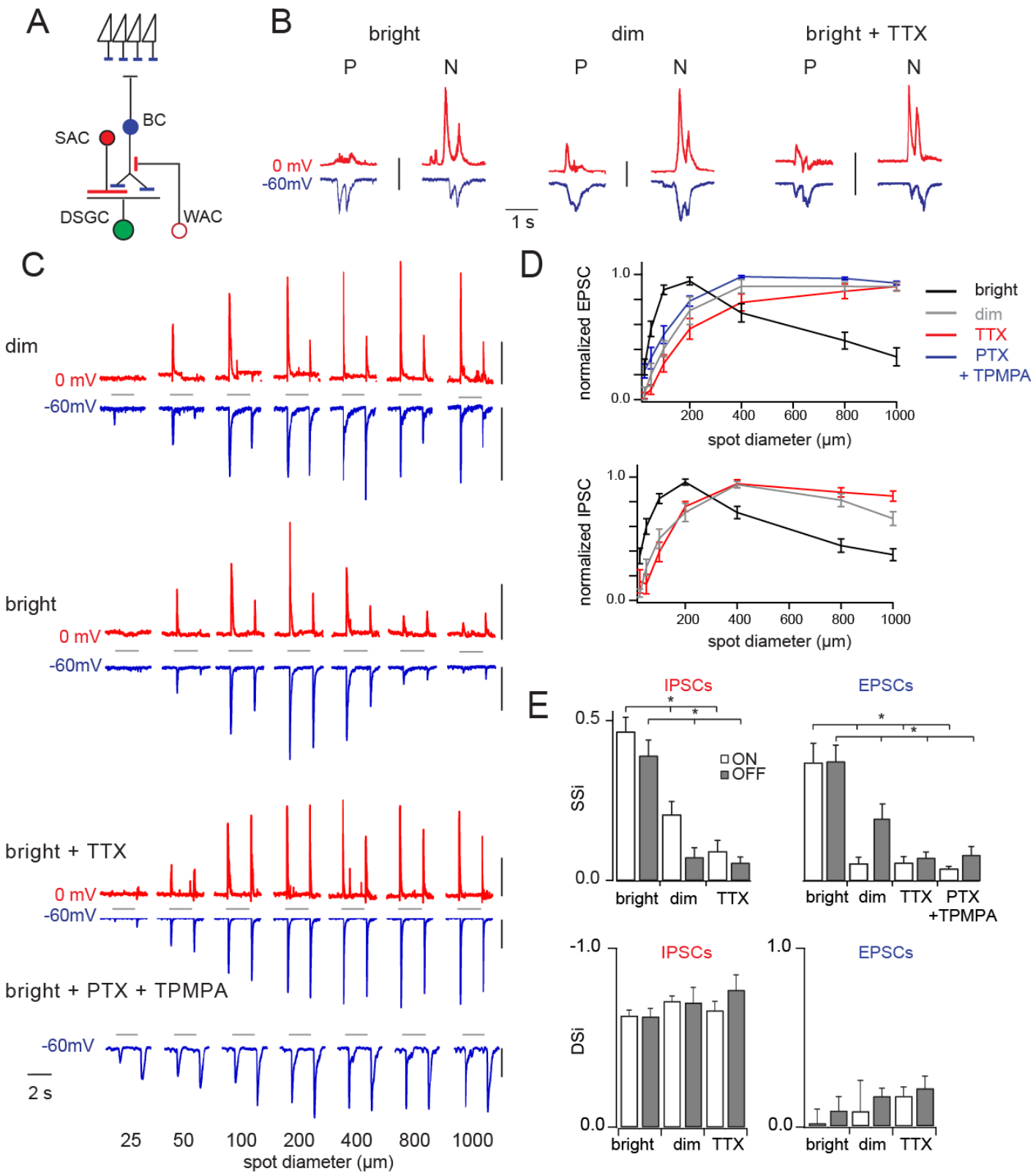

Figure 6: Wide-field inhibition mediated by presynaptic GABA receptors requires voltage-gated Na+ channels

A. A schematic of the DS circuit including a wide-field amacrine cell (WAC). WAC inhibition is applied presynaptically to bipolar cell (BC) terminals that excite both starburst amacrine cells (SACs) and DSGCs. SACs provide DS inhibition directly to DSGCs. For simplicity, a single BC is shown to represent multiple possible types of ON/OFF BCs innervating both SACs and DSGCs. Excitatory synapses are shown in blue, inhibitory synapses are shown in red.

B. Inhibitory (red, IPSCs) and excitatory (blue, EPSCs) synaptic currents measured in voltage-clamped DSGCs (holding potential is indicated on the left) in response to moving spots (400 µm, 1000 µm/s) in preferred (P) and null (N) directions, observed under dim or bright ambient light, or in the added presence of TTX (1 µM) as indicated. Vertical scale bar = 250 pA.

C. Inhibitory and excitatory synaptic currents measured in response to increasing diameter spots (25-1000 µm; indicated at bottom) under dim or bright ambient illumination, or in the added presence of TTX or GABA receptor antagonists (100 µM PTX+100 µM TPMPA) as indicated. Vertical scale bar = 250 pA. Gray horizontal bars indicate the duration of the light stimulus.

D. Normalized peak amplitude of excitatory (*top*) and inhibitory (*bottom*) responses plotted against spot diameter. Responses shown in bright (black) and dim (gray) conditions, or when TTX (red) or GABA receptor antagonists (blue) are applied (n = 12 for bright EPSCs and IPSCs; n = 6 for dim light; n = 12 for TTX; n = 8 for GABA blockers; only ON responses shown for clarity).

E. Average SSi for IPSCs and EPSCs is plotted for the different conditions, as indicated (*top panel*). ON and OFF responses are indicated as open and filled bars, respectively. Asterisks indicate significance of $p < 0.05$ compared to light adapted control. Average DSi is plotted for different conditions, as indicated (*bottom panel*), with negative DSi corresponding to stronger null direction responses.

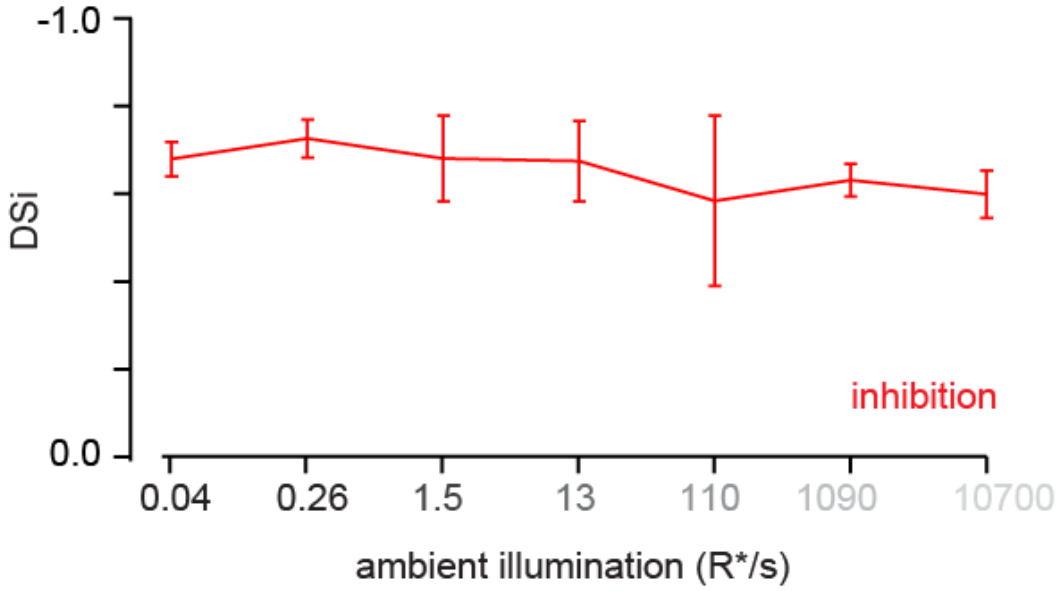

Figure 7: Strength of null direction inhibition does not change with ambient illumination

DSi for IPSCs was calculated as (P-N/P+N), where N is the null direction and P is the preferred direction of spiking responses of DSGCs (n = 2-7 for each light condition). DSi for IPSCs approaches -1, as it is strongest in the DSGC's null direction of spiking across all illumination conditions.

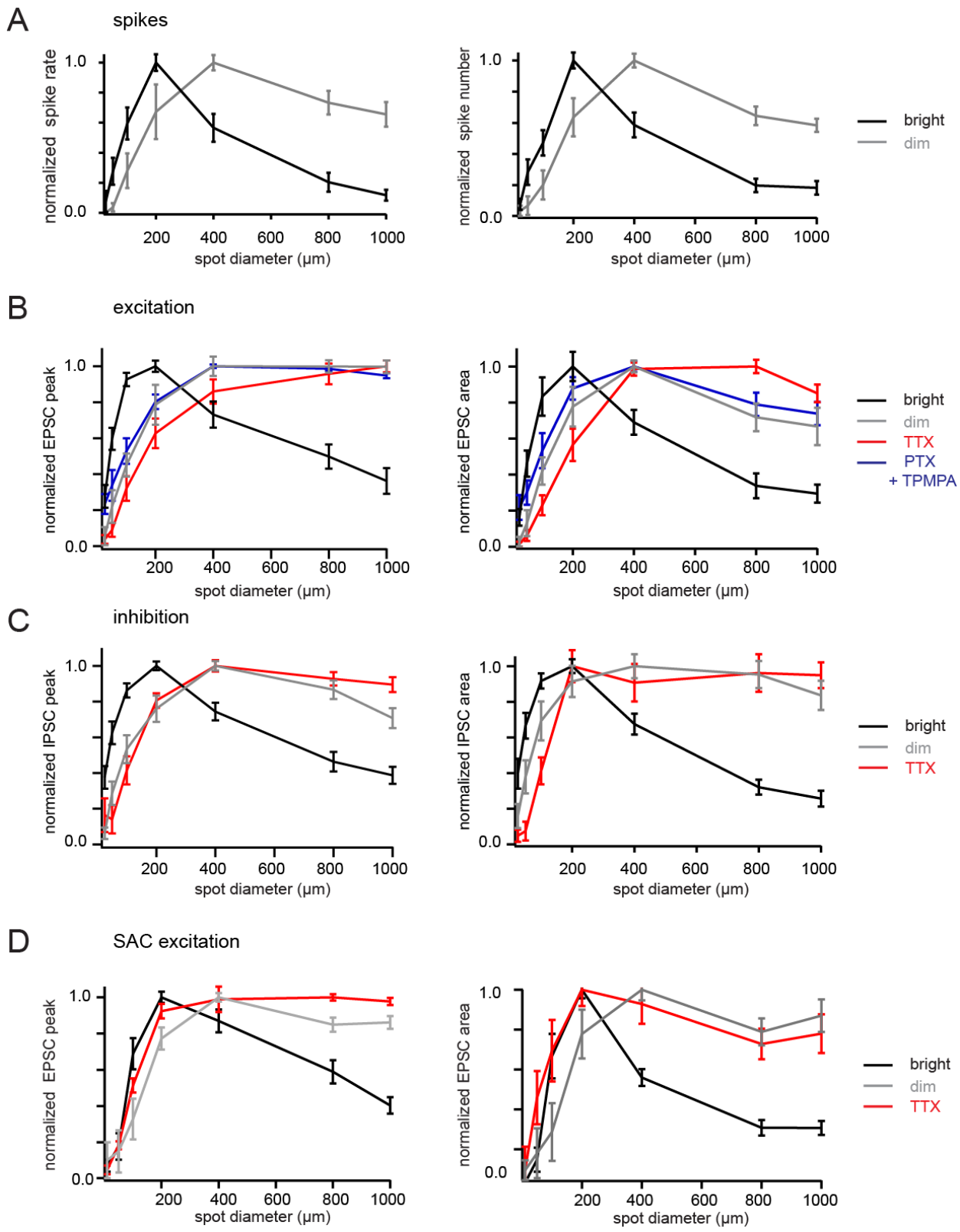

Figure 8: Peak amplitude and the integrated response profiles are qualitatively similar.

A. Spiking responses in bright and dim light expressed as normalized peak spike rate (*left*) or as normalized spike number (*right*).

B. Excitatory synaptic currents to voltage-clamped DSGCs, measured in bright or dim light, or in the presence of TTX or PTX+TPMPA, expressed as normalized current peak (*left*) or normalized integrated current area (charge; *right*).

C. Inhibitory synaptic currents to voltage-clamped DSGCs, measured in bright or dim light, or in the presence of TTX or PTX+TPMPA, expressed as normalized current peak (*left*) or normalized integrated current area (*right*).

D. Excitatory input to SACs (EPSCs) plotted as normalized current peak (*left*) or normalized integrated current area (*right*) in bright or dim light conditions, or in the presence of TTX.

3.3 TTX-sensitive voltage-gated Na+ channels mediate wide-field but not DS inhibition

Presynaptic modulation of local excitation and inhibition could occur either at the level of horizontal cells in the outer retina acting on photoreceptors (or bipolar cell dendrites) or be mediated by WACs in the inner retina, acting at bipolar cell terminals (Shields and Lukasiewicz, 2003, Zaghloul et al., 2007, Baccus et al., 2008, Farrow et al., 2013, Protti et al., 2014). Wide-field inhibition mediated by WACs relies on a spiking mechanism, but horizontal cell inhibition does not. Therefore TTX (1 µM), which blocks voltage-gated Na^+ channels, serves as a valuable tool to distinguish between these distinct sources of inhibition. Next, I examined the effect of blocking voltage-gated Na^+ channels on DS and wide-field inhibition (Figure 6C-E).

In the presence of TTX, moving spots evoked inhibitory and excitatory currents that were indistinguishable from those measured under control conditions (Figure 6B). These results confirm the finding that TTX-sensitive Na^+ channels do not play a strong role in mediating local inhibitory and excitatory inputs to DSGCs (Figure 4B,E; Oesch et

al., 2005, Oesch and Taylor, 2010). In contrast, in the presence of TTX, synaptic responses evoked by large stationary stimuli were augmented compared to responses measured in control (Figure 6C), indicating that wide-field inhibition relies on voltage-gated Na^+ channels. As TTX did not significantly affect responses to the optimum sized spot, the net effect of TTX was a strong reduction in SSi (Figure 6E; n = 14). The reduction of wide-field inhibition observed in the presence of TTX implicates WACs as the principal regulator of size selectivity in the DS circuit. Consistent with the idea that WACs mediate size selectivity via a GABAergic mechanism, the SSi was significantly reduced in the presence of GABA receptor antagonists (Figure 6C-E). This was also found to be true for spiking responses (Figure 9), where GABA antagonists block directional responses as well in most stimulus conditions (Trenholm et al., 2011). These results are not due to response saturation in the absence of GABAergic transmission, since reducing responses with glutamate receptor antagonists did not result in a rescue of surround suppression (Figure 9A, D).

In summary, I have shown that local and wide-field inhibition to DSGCs, stimulated in a biased manner using either small moving or large stationary spots, differ in several respects including: 1) the range over which they operate; 2) their sites of action; 3) their sensitivity to ambient light; and 4) their sensitivity to TTX. DS inhibition acts locally, directly on DSGC dendrites, and remains insensitive to ambient light or Na^+ channel activity, while wide-field inhibition acts on a wide spatial scale, acts presynaptically to the DSGC (likely on presynaptic bipolar cells), is only recruited at bright background light levels and requires Na^+ channels to drive inhibition.

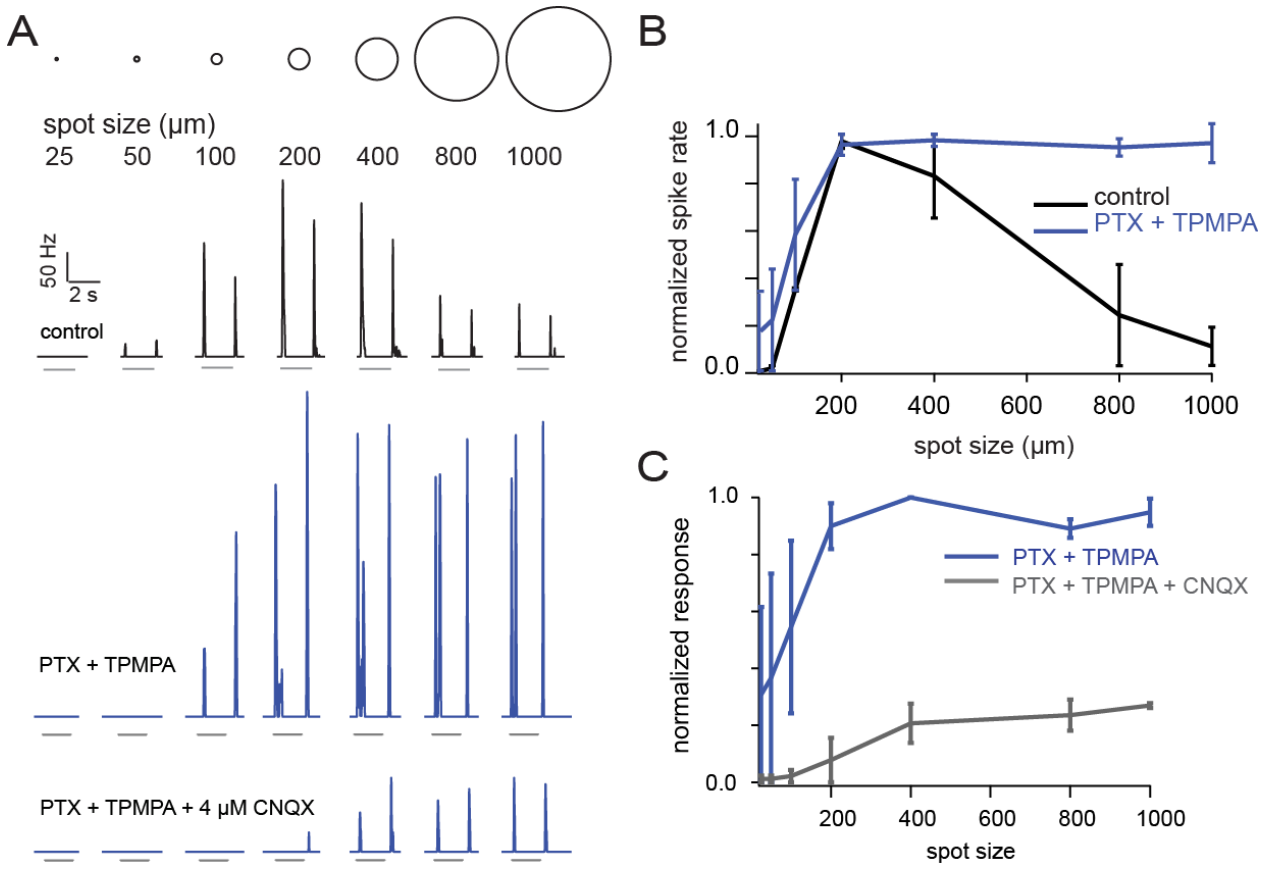

Figure 9: GABA receptor antagonists block surround inhibition even when spike rate is decreased using excitatory synaptic blockers.

A. Spiking response in a DSGC evoked by stationary spot stimuli of varying diameter (7 spots, sizes as indicated) in control (*top*) or in the added presence of PTX + TPMPA (100 μM each; *middle*). Low concentration (4 μM) CNQX was added to reduce spike saturation which may have occluded other sources of surround inhibition under conditions of GABA receptor antagonism (*bottom*).

B. Response profiles for normalized spiking responses in control and in application of PTX + TPMPA (100 μM each). Calculated SSi values were 0.82 ± 0.13 (ON) and 0.87 ± 0.13 (OFF) in control (n = 2) and 0.03 ± 0.03 (ON) and 0.02 ± 0.004 (OFF) in GABA blockers (n = 2; $p < 0.05$ for both ON and OFF).

C. Response profiles normalized within each cell, demonstrating that excitatory blockers drastically reduce response strength. SSi values were 0.027 ± 0.025 for ON and 0.04 ± 0.003 for OFF with GABA blockers alone, and 0.01 ± 0.01 for ON and 0.05 ± 0.004 for OFF with GABA blockers and excitatory blockers together (n = 2, $p > 0.05$ for both ON and OFF, paired t-tests).

3.4 Excitation and inhibition remain balanced during wide-field inhibition

While wide-field inhibition clearly modulates the synaptic inputs to DSGCs, the population data indicated that in some conditions ON IPSCs were more strongly modulated than ON EPSCs, while for OFF responses the opposite trend was observed (Figure 6E). If activation of WACs reduces EPSCs to a greater extent than IPSCs, or vice versa, the critical balance between excitation and inhibition will be disrupted and the DS computation may be perturbed. To investigate whether wide-field inhibition interferes with the balance between inhibition and excitation at the level of individual cells, or even during individual trials, I next measured EPSCs and IPSCs in DSCGs near simultaneously. To do so, the holding potential of the voltage-clamped DSGC was oscillated between the excitatory and inhibitory reversal potentials (0 mV and -60 mV, respectively) at a frequency of 100 Hz, and light-evoked post-synaptic currents were measured following brief capacitive transients (Cafaro and Rieke, 2010). Since the time course of the synaptic responses were relatively slow, the lower sampling of the currents did not strongly distort the overall magnitude of the responses (Figure 10A).

I found that changes in the average peak amplitude of the IPSC and EPSC within a given DSGC were strongly correlated as the size of the spot of light was increased to recruit WACs (Figure 10B,C). This indicated that inhibitory and excitatory inputs remain balanced in individual DSGCs, as different levels of WAC modulation acts presynaptically. Interestingly, the peak amplitude of the ON responses were also correlated with OFF responses (ON EPSC-OFF IPSC, or OFF EPSC-ON IPSC; Figure 8D), although more weakly when compared to ON-ON and OFF-OFF correlations,

suggesting parallel sources of wide-field inhibition acting at ON and OFF bipolar cell terminals. Furthermore, I estimated the variability of the synaptic responses by subtracting the mean response (computed over ~40 trials) from individual trials, resulting in a residual (noise). The correlation strength of the residuals for the optimal spot stimulus was ~0.4 (Figure 10E). Importantly, noise correlations remained constant across spot size (Figure 10E,F), as the mean response decreased with the recruitment of surround inhibition by larger stimuli (Figure 10C). Correlations were significantly reduced when trials were shuffled (offset by one trial), indicating that they did not arise from systematic slow drifts that could potentially arise from a number of sources (Figure 10F). While, a common bipolar cell driving direct excitation and feed-forward inhibition to DSGCs could be the source of correlations, the contribution of co-release of acetylcholine and GABA from SACs onto DSGCs cannot be excluded. Regardless of the precise origin of the correlations, the recruitment of wide-field inhibition does not perturb the inhibition/excitation balance at the level of individual cells or even on an individual trial basis, which is important for high-fidelity stimulus encoding (Cafaro and Rieke, 2010).

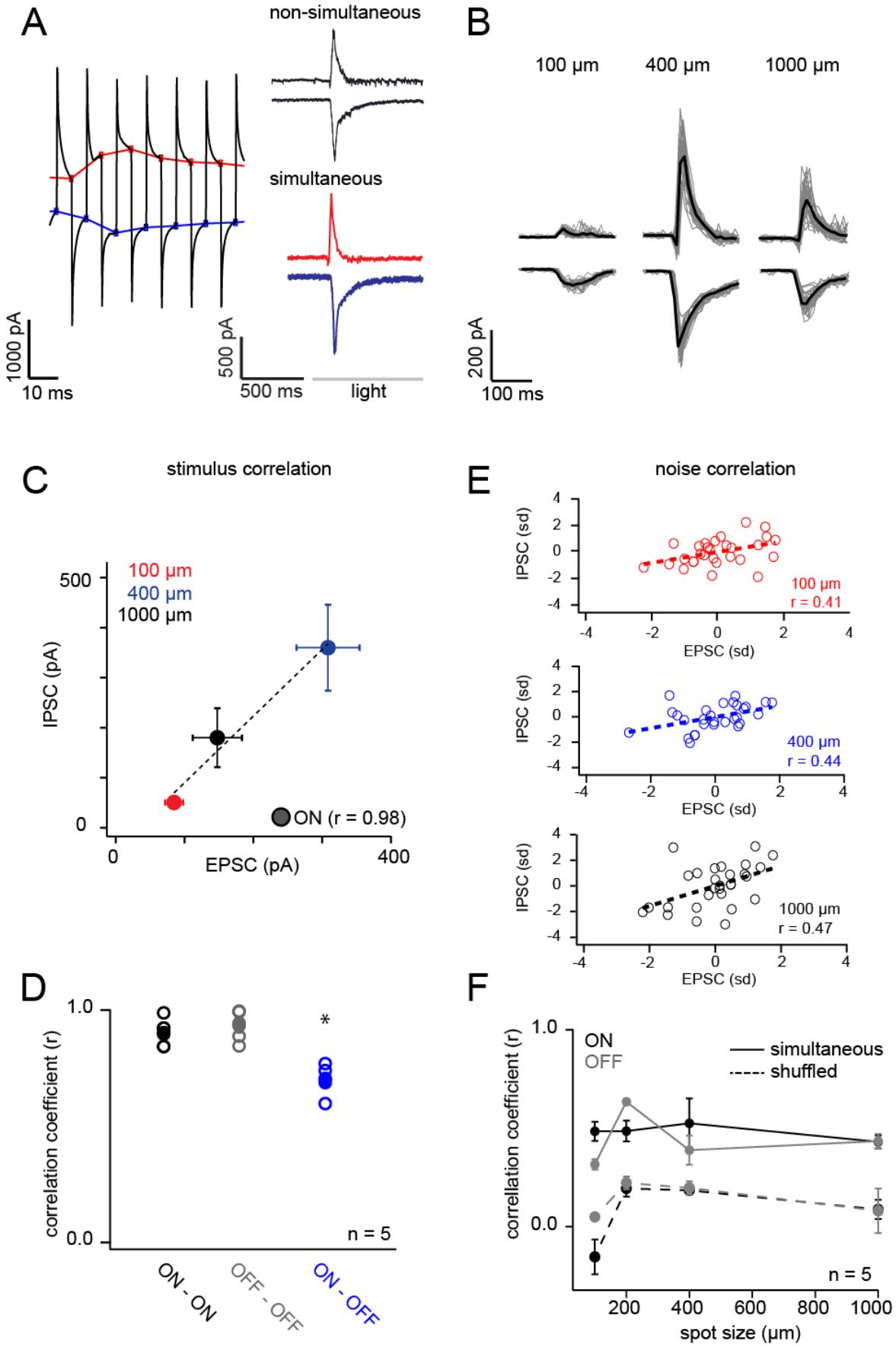
A
non-simultaneous
simultaneous
1000 pA
10 ms
500 pA
500 ms
light
B
100 µm
400 µm
1000 µm
200 pA
100 ms
C
stimulus correlation
100 µm
400 µm
1000 µm
IPSC (pA)
EPSC (pA)
ON (r = 0.98)
D
correlation coefficient (r)
n = 5
ON - ON
OFF - OFF
ON - OFF
E
noise correlation
IPSC (sd)
EPSC (sd)
100 µm
r = 0.41
400 µm
r = 0.44
1000 µm
r = 0.47
F
correlation coefficient (r)
ON
OFF
simultaneous
shuffled
n = 5
spot size (µm)

Figure 10: Wide-field inhibition does not disrupt the inhibition/excitation balance in DSGCs

A. Light-evoked response measured while the membrane potential was oscillated between the reversal potential for excitation (0 mV) and inhibition (-60 mV) at 100 Hz (left). The light-evoked inhibitory (red) and excitatory (blue) synaptic currents were estimated by measuring current after the capacitive transients had settled. Synaptic responses measured from the same cell at different times (top right) or nearly simultaneously (bottom right) are shown. Light stimulus was a 400 µm spot, indicated by gray bar.

B. Inhibitory and excitatory responses measured near simultaneously evoked by 100 µm, 400 µm or 1000 µm spots (measured in bright light conditions). Black traces indicate the average responses, while the gray traces represent individual trials (40 trials).
C. The average IPSC and EPSC peak amplitudes measured near simultaneously in a DSGC are strongly correlated (Pearson's correlation coefficient, $r = 0.98$), indicating that wide-field inhibition decreases the strength of inhibition and excitation in parallel. The dotted trend lines represent linear regression fits.

D. The correlation coefficient plotted for ON IPSCs-ON EPSCs (black), OFF IPSCs-OFF EPSCs (gray), and ON EPSCs-OFF IPSCs or OFF IPSCs – ON EPSCs (blue dots). Filled circles indicate the population average r ($n = 5$) while open circles indicate r of individual cells (* indicate $p < 0.01$; paired t-tests).

E. Noise correlations for trials shown in **B.** Each point indicates the deviation of the peak amplitude of an individual response from the average response, normalized by the standard deviation of the responses measured over 40 trials. Correlation coefficients for each set of responses evoked by different size stimuli (100 µm, 400 µm or 1000 µm diameter spots) are indicated. Dotted trend lines represent linear regression between EPSC and IPSC residuals.

F. The correlation coefficient (average ± SEM) is plotted against spot diameter for both ON (black) and OFF (gray) responses. The correlation coefficient was significantly reduced when trials were shuffled (dashed lines; $n = 5$; $p < 0.1$ for each pairwise comparison between shuffled and non-shuffled responses of a given size).

3.5 Wide-field modulation of starburst amacrine cell activity

One way in which WACs could modulate excitatory and inhibitory responses in DSGCs in parallel is by acting on presynaptic inputs that drive both SACs and DSCGs (Figure 4A). To test whether WACs mediate inputs to SACs, I directly recorded EPSCs

in SACs (held at -60 mV). Indeed, these measurements revealed response profiles to increasing spot stimuli that were similar to those measured in DSGCs (Figure 11B,C). The spatial selectivity of excitation was significantly reduced in the presence of TTX and under dim light conditions (Figure 11B,E). The qualitative effects of TTX/dim light did not change whether the response was quantified as the EPSC peak or the integrated current (Figure 7). Similar to EPSCs, IPSCs measured in SACs also exhibited a TTX-sensitive surround (Figure 11B,D,E). However, these data should be interpreted with caution, as putative direct WAC input to SACs could be masked by increases in reciprocal SAC-SAC inhibition (Lee and Zhou, 2006) that are expected to be augmented in the presence of TTX. Consistent with the hypothesis, my finding that the input properties of SACs matched their output properties (measured as IPSCs in DSGCs) suggests that WACs act at sites upstream to the SAC, i.e. at the bipolar cell axonal terminals providing excitation to SACs and DSGCs.

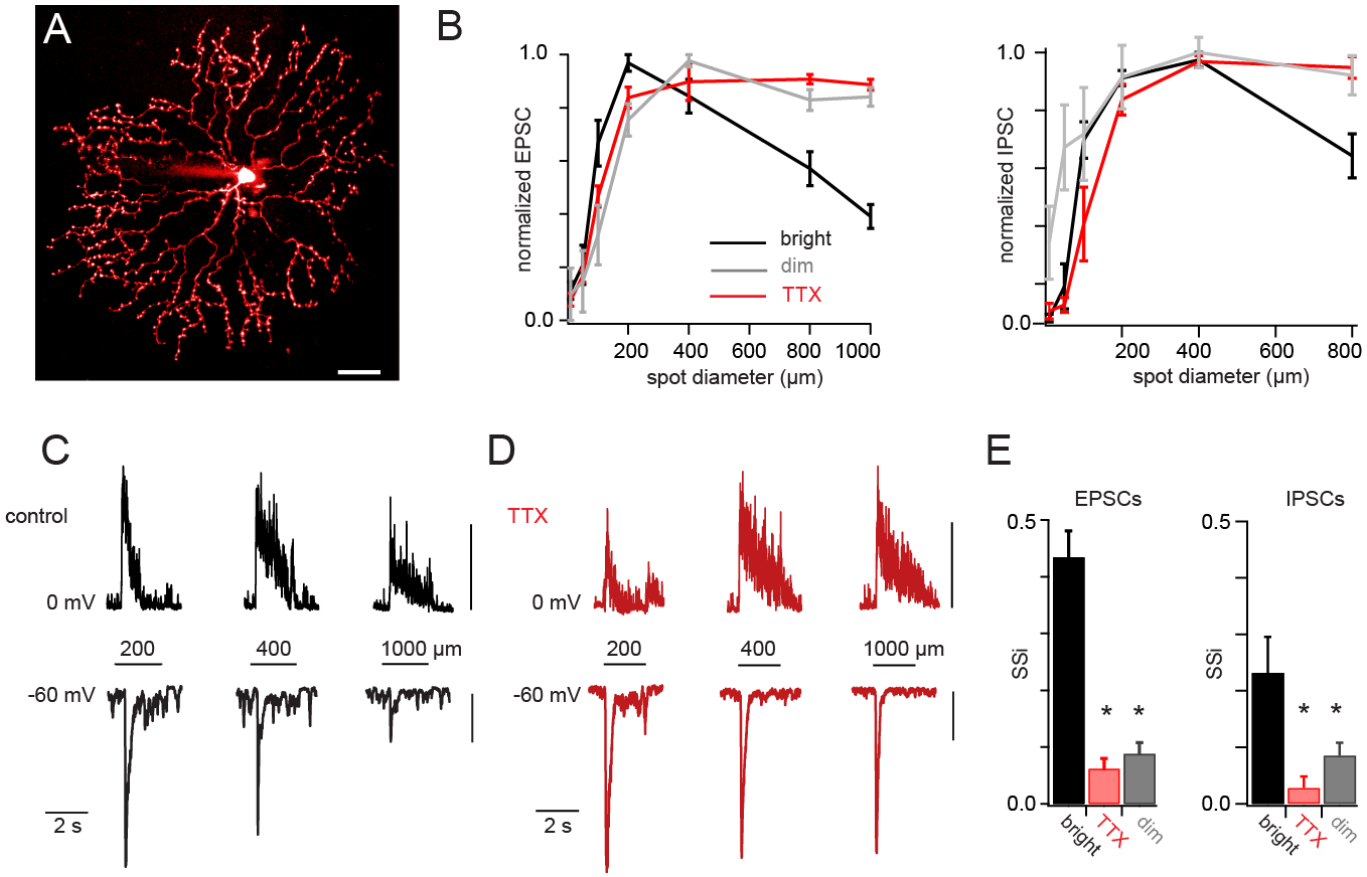

Figure 11: Starburst amacrine cells are subject to presynaptic TTX-sensitive wide-field inhibition

A. A maximum projection of a 2-photon image stack of an Alexa-488 filled starburst amacrine cell (scale bar = 20 µm).

B. Normalized EPSC (*left*) and IPSC (*right*) peak amplitude is plotted against spot size (n = 5 to 6 cells for each condition).

C. Example EPSCs (V_{hold} = -60 mV; *bottom*) and IPSCs (V_{hold} = 0 mV; *top*) measured in a voltage-clamped SAC evoked by spots of different diameters (as indicated) under bright background light conditions or in the added presence of TTX (**D**; scale bars = 100 pA).

E. The average SSi measured under different conditions (n = 5-8). Asterisks indicate $p < 0.05$.

3.5 Wide-field amacrine cells confer spatial sensitivity without affecting directional preference

To better understand the impact of wide-field inhibition on DS processing, I designed 3 stimulus paradigms to differentially activate WACs in the periphery, while measuring DS responses of DSGCs in response to grating stimuli (0.05 cyc/deg, 2 Hz, moving in 8 directions; Figure 12A). First, I stimulated peripheral WACs using an annulus (inner diameter 500 µm, outer diameter 2000 µm) in which the spatial frequency of the surround grating was adjusted to strongly (0.1cyc/deg) or weakly stimulate WACs (0.4 cyc/deg, see Figure 18). To exclude possible edge effects of the stimuli, the outer grating was separated from the inner grating with a 100 µm thick gray ring and the outer grating was moved orthogonally to the cell's preferred-null axis. In a second paradigm, I compared responses to large gratings (0.0125 cyc/deg) presented through different sized apertures (full field, 2000 µm; or centre alone, 500 µm). Full field gratings would stimulate both wide-field and local inhibition while the stimuli presented through the aperture would be biased towards stimulating only local inputs. In the third paradigm I compared spiking responses to gratings drifting in 8 directions under dim vs. bright conditions (10^{-1} R*/s vs. 10^{1} R*/s), where I have shown wide-field inhibition to be stronger in the latter condition (Figure 5F).

Regardless of the stimulus paradigm used, the condition designed to recruit wide-field inhibition decreased the overall strength of the centre response (Figure 12A,B) validating the experimental design. The decrease in response amplitude was associated with a mild sharpening of the directional tuning curve (Figure 12C), which is consistent with the role of postsynaptic processing (Oesch et al., 2005, Priebe and Ferster, 2008).

However, all three manipulations failed to cause any statistically significant improvements in the DSi (Figure 12D). In addition, regardless of the absolute magnitude of the response, increasing wide-field inhibition did not significantly alter the DSGC's preferred direction (Figure 12E). Taken together, these data indicated that the direction coding properties of the DSGC are not strongly affected by wide-field inhibition, consistent with notion that local excitation/inhibition remain balanced under different ambient light conditions (Figure 10).

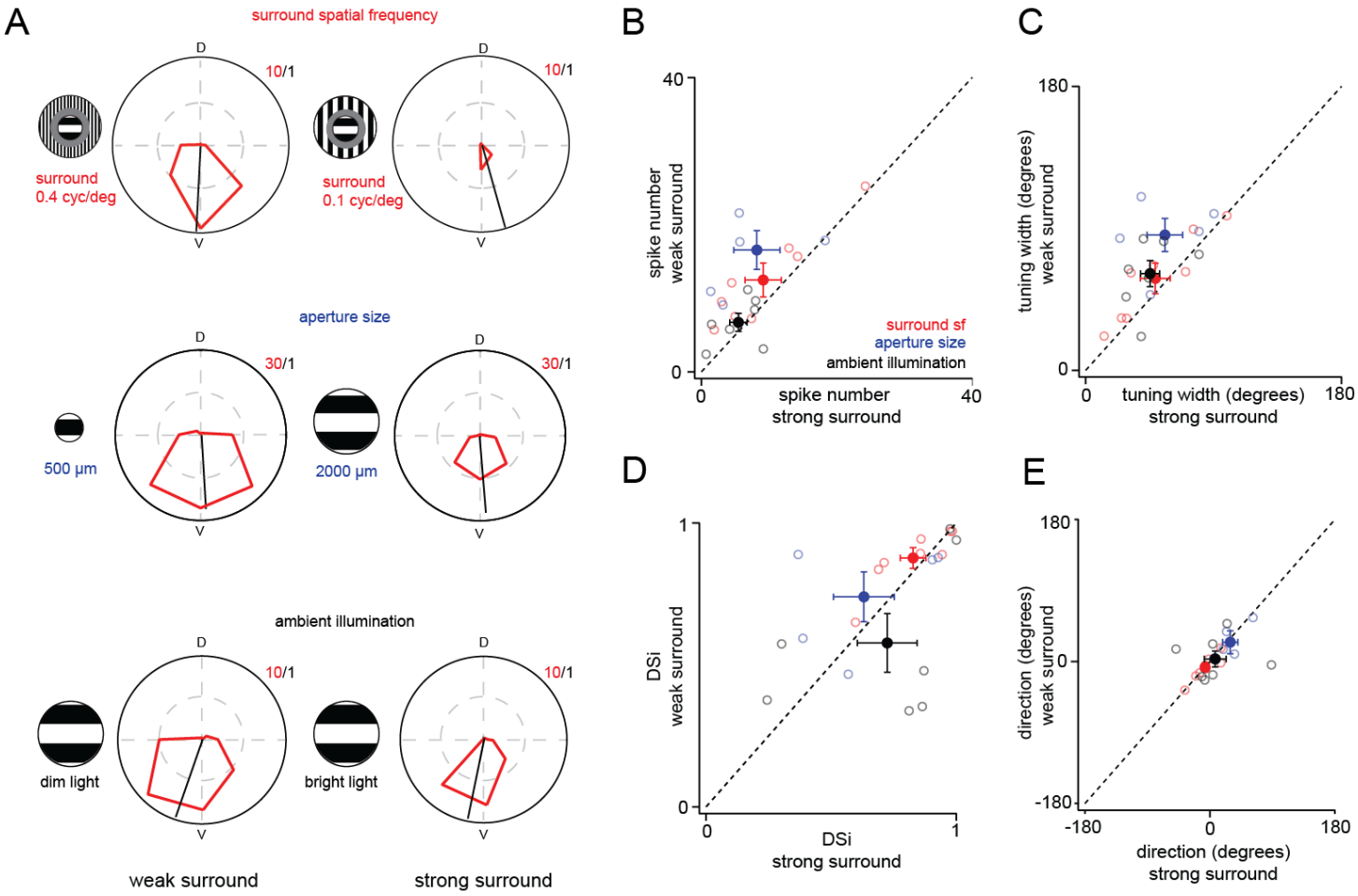

Figure 12: Wide-field inhibition does not change the DSGC's preferred direction but sharpens its directional tuning

A. Polar plots comparing spiking responses in DSGCs (average number of spikes/cycle, red) evoked by centre gratings moving in 8 directions under conditions in which WACs are weakly (*left column*) or strongly activated (*right column*). WAC activity was biased by changing spatial frequency of the surround grating (drifting at 2Hz; *top*), the aperture size (*middle*) or ambient illumination (*bottom*). The black line indicates the direction (derived from the vector sum of responses measured in all directions) and the magnitude of DSi (0 to 1). Dorsal (D) and ventral (V) poles of the retina are indicated. For clarity, illustrations of stimuli are not drawn to scale.

B. The magnitude of the preferred direction response (average number of spikes/cycle) of single cells evoked while weakly or strongly stimulating the surround are plotted against each other (conditions as shown in **A**; filled markers represent mean, open markers represent individual cells; n = 8 for changing surround spatial frequency, n = 5 for changing aperture size, and n = 7 for changing background illumination; $p < 0.05$ for all conditions).

C. The widths of the directional tuning curves (estimated by a Gaussian fit) for each cell measured under weak and strong surround stimulation conditions are plotted against each other (similar conditions and n-values as in **B**; $p \leq 0.05$ for all conditions).

D. The DSi measured in individual DSGCs under weak and strong surround conditions are plotted against each other (similar conditions and n-values as in **B**; $p > 0.1$ for all conditions).

E. Plotting the angle of the preferred direction measured in individual cells under conditions of weak and strong surround stimulation against each other reveals no change in directional preference ($p > 0.1$ for all conditions).

3.5 WACs control spatial but not temporal tuning of the DS circuit

While the data so far clearly indicate a role for wide-field inhibition in shaping the spatial selectivity of DSGCs, it does not address whether such preferences depend on the temporal frequency of the stimulus, as often is the case for other types of ganglion cells (Frishman et al., 1987). Furthermore, optomotor behaviours that rely on directional signals from the retina exhibit distinct transitions in their spatiotemporal tuning properties during changes in ambient light conditions (Umino et al., 2008; Figure 13A,B; also see Discussion). Thus, I next examined the spatial tuning of DSGCs at various temporal

frequencies in both dim and bright light conditions. If responses were temporally tuned, it would be expected that the responses would align with the temporal frequency axis (with a maximum at the ideal temporal frequency) and be invariant with the spatial frequency axis (Figure 13A) when temporal frequency is plotted as a function of spatial frequency. Alternatively, if responses were tuned to velocity, then the temporal and spatial aspects would be inseparable and the responses would align with the diagonal axis between both spatial and temporal frequencies (Figure 13B).

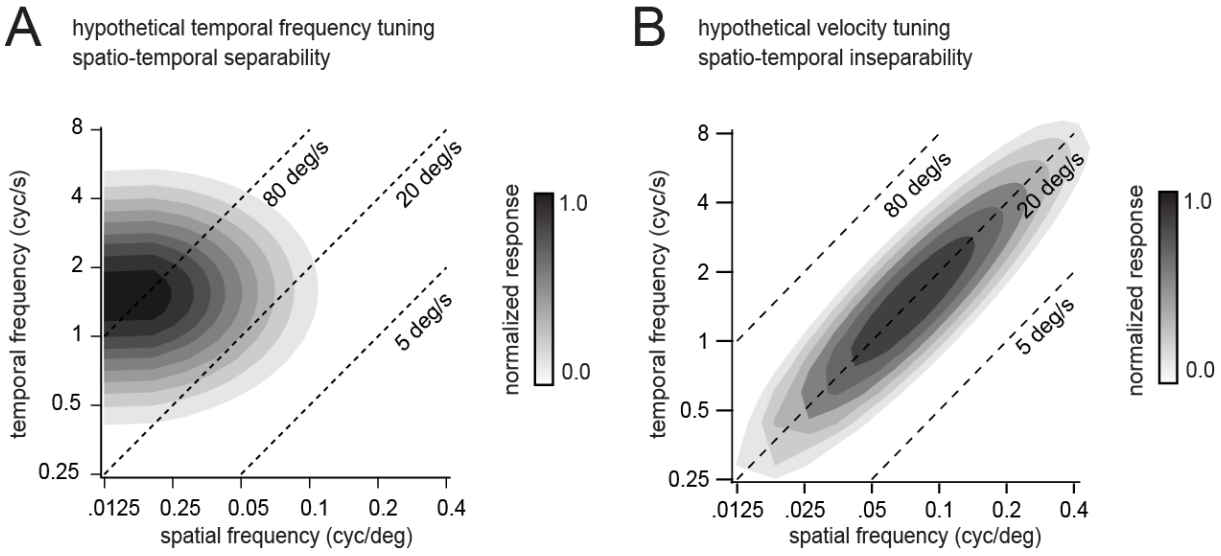

Figure 13: Hypothetical tuning curves demonstrating spatiotemporal separability

A. A hypothetical contour plot showing maximum responses evoked by sine wave gratings of varying spatial and temporal frequencies. As the preferred spatial frequency is similar at each temporal frequency, responses are considered "separable" with a velocity tuning index (VTi) equal to 0.

B. A hypothetical contour plot depicting an alternative scenario in which preferred spatial frequency is dependent on temporal frequency in such a way that the maximal responses fall on the diagonal or velocity axis (dotted lines indicate different velocities). Here the responses are considered "inseparable" in a way that represents speed tuning (VTi = 1). Note: The spatiotemporal tuning of optomotor responses measured in mouse are temporally tuned under dim light conditions but speed tuned (inseparable) under bright light conditions (Umino et al., 2008).

Under dim light conditions ($<10^{-1}$ R*/s) I found that the DSGC's spiking responses remained poorly spatially tuned at all temporal frequencies tested (Figure 14A). Thus, spatiotemporal frequencies that evoked maximal responses were orientated along the temporal frequency axis. Under brighter ambient illumination ($>10^{1}$ R*/s), DSGCs showed a shift in spatial tuning (Figure 14B) consistent with the idea that WACs become functional at these ambient light levels. However, only a marginal change in temporal frequency preference was observed, suggesting that WACs do not modulate temporal tuning of the DS circuit (Figure 14C,D). Moreover, the broad temporal tuning (with peak ~1-2 Hz; Figure 14D) suggests that responses were primarily mediated by rod photoreceptors in both dim and bright experimental conditions (Wang et al., 2011). Thus, over a small range of ambient light levels (10^{-1} - 10^{1} R*/s), the DSGCs spatiotemporal profile switches from being temporally tuned, to being tuned to both the spatial and temporal frequency components of the stimulus (Figure 14A, B). Response attenuation to large bars is therefore only present in bright light, and is not dependent on the temporal frequency in any light condition.

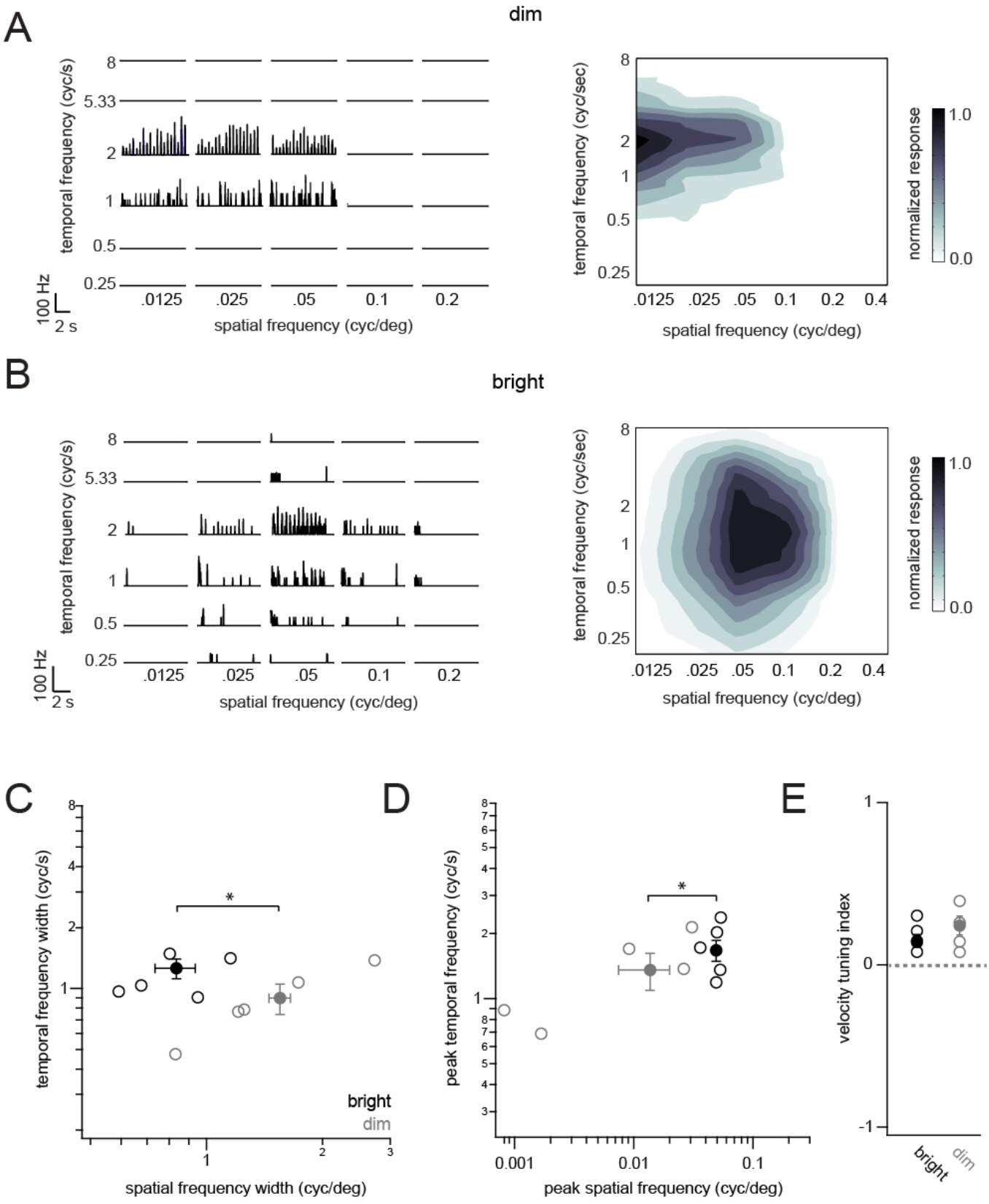
A
dim
temporal frequency (cyc/s)
8
5.33
2
1
0.5
0.25
100 Hz
2 s
.0125
.025
.05
0.1
0.2
spatial frequency (cyc/deg)
temporal frequency (cyc/sec)
0.4
normalized response
1.0
0.0
B
bright
C
D
E
temporal frequency width (cyc/s)
spatial frequency width (cyc/deg)
peak temporal frequency (cyc/s)
peak spatial frequency (cyc/deg)
0.001
0.01
velocity tuning index
-1
*

Figure 14: Spatiotemporal tuning properties of DSGCs are modified by ambient light level

A. Example recordings illustrating DSGC's preferred direction spiking responses evoked by stimuli of different spatiotemporal frequencies (as indicated), measured under dim light conditions. Contour plot illustrating the normalized steady-state response evoked by gratings of 6 spatial and 16 temporal frequencies

B. Example recordings and contour plots illustrating tuning for spiking responses measured in a DSGC evoked by gratings moving in the DSGC's preferred direction (as in **A**) measured under bright light conditions.

C. The spatial and temporal frequency tuning widths (estimated with a 2-D Gaussian function) are plotted against each other for different conditions shown in **A** and **B**. (Bright light conditions, black symbols; n = 6; dim light conditions, gray symbols; n = 4). Open symbols represent individual cells, filled symbols represent averages (* indicate $p < 0.05$ in comparison to light adapted conditions).

D. The preferred spatial frequency is plotted against preferred temporal frequency for each cell, measured under different conditions as in **C**.

E. The velocity tuning index (see Methods) was computed for bright and dim conditions. See also Supplementary Figure 3E for a more detailed statistical analysis showing the lack of velocity tuning of DSGC responses.

Further statistical analysis of the data confirmed the lack of dependence between spatial and temporal tuning giving rise to a velocity tuning index (VTi; see Methods) that was near zero for both dim and light conditions (Figure 14E). The separable spatiotemporal tuning described here for mouse DSGCs are comparable to tuning of rabbit DSGCs (He and Levick, 2000, Grzywacz and Amthor, 2007) and along with the separability of other stimulus dimensions (e.g. contrast; Nowak et al., 2011), is likely to facilitate the decoding of directional and non-directional signals by higher visual centers (van Hateren, 1990). To more carefully ascertain the lack of dependence between spatial and temporal frequency tuning I compared the goodness of 2D Gaussian fits of the data in which the co-efficient of correlation parameter between spatial tuning and temporal

tuning was free to vary (see Methods), or held fixed at zero (Perrone and Thiele, 2001), and found that there was no significant change in the goodness of fit between fitting strategies ($p = 0.2$; paired t-test, Figure 15C). This relatively liberal assessment (Priebe et al., 2003) indicated that spatial and temporal tuning was separable in both dim and bright conditions. The velocity tuning index (VTi; see Methods) derived from these measurements was near zero for both dim and light conditions. Thus, these statistics confirm spatial and temporal tuning are separable in DSGCs in both dim and bright conditions.

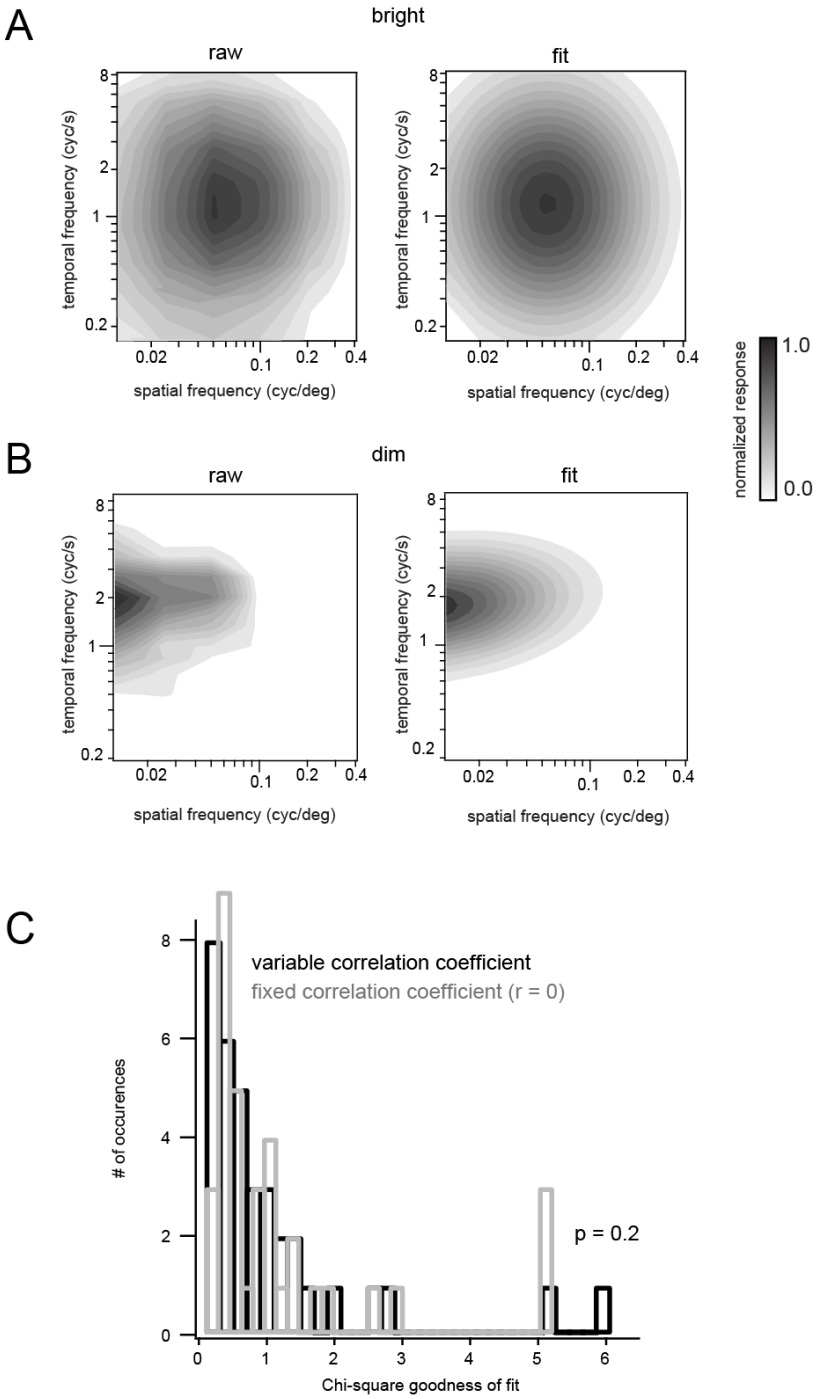

Figure 15 Spiking profiles of DSGCs exhibit spatiotemporal separability

A. Contour plots representing raw data (*left*) and 2D Gaussian fits of data (*right*) obtained from spiking responses of a DSGC responding to varying spatial and temporal frequencies in bright conditions.

B. Similar to C, but responses were measured under dim background conditions.

C. Histogram displaying the goodness of fit for 2D Gaussian fits of spatiotemporal tuning profiles. Black bars represent the Chi-square values for fits in which the co-efficient of correlation between spatial and temporal frequency was free to vary, while gray bars represent fits in which this parameter was fixed to zero. The average Chi-square values were 1.04 ± 0.22 with a variable correlation coefficient and 1.19 ± 0.23 with a fixed value (n = 35), and were not statistically different, indicating no relationship between spatial frequency and temporal frequency tuning (i.e. responses were not speed tuned).

To understand the biophysical basis of the spatiotemporal tuning in DSGCs, I next examined the EPSCs (evoked by preferred direction stimuli) and IPSCs (evoked by null direction stimuli; Figure 16A) in response to moving gratings of different temporal or spatial frequencies under different ambient light and pharmacological conditions. When spatiotemporal profiles of DSGCs were measured under dim light conditions, excitatory and inhibitory synaptic responses exhibited a weak spatial selectivity and responses aligned along the temporal frequency axis (Figure 16B), similar to results derived from DSGC spiking. On the other hand, in bright light, synaptic responses became strongly spatially tuned (Figure 16B), but did not exhibit significant alterations of their temporal frequency preferences (Figure 16B,E). Under both conditions synaptic inputs were not velocity tuned (Figure 16F). The finding that the tuning profiles of the synaptic responses were similar to those of the spiking responses (in dim and bright conditions) suggests that spatiotemporal tuning properties of DSGCs are acquired presynaptically. The voltage clamp tuning profiles were acquired after presentation of the stimuli for seven seconds; however the initial transient responses were excluded (Figure 17A-C). When spatiotemporal profiles of excitatory and inhibitory synaptic inputs were measured in the presence of TTX, I found that the band-pass spatial tuning profile evident in bright light levels reverted back to low-pass in the presence of TTX (for both

IPSCs and EPSCs; Figure 16A,C-E). This was also true or when GABA receptor antagonists were applied (EPSCs; Figure17D,E). Interestingly, neither TTX nor GABA receptor antagonists (PTX + TPMPA) had any significant effect on the DSGC's temporal frequency tuning profile (Figure 16D-E). Taken together, these results support the conclusion that WACs strongly contribute to the spatial tuning without significantly altering the temporal frequency profile of the DSGC. The effects of WACs on the spatial coding of DSGCs are summarized in Figure 18, illustrating spatial selectivity changes at the peak temporal frequency only (1-2 cycles/s).

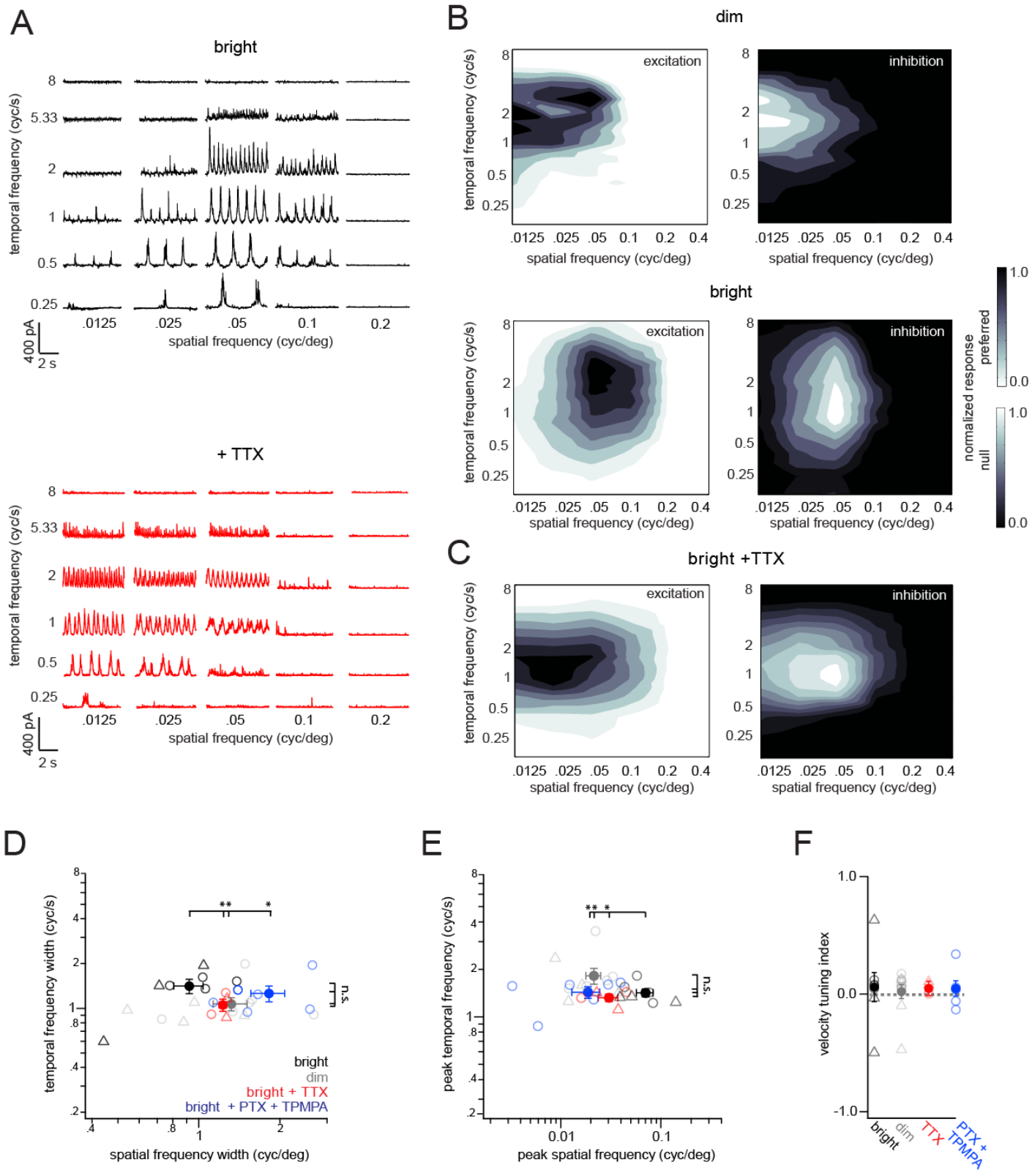

Figure 16: Wide-field amacrine cells confer spatial selectivity to an otherwise temporally tuned DSGC circuit

A. Example recordings illustrating IPSCs (V_{hold} = 0 mV) evoked by stimuli moving in the DSGC's null direction measured under bright conditions in control Ringer's (*top*) or in the added presence of TTX (*bottom*). The spatial and temporal frequencies are indicated. Responses to movement were quantified after the brief onset response to the stimulus presentation.

B. Contour plots illustrating the spatiotemporal tuning profiles of EPSCs and IPSCs in dim (*top*) and bright (*bottom*) ambient light conditions.

C. Blocking voltage-dependent Na^+ channels (1 μM TTX) resulted in the loss of spatial but not temporal tuning of both excitation and inhibition.

D. The spatial and temporal frequency tuning widths (estimated with a 2-D Gaussian function) are plotted against each other for different conditions shown in **B** and **C**. As EPSCs (circles) and IPSCs (triangles) exhibited similar tuning (Supplementary Figure 5) responses were pooled to compare spatiotemporal profiles in different conditions (bright light, black symbols; n = 6; dim light, gray symbols, n = 14; TTX, red symbols; n = 4; PTX+TPMPA, blue symbols, n = 6). Open symbols represent individual cells, filled symbols represent averages (* indicate $p < 0.01$ in comparison to light adapted conditions).

E. The preferred spatial frequency is plotted against preferred temporal frequency for each cell, measured under different conditions as in **D**.

F. The velocity tuning index was computed for conditions in which WAC activity was high (bright light) or low (dim, TTX, PTX).

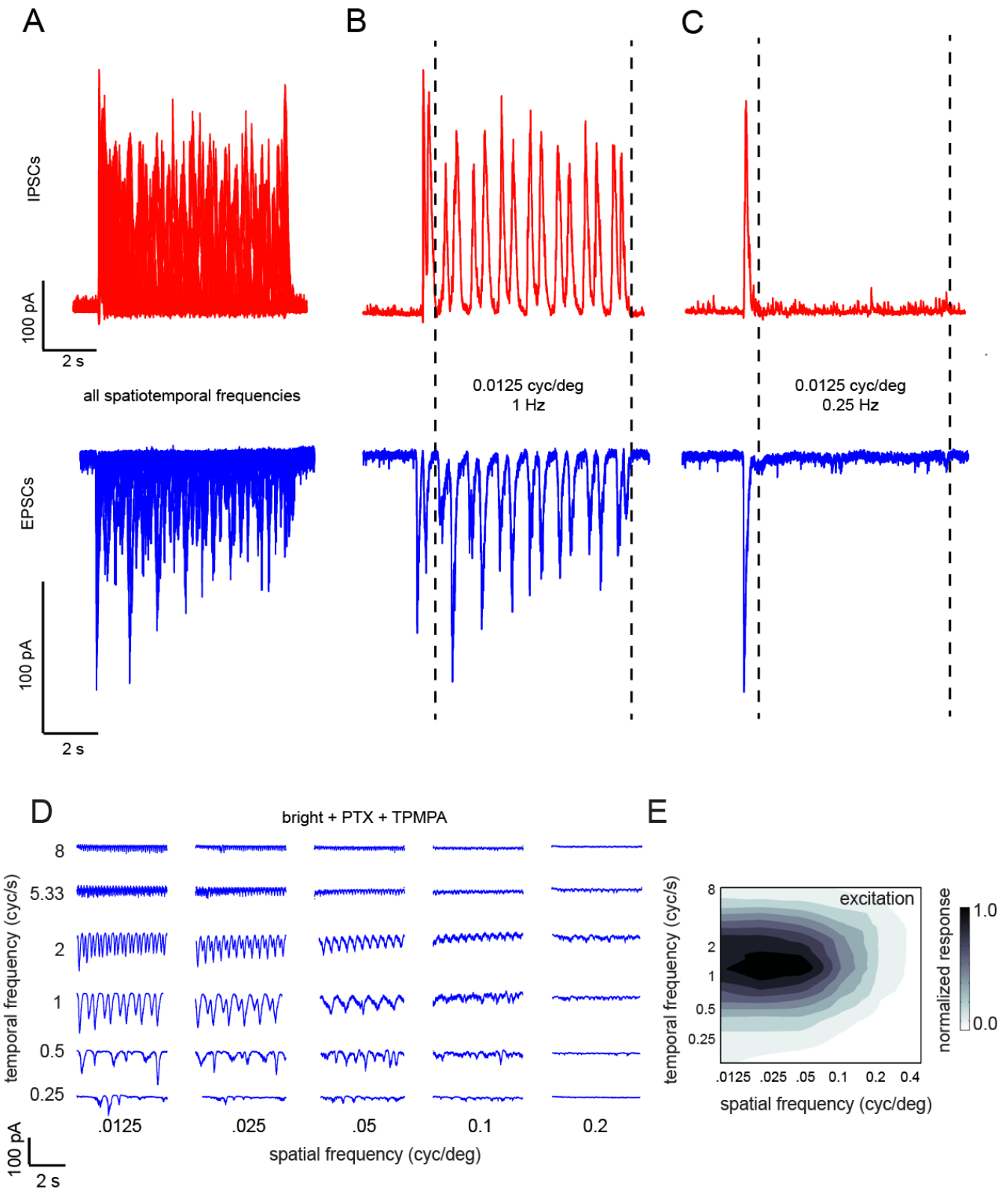
A
B
C
IPSCs
100 pA
2 s
all spatiotemporal frequencies
0.0125 cyc/deg
1 Hz
0.0125 cyc/deg
0.25 Hz
EPSCs
100 pA
2 s
D
bright + PTX + TPMPA
temporal frequency (cyc/s)
8
5.33
2
1
0.5
0.25
.0125
.025
.05
0.1
0.2
spatial frequency (cyc/deg)
100 pA
2 s
E
excitation
temporal frequency (cyc/s)
8
2
1
0.5
0.25
.0125 .025 .05 0.1 0.2 0.4
spatial frequency (cyc/deg)
normalized response
1.0
0.0

Figure 17: Synaptic inhibitory and excitatory responses to drifting sine wave gratings

A. IPSCs (Vhold ~0 mV; *top panels*) and EPSCs (Vhold ~ -60 mV; *bottom panels*) measured in DSGCs in the presence of TTX, evoked by drifting grating of 96 spatiotemporal frequencies are overlaid. The IPSCs were evoked by stimuli moving in the DSGC's null direction while the EPSCs were evoked by stimuli moving in the preferred direction. Each stimulus was presented for 7 seconds (inter-stimulus interval of 7 seconds).

B. Examples of single trial IPSCs and EPSCs evoked at 1Hz drifting grating (0.0125 cyc/deg).

C. Example IPSCs and EPSCs evoked at a non-optimal stimulus frequency. Responses were quantified in the region in between the vertical dashed lines, avoiding the initial transient response.

D. Example recordings illustrating EPSCs in the presence of GABA blockers (PTX+TPMPA), evoked by moving gratings moving in the DSGC's preferred direction at different spatiotemporal frequencies, as indicated.

E. Contour plot illustrating the spatiotemporal tuning profiles of EPSCs in the presence of GABA receptor antagonists (PTX + TPMPA). Note presence of temporal but not spatial tuning.

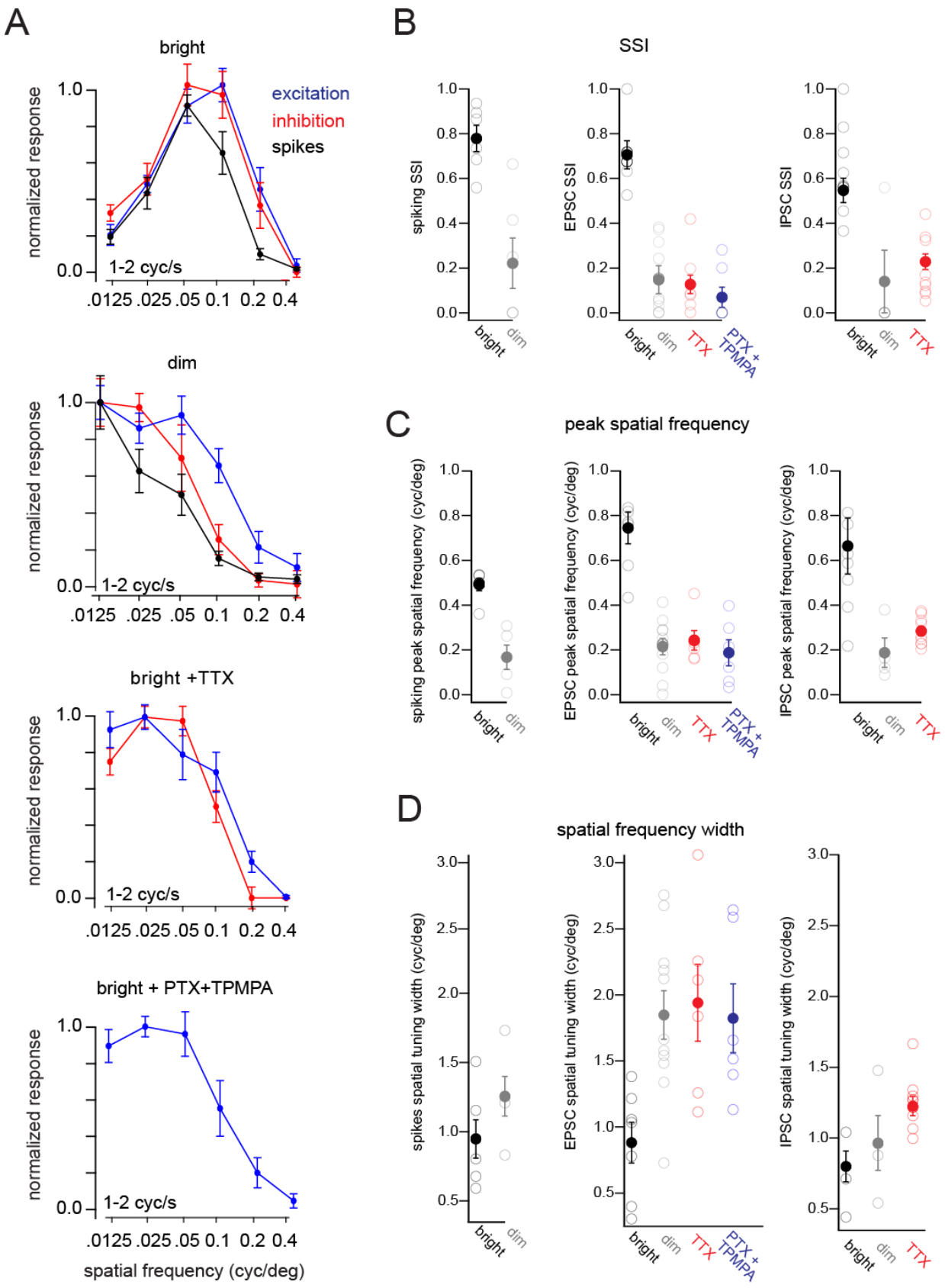
A
bright
normalized response
1.0
0.0
excitation
inhibition
spikes
1-2 cyc/s
.0125 .025 .05 0.1 0.2 0.4
dim
bright +TTX
bright + PTX+TPMPA
spatial frequency (cyc/deg)
B
SSI
spiking SSI
EPSC SSI
IPSC SSI
bright
dim
TTX
PTX + TPMPA
C
peak spatial frequency
spiking peak spatial frequency (cyc/deg)
EPSC peak spatial frequency (cyc/deg)
IPSC peak spatial frequency (cyc/deg)
D
spatial frequency width
spikes spatial tuning width (cyc/deg)
EPSC spatial tuning width (cyc/deg)
IPSC spatial tuning width (cyc/deg)

Figure 18: Wide-field amacrine cells affect DSGCs' spatial selectivity

A. Averaged responses to sine wave gratings of varying spatial frequencies drifting at 1-2 Hz under different conditions (bright, dim, TTX, and PTX+TPMPA conditions).

B. SSI calculated for moving stimuli is shown across conditions for spikes (*left*), excitation (*middle*) and inhibition (*right*); $p < 0.01$ for all comparisons against SSi in light adapted condition. In B-D, open symbols represent individual cells, closed symbols represent the mean response in each condition.

C. Plots of the spatial frequency at which maximal responses are observed; $p < 0.01$ for all comparisons with peak spatial frequency in light adapted condition.

D. The width (standard deviation of a Gaussian fit) of the spatial frequency profile of spiking; $p < 0.1$ for all comparisons with the width measured in light adapted conditions.

Spatiotemporal separability observed in the responses of DSGCs was easily captured in a simplified linear-nonlinear model in which centre excitation and surround inhibition occurred coincidently (Hoggarth et al., 2015), which contrasts with classical linear models in which surround inhibition appears delayed (Enroth-Cugell et al., 1983). We hypothesized that DSGCs exhibit an inhibitory receptive field comprised of nonlinear rectifying subunits (Olveczky et al., 2003, Passaglia et al., 2009, Takeshita and Gollisch, 2014), which produces a tonic inhibition (0 delay), as individual subunits are asynchronously activated by different phases of the grating, as would be expected by a non-linear (extra-classical) surround mechanism (Zaghloul et al., 2007).

To test whether DSGC surround inhibition relies on non-linear subunits, I presented separate gratings to both the center and the surround to measure the spatial preferences of the wide-field inhibition (Figure 19A). Indeed I found that wide-field inhibition is largely independent of spatial frequency presented to the surround, once stimuli were larger than a certain size (bar width of ~75 μm; Figure 17B,C), a characteristic feature of non-linear surround mechanisms (Hochstein and Shapley, 1976a,

Olveczky et al., 2003). Thus, it appears that presynaptic inhibition arising from a non-linear inhibitory receptive field gives rise to separable spatiotemporal tuning of DSGCs.

In summary, I have shown that DSGCs exhibit wide-field inhibition which operates independently from the inhibitory mechanisms driving direction-selectivity. This wide-field inhibition likely arises from a WAC presynaptic to DSGC inputs, allowing DS to remain balanced. Wide-field inhibition is modulated by ambient light, and only 'switches on' above cone threshold, after which it confers the DSGC with spatial selectivity. Finally, I have shown evidence to suggest that WAC dendrites utilize non-linear subunits to drive surround inhibition in DSGCs.

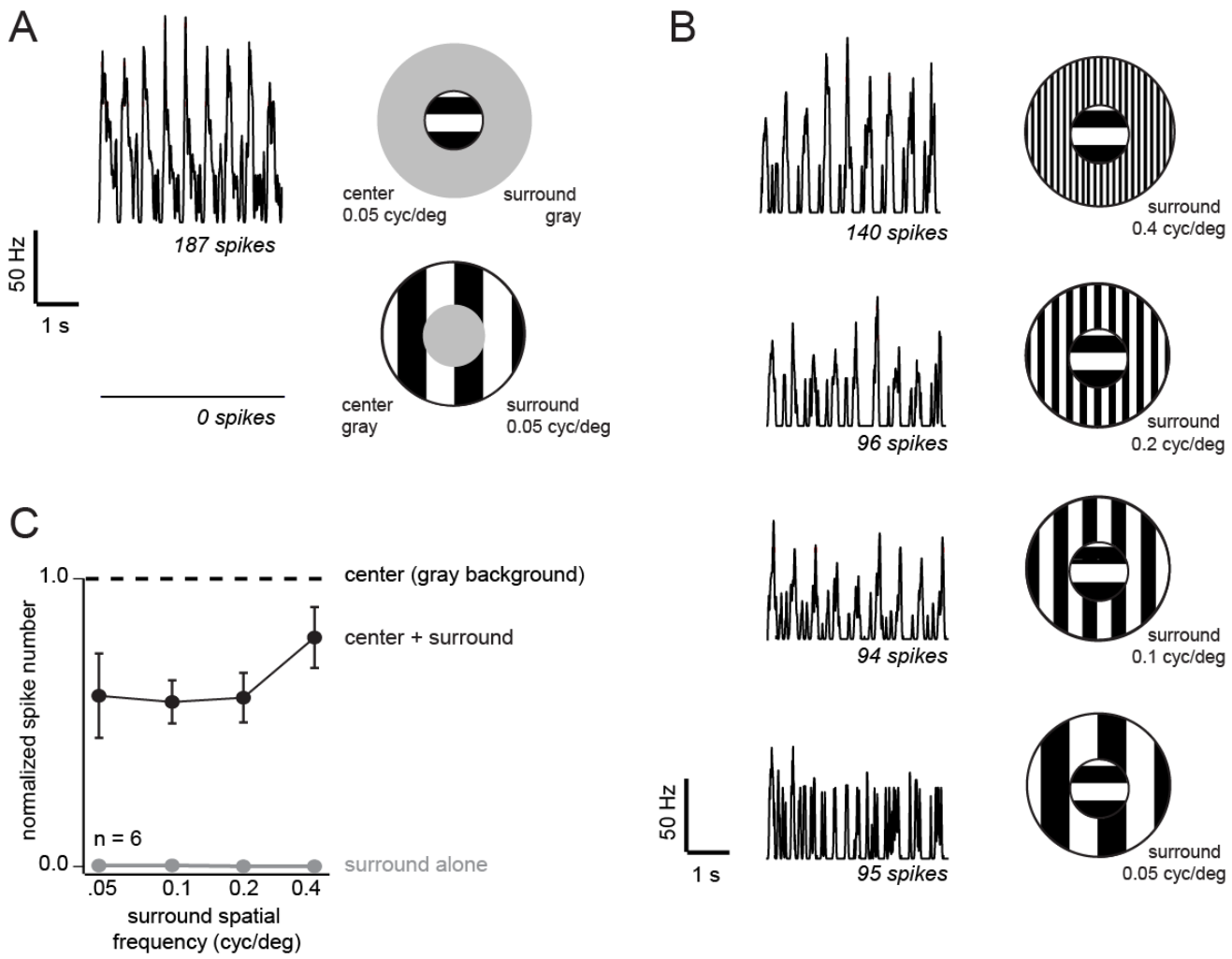

Figure 19: Spatial frequency dependence of wide-field inhibition.

A. Response to a centre grating alone, presented in the DSGC's preferred direction through an aperture (diameter of 500 µm; *top*). Below, response to the annulus alone (outer diameter 2000 µm, inner diameter 500 µm). All gratings were drifting at a temporal frequency of 2 Hz. Only steady-state responses are shown (initial transients were blanked).

B. Surround gratings (drifting at a direction orthogonal to the preferred-null axis) were presented at varying spatial frequencies while the frequency of the center grating was held constant at 0.05 cyc/deg (as in A).

C. A plot of the spiking response as a function of spatial frequency of the surround grating (black; n=6). Responses are normalized within each cell to responses evoked by center gratings presented alone (dotted line; n = 6). The spiking responses to the surround grating presented alone are plotted in gray (n = 6).

4. Discussion

4.1 Multiple Layers of Inhibition in the DS Circuit are Represented by Spiking and Non-spiking Amacrine Cells

The DS circuit in the retina is becoming one of the most well understood neural circuits in the brain, both at the physiological (for review see: Borst and Euler, 2011; Vaney et al., 2012), and anatomical level (Briggman et al., 2011, Helmstaedter et al., 2013, Kim et al., 2014). Work over the last 30 years has firmly established a key role for SACs in driving the directionality of motion detection by the DS circuit but the role for other types of amacrine cells is less well defined. A number of anatomical (Dacheux et al., 2003; Famiglietti, 1983) and physiological (Chiao and Masland, 2003; Fried et al., 2005; Rivlin-Etzion et al., 2012; Stasheff and Masland, 2002) studies have implicated the role for additional amacrine cells in controlling the DS circuit, but the evidence is usually indirect or speculative. Here, I have identified for the first time another major element in the circuit: a spiking GABAergic wide-field amacrine cell. My results demonstrate how WACs interact with known elements of the DS circuitry to provide adaptable spatial selectivity in varying light conditions, further elaborating the functional and anatomical complexity of this circuit.

Multiple layers of inhibition in the DS circuit differ in three major ways. First, wide-field inhibition relies on spiking, while local DS inhibition does not (see TTX application in Figures 6,11,16). Secondly, wide-field inhibition is directed presynaptically, while DS inhibition is directed postsynaptically (acting directly on the ganglion cell, see diagram Figure 8A). Third, wide-field inhibition can actively alter its level of activity based on background light levels, while DS inhibition remains constant

(Figure 6,7,12; further discussed in section 4.2). This discussion will address each of these differences and the potential benefits for DS coding in the retina.

I have shown a role for a spiking amacrine cell that controls spatial tuning of the DS circuit and is regulated by ambient light levels to relieve inhibitory control of spatial tuning during adaptation to dark conditions. That a spiking cell would be the target of regulation is somewhat unsurprising. Spiking activity is a popular target for circuit modulation – including spiking dendrites in the hippocampus during induction of brain waves (Chiovini et al., 2014) and regulation of spike bursts and frequency in the thalamus (Deschenes et al., 1984). The activation/inactivation of spiking activity can be a selective switch target, and either depolarization (leading to sodium channel inactivation) or hyperpolarization (leading to a failure to reach spike threshold) can drive a neuron away from a spiking modality into a separate integration mode. Further, these modifications are specific to spiking cells, and non-spiking cells such as the starburst amacrine cell would be insensitive to global adaptational strategies which target spiking cells. By combining the inhibitory influences of both spiking and non-spiking amacrine cells (WACs and SACs, respectively), the DS circuit can selectively adapt specific properties (ie spatial tuning) to ambient light. Evidence that wide-field inhibition is mediated by spiking GABAergic WACs largely relies on pharmacology, particularly on the effects of TTX. Thus I considered carefully where TTX could be acting in the DS circuit. SACs express predominantly TTX-insensitive Na^+ channels (Oesch and Taylor, 2010), excluding them as a target for TTX. On average, I did observe a mild decrease in excitation/inhibition evoked by small spots in the presence of TTX, which could be due to an effect on spiking AII amacrine cells, bipolar cells which express TTX-sensitive Na^+ channels (Cui and

Pan, 2008), and/or non-canonical excitatory amacrine cells which have been recently shown to contact DSGCs (Lee et al., 2014) and express TTX-sensitive Na^+ channels (Grimes et al., 2011). However, the most striking effect was that TTX increased the amplitude of both EPSCs and IPSCs evoked by large spots (400-1000 μm, Figure 8C) clearly indicating a presynaptic inhibitory mechanism that relies on spiking. Thus, the most likely candidates for mediating TTX-dependent wide-field inhibition are spiking WACs (Cook and McReynolds, 1998, Demb et al., 1999, Taylor, 1999, Zaghloul et al., 2007, Zhang et al., 2012, Farrow et al., 2013, Protti et al., 2014, Venkataramani et al., 2014). This may be directly tested in the future, potentially using experiments which exclusively activate WACs optogenetically via channelrhodopsin.

Given that DSGCs critically rely on the balance of inhibition and excitation to compute direction, it could be expected that the DS inhibition provided by SACs would be unaffected by ambient light, if consistent representation of directional information is prioritized by the retina. By the same rationale, the involvement of WACs in the DS circuit was surprising, as having an additional source of GABAergic innervation that varies with ambient light might be expected to interfere with the DSGC's computational abilities. However, I have shown that this conundrum is easily solved by having wide-field inhibition selectively modulate local synaptic inputs to DSGCs (presynaptically), rather than providing both pre- and post-synaptic inhibition, as is observed for many other types of ganglion cells (Cook and McReynolds, 1998, Demb et al., 1999, Taylor, 1999, Zaghloul et al., 2007, Zhang et al., 2012, Farrow et al., 2013, Protti et al., 2014). The separation of inhibition into pre- and post- synaptic modalities allows for inhibitory computations that can be mutually exclusive and act without interference.

Three lines of evidence point to the bipolar cell terminals as being the main presynaptic targets for WAC inhibition. First, TTX-sensitive surround inhibition was observed in the presence of cholinergic receptor antagonists (data not shown), excluding potential inhibition directed to the excitatory contributions from SACs. Second, bipolar cell mediated EPSCs measured in voltage-clamped SACs also exhibit a TTX-sensitive surround, further demonstrating that bipolar cell excitation is under WAC inhibitory control. Third, we did not find physiological (Figure 11) or anatomical (see electron microscopy data in Figure 8 of Hoggarth et al., 2015) evidence for a direct WAC inhibition to SACs. Taken together, the results suggest that the major actions of WACs are mediated on the bipolar cell terminals. This contrasts with SAC-mediated inhibition which is expressed postsynaptically (Yonehara et al., 2013, Chen et al., 2014, Park et al., 2014).

The finding that surround inhibition is directed presynaptically does not directly implicate WACs in mediating this inhibition. Alternatively, if horizontal cells were inhibiting bipolar cell responses but acting in the outer retina, the suppression of EPSCs and IPSCs I observed in control conditions (Figure 8C) would still be expected. In other types of ganglion cells, previous studies have shown that TTX does not completely block surround inhibition, suggesting an additional role for the non-spiking horizontal cells in mediating surround inhibition (Cook and McReynolds, 1998, Taylor, 1999, Demb et al., 2001, McMahon et al., 2004, Protti et al., 2014, Venkataramani et al., 2014). The near complete block of surround inhibition by TTX observed even for large stimuli was somewhat surprising, given that the modulation of horizontal cell membrane potential has previously been show to strongly influences DSGC activity (Mangel, 1991) and would

have been expected to participate in surround inhibition. However, several factors may have masked horizontal cell mediated surround inhibition in my experiments. These include circuit nonlinearities in the inner retina such as a spike in the bipolar cell terminal (Baden et al., 2013) or the fact that horizontal cell feedback is so strong that it reverses the polarity of the responses (Szikra et al., 2014), which would be difficult to detect in the ON-OFF DSGC. It is also possible that horizontal cell feedback is more important for shaping the ganglion cell responses in the temporal domain under extremely high photopic conditions (Pandarinath et al., 2010), which I have not specifically tested here (background light levels were chosen to straddle to photopic-scotopic range to accentuate the switching phenomenon). Also, it has been shown that horizontal cell GABA release may be impaired in standard recording conditions (Deniz et al., 2011). Thus, while I have revealed a clear role for WACs in spatial processing in the DS circuit, the specific role of horizontal cells remains to be evaluated. The evidence presented in this thesis however lends to the contribution of a wide-field amacrine cell in mediated presynaptic inhibition.

4.2 WACs and SACs are differentially modulated by ambient light

How are WACs and SACs differentially modulated by light? Since DSGCs and SACs respond robustly under dim conditions, it was surprising that WACs were non-functional under the same experimental conditions. As WACs contacting the DS circuit may receive inputs from a different set of bipolar cells than DSGCs (their small, dendrite-like processes do not co-stratify with SACs and DSGCs; Badea and Nathans, 2004, Lin and Masland, 2006), it is possible that under dim light conditions they receive relatively weaker excitation that fails to bring them to spike threshold. Indeed, other retinal circuits including those driving the ON alpha ganglion cells exhibit a dramatic increase in

excitation over this critical range of intensities (Farrow et al., 2013, Grimes et al., 2014). However, changes in the strength of excitatory input cannot completely account for the current phenomenon. Under bright conditions, weaker responses evoked by low contrast stimuli were still associated with an equally strong surround (Farrow et al., 2013, Hoggarth et al., 2015). These results indicate that critical ambient light-induced changes lead to differences in the excitation – inhibition or input – output function of the WACs, rather than solely from changes in excitation strength.

The precise physiological mechanisms driving differential activity in different light conditions is a major question in the field of retinal neurophysiology (Demb and Singer, 2015). The mechanism by which WACs are driven to inactivation in dim light conditions remains unanswered. However, recent studies implicate multiple mechanisms which may result in shifting WACs into a non-linear state (Farrow et al., 2013, Grimes et al., 2014). Under bright light, response kinetics accelerates making conditions more favourable for spike generation. Moreover, recently it has been shown that in the dark, ON cone bipolar cells release glutamate tonically, which is likely to keep amacrine cells in a depolarized state, which may drive Na^+ channels into inactivation (Grimes et al., 2014). In bright light however the resting membrane potential of cone bipolar cells is hyperpolarized, which may lead to de-inactivation allowing for Na^+ channels to resume driving spiking activity. Furthermore, light-dependent changes in gap junction coupling between ganglion and amacrine cells (Hu et al., 2010) as well as between amacrine and bipolar cells (Farrow et al., 2013), has also been hypothesized to play a role in switching WACs into an inactive state. Changes in coupling have been previously shown to drive circuits to switch from one state to another in the visual system (Dedek et al., 2008,

Pandarinath et al., 2010). Future investigations into which of these processes are specifically manipulated across light conditions will confirm the factors underlying the emergence of WAC dependent long-range inhibition.

4.3 Wiring specificity of multiple amacrine cells in the DS circuit

Anatomical evidence for presynaptic modulation of release from ON bipolar cell terminals driving DSGCs has been previously documented (Dacheux et al., 2003, Famiglietti, 2005). However, recent studies using optical approaches to directly probe synaptic activity at bipolar cell terminals (Yonehara et al., 2013, Park et al., 2014) indicated the absence of directional inhibition at bipolar cell terminals and suggested that SACs act exclusively on DSGC dendrites. Here using large static or moving stimuli I have clearly revealed a role for presynaptic inhibition (Figure 8,14). The observed decrease in excitation cannot be explained by increases in inhibition onto DSGCs, as wide-field inhibition reduces both the inhibitory and excitatory currents to DSGCs in parallel. Additionally, a recent study found light-evoked Ca^{2+} responses in terminals of bipolar cells which co-stratified with SACs were diminished as the size of the stimuli was increased (Chen et al., 2014), consistent with WAC inhibition. A demonstration of a second major source of inhibition to the DS circuit prompts a careful consideration of WAC-mediated inhibition when presynaptic mechanisms of inhibition in the DS circuit are being evaluated. Therefore, it is an important goal to determine where the WAC synapses are formed in the DS circuit and how this wiring specificity influences the responses of both SACs and DSGCs.

The first clues that SACs mediate local DS inhibition came from anatomical studies showing that SAC dendrites co-stratify with those of DSGCs (Famiglietti, 1983).

WACs are the lead candidates for mediating TTX sensitive wide-field inhibition to ganglion cells (Volgyi et al., 2001, Baccus et al., 2008, Zhang et al., 2012, Farrow et al., 2013), but previously anatomical evidence that WACs co-stratify with the DS circuit was absent. WACs span large areas of the retina and send their processes to distinct strata within the inner-plexiform layer (Badea and Nathans, 2004; Lin and Masland, 2006; Pérez De Sevilla Müller et al., 2007). While this class of amacrine cells has been anatomically well described and is known to consist of at least 16 subtypes, whether any of these known types have been described here physiologically is not clear.

Delineating the specific connectivity between WACs and particular subtypes of bipolar cells remains a challenge. I have demonstrated that inhibition arises at the level of the bipolar cell terminals contacting ON and OFF SACs and DSGCs. The finding that the variance of the inhibitory and excitatory currents measured near simultaneously (presumably arising largely from incident bipolar cell and SAC input) was strongly correlated, suggesting a common origin. Whether this corresponds to a single WAC contacting overlapping sets of bipolar cell subtypes subserving SACs and DSGCs (Helmstaedter et al., 2013), or whether WACs contact a single type of bipolar cell that provides common input to SACs and DSGCs, could not be unambigously distinguished. Together with previous anatomical characterization (Briggman et al., 2011), current anatomical work additionally provides evidence for WACs forming synapses exclusively on the bipolar cell terminals presynaptic to DSGCs (Hoggarth et al., 2015).

.

4.4 On plasticity and adaptation of direction coding in the face of changing illumination and decreased inhibition

This thesis work represents the second recent study outlining the potential ways in which activity in the DS circuit may be modified as an adaptive response to the persistent characteristics of light stimulation. The first example of activity-dependent changes in DSGCs' responses was a recent study in which constant activation of DSGCs via prolonged exposure to moving stimuli could temporarily reverse their observed direction preference in certain experimental conditions (Rivlin-Etzion et al., 2012, Vlasits et al., 2014). While short term plasticity has been observed at bipolar cell terminals (Vickers et al., 2012), the output of ganglion cells is thought to be constant, reliably translating visual stimuli into neural impulses (However, see Vlasits et al., 2014). The computational benefit of altering the preferred direction of the DSGC remains unknown. Therefore, this thesis work represents the only findings to date in which changes in the DS circuit in response to the environment serves a clear beneficial role.

Selectively decreasing wide-field inhibition either pharmacologically or by decreasing ambient light levels did not change the directional preferences of DSGCs, but resulted in a loss in their spatial selectivity with little effect on their temporal frequency tuning. Thus, spatial tuning seems to be an additional feature of the DS circuit that is encoded independently of direction. The benefits of a mechanism by which direction and size coding are independently processed at distinct synaptic loci are clear. Under low light conditions where photons are limited, retinal circuits are required to pool light information from wide areas in order to detect weak signals. In these regimes, inhibitory suppressive mechanisms could degrade signals. To avoid this, retinal circuits functionally

re-wire to decrease inhibition. However, while reducing inhibition, directional selectivity must be maintained under low light as it is likely a key feature important for survival. Thus, SAC function is maintained across all conditions. On the other hand, in bright conditions, surround inhibition serves to reduce intrinsic noise and spatial redundancy (Barlow, 1961). The differential regulation of WAC and SAC output by ambient light, along with the specific wiring of WACs to presynaptic bipolar cell terminals, allows the DS circuit to operate across a wide range of light intensities, changing the circuit's size selectivity while remaining in a balanced state for optimum DS function (Cafaro and Rieke, 2010).

4.5 The role of wide-field amacrine cells in coding other visual stimuli

The presence of WACs in the DS circuit may in the future be used as rationale to assign alternate coding abilities common in circuits containing WACs to DSGCs. While here I have demonstrated a role for WACs on the spatial tuning of DSGCs, this does not fully encompass the role of WAC to bipolar cell inhibition across the retina, or even likely within the DS circuit. However, in this section I will argue that two commonly attributed roles of WACs, namely object motion sensitivity and orientation selectivity, are likely not present in mouse DSGCs studied here.

WACs have previously been shown to be important for conveying object motion sensitivity (OMS), in which subtypes of ganglion cells (which in rabbit retina include ON and OFF type brisk-transient GCs, local edge detector cells, and ON-OFF DSGCs) are sensitive only to motion within their receptive field center when that motion is discontinuous with the motion present in the surround (Olveczky et al., 2003, Baccus et al., 2008). This response type is often used to describe sensitivity to motion of objects

which move through a ganglion cell's receptive field, but not motion of the entire visual scene, such as that present during head or eye movements. OMS has been proposed to serve an important role for selective feature detection, which has a behaviourally relevant role and is theoretically used for detecting predators (Zhang et al., 2012). The WAC inputs to the DS circuit share many features with known OMS neural machinery (Olveczky et al., 2003). Additionally, the observation that wide-field inhibition acts independently of spatial frequency (Figure 19) would predict that any motion in the surround would supress responses in the center, consistent with OMS (Olveczky et al., 2003, Baccus et al., 2008). In addition, retinal circuits which drive OMS have been shown to rely on presynaptic inhibition (Baccus et al., 2008). I also found that surround suppression acted independently of direction, as in OMS detection (Baccus et al., 2008). However, many observations contradict expectations from OMS behaviour and I found numerous discrepancies from the predications of an OMS surround. First, I found that DSGCs strongly responded to continuous motion which spanned the entire retina (presented through a 2000 μm annulus, similar in size to the area of retina exposed to light, see Methods) at specific spatial and temporal frequencies (Figure 14, 16). This directly contradicts the expectation that an OMS cell would be insensitive to global motion. Second, while the surround responses here were found to not depend on the spatial frequency of the stimulus presented to the surround (Figure 19), Chiao and Masland (2003) found that surround inhibition in DSGCs is highly dependent on the spatial phase difference between the object and the surround. Even when object and background are moving coherently but are out of phase, inhibition is reduced. Thus, depending on the context of the stimulus, the DSGC may or may not respond to global

motion. However, since the stimulus presented to the center was presented through a 500 µm annulus in my experiments (Figure 19), the spatial dependence of the surround may have been occluded (Chiao and Masland, 2003). Third, the absence of temporal frequency dependence on wide-field inhibition (Figure 14; see Model predictions in Hoggarth et al 2015) predicts a suppressive phenomenon which acts without delay, in contrast with the brief delays which permit OMS coding (Olveczky et al., 2003, Baccus et al., 2008). Fourth, OMS depends on excitation and inhibition being temporally uncoupled (Baccus et al., 2008). In the DS circuit, excitation and inhibition can arrive locally from a common source – cholinergic excitation and GABAergic inhibition from SACs. Therefore, it is unlikely that excitation and inhibition would display the temporal characteristics required for OMS. Finally, since both OMS and spatial selectivity rely on spiking wide-field amacrine cells, which are modulated by background light conditions, it would be predicted that OMS characteristics would also depend on background light, which has not been observed. OMS, similar to DS, would likely be critical for survival and would serve the animal best to be conserved across light levels (Zhang et al., 2012). Future experiments may explore the light sensitivity of OMS behaviours to test if the subserving WACs in OMS circuits switch based on background light. However, based on the available evidence, the mouse DS circuit with light-sensitive, WAC-driven spatial selectivity does not demonstrate OMS behaviour.

WACs have recently been shown to contribute to orientation selectivity (OS) in the retina (Murphy-Baum and Taylor, 2015). OS describes the selectivity of visual neurons to the angle of an edge in the visual field .OS has classically been attributed to the convergence of multiple center-surround ganglion cell receptive fields downstream of

the retina in higher visual centers, in the Nobel Prize winning work of Hubel and Wiesel (1962). However, more recently, a secondary mechanism for OS originating in the retina has been described (Murphy-Baum and Taylor, 2015, Nath and Schwartz, 2016, Venkataramani and Taylor, 2016). The basis of OS in the retina relies on inhibition from WACs, which are preferentially stimulated by specific orientations of light in their receptive fields, which are closely matched by their dendritic fields. WACs have long processes which extend millimetres on the retina (see Discussion section 4.3). A narrow bar stimuli therefore would maximally recruit a specific WAC dendrite when in the appropriate orientation (Murphy-Baum and Taylor, 2015). Non-branching WAC processes presynaptic to the DS circuit appear to be suited to similar OS characteristics (Hoggarth et al., 2015). However, a recent study has shown that DSGCs are not also OS (Nath and Schwartz, 2016). This may be explained by summation of signals from many individual WAC dendrites prior to being passed to bipolar cells, either through gap junction coupling (Volgyi et al., 2001) or active signal conduction within a single WAC combining input from separate neurites. Alternatively, multiple different individual OS inputs may be combined postsynaptically in the DSGC, effectively cancelling OS. This would predict that individual synaptic inputs may have OS characteristics, which could be tested using functional imaging in a future study. Finally, while OS (when measured in V1) was found to be conserved across ambient light conditions (Duffy and Hubel, 2007), it is unknown whether OS originating in the retina would show similar properties.

While this study has shown a role of WACs in the DS circuit, for the reasons outlined above this likely does not lead to either OMS or OS responses. However, surround inhibition from WACs may contribute to other visual coding properties, which

have not yet been tested. The presence of multiple inhibitory interneurons in the DS circuit should be considered in future studies, and may lead to additional roles not described here, especially using novel stimuli (Roska and Werblin, 2003).

4.6 Relating DS circuit properties to behaviour

Recent anatomical studies indicate that in addition to the visual forming areas in the brain, ON-OFF DSGCs (studied here) also project to the accessory optic system (AOS) (Kay et al., 2011, Dhande et al., 2013), where together with ON DSGCs they help drive optomotor behaviours (Oyster et al., 1980, Yonehara et al., 2009). Interestingly, under dim conditions, optomotor behaviours have been shown to be tuned to temporal frequency of moving stimuli in the dark (Umino et al., 2008), similar to the findings here of ON-OFF DSGCs. However, under bright conditions, optomotor responses change to preferring speed (Umino et al., 2008), while the responses of DSGCs change to preferring spatial and temporal frequency independently (Figure 16). This mismatch between DSGC response properties and observed behaviour suggests that speed tuning arises in higher visual centres by combining inputs from individual units (potentially ON and ON-OFF types of DSGCs) that are not speed tuned themselves but exhibit distinct spatiotemporal tuning properties (Simoncelli and Heeger, 1998, 2001), possibly in a manner analogous to a model for orientation tuning in VI, where orientation selective receptive fields of simple and complex cells are derived from combinations of non-orientation selective center-surround receptive fields of ganglion cells (Hubel and Wiesel, 1962). Whether the switching phenomena of speed tuning in visual behaviours driven by DSGCs are derived

from the switching phenomenon of WACs providing inhibition to DSGCs in the retina is a potential topic of future study.

4.8 Conclusion

I have shown that changing ambient light levels leads to the recruitment of additional neural elements (spiking WACs) that endow the mammalian retinal direction coding circuit with extra computational abilities, specifically spatial selectivity. Furthermore, I have also shown how the distinct physiological properties of the SACs and WACs underlying the extraction of each feature allows the DS circuit to operate in different modes according to ambient illumination (spatial and temporal coding vs temporal coding only). The simple anatomical arrangement of dual GABAergic inhibitory interneurons (pre- vs post-synaptic) allows each to coordinate to control the visual function of DSGCs without mutual interference, a finding which lends to the complex and multi-faceted visual functions of retinal circuits.

5. Bibliography

Baccus SA, Olveczky BP, Manu M, Meister M (2008) A retinal circuit that computes object motion. J Neurosci 28:6807-6817.

Badea TC, Nathans J (2004) Quantitative analysis of neuronal morphologies in the mouse retina visualized by using a genetically directed reporter. The Journal of Comparative Neurology 480:331-351.

Baden T, Berens P, Bethge M, Euler T (2013) Spikes in mammalian bipolar cells support temporal layering of the inner retina. Curr Biol 23:48-52.

Barlow HB (1961) The coding of sensory messages. In: Current Problems in Animal Behaviour, vol. 331-360 (W.H. Thorpe, O. L. Z., ed), pp 331-360: Cambridge Univ. Press.

Barlow HB, Fitzhugh R, Kuffler SW (1957) Change of organization in the receptive fields of the cat's retina during dark adaptation. J Physiol 137:338-354.

Barlow HB, Levick WR (1965) The mechanism of directionally selective units in rabbit's retina. J Physiol 178:477-504.

Bloomfield SA (1992) Relationship between receptive and dendritic field size of amacrine cells in the rabbit retina. J Neurophysiol 68:711-725.

Borst A, Euler T (2011) Seeing Things in Motion: Models, Circuits, and Mechanisms. Neuron 71:974-994.

Brainard DH (1997) The Psychophysics Toolbox. Spat Vis 10:433-436.

Briggman KL, Helmstaedter M, Denk W (2011) Wiring specificity in the direction-selectivity circuit of the retina. Nature 471:183-188.

Cafaro J, Rieke F (2010) Noise correlations improve response fidelity and stimulus encoding. Nature 468:964-967.

Caldwell JH, Daw NW, Wyatt HJ (1978) Effects of picrotoxin and strychnine on rabbit retinal ganglion cells: lateral interactions for cells with more complex receptive fields. J Physiol 276:277-298.

Chen M, Lee S, Park SJ, Looger LL, Zhou ZJ (2014) Receptive field properties of bipolar cell axon terminals in the direction-selective sublaminas of the mouse retina. J Neurophysiol.

Chiao CC, Masland RH (2003) Contextual tuning of direction-selective retinal ganglion cells. Nat Neurosci 6:1251-1252.

Chiovini B, Turi GF, Katona G, Kaszas A, Palfi D, Maak P, Szalay G, Szabo MF, Szabo G, Szadai Z, Kali S, Rozsa B (2014) Dendritic spikes induce ripples in parvalbumin interneurons during hippocampal sharp waves. Neuron 82:908-924.

Cook PB, McReynolds JS (1998) Lateral inhibition in the inner retina is important for spatial tuning of ganglion cells. Nat Neurosci 1:714-719.

Cui J, Pan ZH (2008) Two types of cone bipolar cells express voltage-gated Na+ channels in the rat retina. Vis Neurosci 25:635-645.

Dacheux RF, Chimento MF, Amthor FR (2003) Synaptic input to the on-off directionally selective ganglion cell in the rabbit retina. The Journal of Comparative Neurology 456:267-278.

Dedek K, Pandarinath C, Alam NM, Wellershaus K, Schubert T, Willecke K, Prusky GT, Weiler R, Nirenberg S (2008) Ganglion cell adaptability: does the coupling of horizontal cells play a role? PLoS One 3:e1714.
Demb JB, Haarsma L, Freed MA, Sterling P (1999) Functional circuitry of the retinal ganglion cell's nonlinear receptive field. J Neurosci 19:9756-9767.
Demb JB, Singer JH (2015) Functional Circuitry of the Retina. Annual Review of Vision Science 1:263-289.
Demb JB, Zaghloul K, Haarsma L, Sterling P (2001) Bipolar cells contribute to nonlinear spatial summation in the brisk-transient (Y) ganglion cell in mammalian retina. J Neurosci 21:7447-7454.
Deniz S, Wersinger E, Schwab Y, Mura C, Erdelyi F, Szabo G, Rendon A, Sahel JA, Picaud S, Roux MJ (2011) Mammalian retinal horizontal cells are unconventional GABAergic neurons. J Neurochem 116:350-362.
Deschenes M, Paradis M, Roy JP, Steriade M (1984) Electrophysiology of neurons of lateral thalamic nuclei in cat: resting properties and burst discharges. J Neurophysiol 51:1196-1219.
Dhande OS, Estevez ME, Quattrochi LE, El-Danaf RN, Nguyen PL, Berson DM, Huberman AD (2013) Genetic dissection of retinal inputs to brainstem nuclei controlling image stabilization. J Neurosci 33:17797-17813.
Duffy KR, Hubel DH (2007) Receptive field properties of neurons in the primary visual cortex under photopic and scotopic lighting conditions. Vision Res 47:2569-2574.
Enroth-Cugell C, Jakiela HG (1980) Suppression of cat retinal ganglion cell responses by moving patterns. J Physiol 302:49-72.
Enroth-Cugell C, Robson J (1966) The contrast sensitivity of retinal ganglion cells of the cat. J Physiol 187:517-552.
Enroth-Cugell C, Robson JG, Schweitzer-Tong DE, Watson AB (1983) Spatio-temporal interactions in cat retinal ganglion cells showing linear spatial summation. J Physiol 341:279-307.
Euler T, Detwiler PB, Denk W (2002) Directionally selective calcium signals in dendrites of starburst amacrine cells. Nature 418:845-852.
Famiglietti EV (2005) Synaptic organization of complex ganglion cells in rabbit retina: type and arrangement of inputs to directionally selective and local-edge-detector cells. J Comp Neurol 484:357-391.
Famiglietti EV, Jr. (1983) On and off pathways through amacrine cells in mammalian retina: the synaptic connections of "starburst" amacrine cells. Vision Res 23:1265-1279.
Famiglietti EV, Jr., Kolb H (1975) A bistratified amacrine cell and synaptic cirucitry in the inner plexiform layer of the retina. Brain Res 84:293-300.
Famiglietti EV, Jr., Kolb H (1976) Structural basis for ON-and OFF-center responses in retinal ganglion cells. Science 194:193-195.
Farrow K, Teixeira M, Szikra T, Viney TJ, Balint K, Yonehara K, Roska B (2013) Ambient illumination toggles a neuronal circuit switch in the retina and visual perception at cone threshold. Neuron 78:325-338.
Flores-Herr N, Protti DA, Wassle H (2001) Synaptic currents generating the inhibitory surround of ganglion cells in the mammalian retina. J Neurosci 21:4852-4863.

Fried SI, Mu¨nch TA, Werblin FS (2005a) Directional Selectivity Is Formed at Multiple Levels by Laterally Offset Inhibition in the Rabbit Retina. Neuron 46:117-127.
Fried SI, Munch TA, Werblin FS (2005b) Directional selectivity is formed at multiple levels by laterally offset inhibition in the rabbit retina. Neuron 46:117-127.
Frishman LJ, Freeman AW, Troy JB, Schweitzer-Tong DE, Enroth-Cugell C (1987) Spatiotemporal frequency responses of cat retinal ganglion cells. J Gen Physiol 89:599-628.
Gale SD, Murphy GJ (2014) Distinct representation and distribution of visual information by specific cell types in mouse superficial superior colliculus. J Neurosci 34:13458-13471.
Gollisch T, Meister M (2010) Eye smarter than scientists believed: neural computations in circuits of the retina. Neuron 65:150-164.
Grimes WN, Schwartz GW, Rieke F (2014) The synaptic and circuit mechanisms underlying a change in spatial encoding in the retina. Neuron 82:460-473.
Grimes WN, Seal RP, Oesch N, Edwards RH, Diamond JS (2011) Genetic targeting and physiological features of VGLUT3+ amacrine cells. Vis Neurosci 28:381-392.
Grzywacz NM, Amthor FR (2007) Robust directional computation in on-off directionally selective ganglion cells of rabbit retina. Vis Neurosci 24:647-661.
Grzywacz NM, Amthor FR, Merwine DK (1994) Directional hyperacuity in ganglion cells of the rabbit retina. Vis Neurosci 11:1019-1025.
Hartline HK, Ratliff F (1957) Inhibitory interaction of receptor units in the eye of Limulus. J Gen Physiol 40:357-376.
He S, Levick WR (2000) Spatial-temporal response characteristics of the ON-OFF direction selective ganglion cells in the rabbit retina. Neurosci Lett 285:25-28.
Hecht S, Shlaer S, Pirenne MH (1942) ENERGY, QUANTA, AND VISION. J Gen Physiol 25:819-840.
Helmstaedter M, Briggman KL, Turaga SC, Jain V, Seung HS, Denk W (2013) Connectomic reconstruction of the inner plexiform layer in the mouse retina. Nature 500:168-174.
Hirasawa H (2003) pH Changes in the Invaginating Synaptic Cleft Mediate Feedback from Horizontal Cells to Cone Photoreceptors by Modulating Ca2+ Channels. The Journal of General Physiology 122:657-671.
Hochstein S, Shapley RM (1976a) Linear and nonlinear spatial subunits in Y cat retinal ganglion cells. J Physiol 262:265-284.
Hochstein S, Shapley RM (1976b) Quantitative analysis of retinal ganglion cell classifications. J Physiol 262:237-264.
Hoggarth A, McLaughlin AJ, Ronellenfitch K, Trenholm S, Vasandani R, Sethuramanujam S, Schwab D, Briggman KL, Awatramani GB (2015) Specific wiring of distinct amacrine cells in the directionally selective retinal circuit permits independent coding of direction and size. Neuron 86:276-291.
Hu EH, Pan F, Volgyi B, Bloomfield SA (2010) Light increases the gap junctional coupling of retinal ganglion cells. J Physiol 588:4145-4163.
Hubel DH, Wiesel TN (1962) Receptive fields, binocular interaction and functional architecture in the cat's visual cortex. J Physiol 160:106-154.
Kolb H (1974) The connections between horizontal cells and photoreceptors in the retina of the cat: electron microscopy of Golgi preparations. J Comp Neurol 155:1-14.

Kolb H (2003) How the retina works. American scientist 91:28-35.
Krekelberg B, van Wezel RJ (2013) Neural mechanisms of speed perception: transparent motion. J Neurophysiol 110:2007-2018.
Kuffler SW (1953) Discharge patterns and functional organization of mammalian retina. J Neurophysiol 16:37-68.
Lee S, Chen L, Chen M, Ye M, Seal RP, Zhou ZJ (2014) An Unconventional Glutamatergic Circuit in the Retina Formed by vGluT3 Amacrine Cells. Neuron 84:708-715.
Lee S, Zhou ZJ (2006) The synaptic mechanism of direction selectivity in distal processes of starburst amacrine cells. Neuron 51:787-799.
Li PH, Gauthier JL, Schiff M, Sher A, Ahn D, Field GD, Greschner M, Callaway EM, Litke AM, Chichilnisky EJ (2015) Anatomical identification of extracellularly recorded cells in large-scale multielectrode recordings. J Neurosci 35:4663-4675.
Lin B, Masland RH (2006) Populations of wide-field amacrine cells in the mouse retina. The Journal of Comparative Neurology 499:797-809.
Mach E (1865) Über die Wirkung der räumlichen Vertheilung des Lichtreizes auf die Netzhaut. Sitzungsberichte der mathematisch-naturwissenschaftlichen Classe der kaiserlichen Akademie der Wissenschaften 52:303-322.
MacNeil MA, Masland RH (1998) Extreme diversity among amacrine cells: implications for function. Neuron 20:971-982.
Mangel SC (1991) Analysis of the horizontal cell contribution to the receptive field surround of ganglion cells in the rabbit retina. J Physiol 442:211-234.
Masland RH (2001) The fundamental plan of the retina. Nat Neurosci 4:877-886.
Masland RH (2012) The tasks of amacrine cells. Vis Neurosci 29:3-9.
McMahon MJ, Packer OS, Dacey DM (2004) The classical receptive field surround of primate parasol ganglion cells is mediated primarily by a non-GABAergic pathway. J Neurosci 24:3736-3745.
Morgan IG, Boelen MK (1996) A retinal dark-light switch: a review of the evidence. Vis Neurosci 13:399-409.
Murphy-Baum BL, Taylor WR (2015) The Synaptic and Morphological Basis of Orientation Selectivity in a Polyaxonal Amacrine Cell of the Rabbit Retina. J Neurosci 35:13336-13350.
Nath A, Schwartz GW (2016) Cardinal Orientation Selectivity Is Represented by Two Distinct Ganglion Cell Types in Mouse Retina. J Neurosci 36:3208-3221.
Nelson R, Kolb H (1983) Synaptic patterns and response properties of bipolar and ganglion cells in the cat retina. Vision Res 23:1183-1195.
Nowak P, Dobbins AC, Gawne TJ, Grzywacz NM, Amthor FR (2011) Separability of stimulus parameter encoding by on-off directionally selective rabbit retinal ganglion cells. J Neurophysiol 105:2083-2099.
O'Malley DM, Sandell JH, Masland RH (1992) Co-release of acetylcholine and GABA by the starburst amacrine cells. J Neurosci 12:1394-1408.
Oesch N, Euler T, Taylor WR (2005) Direction-selective dendritic action potentials in rabbit retina. Neuron 47:739-750.
Oesch NW, Taylor WR (2010) Tetrodotoxin-resistant sodium channels contribute to directional responses in starburst amacrine cells. PLoS One 5:e12447.

Olveczky BP, Baccus SA, Meister M (2003) Segregation of object and background motion in the retina. Nature 423:401-408.
Oyster CW, Takahashi E, Collewijn H (1972) Direction-selective retinal ganglion cells and control of optokinetic nystagmus in the rabbit. Vision Res 12:183-193.
Pandarinath C, Bomash I, Victor JD, Prusky GT, Tschetter WW, Nirenberg S (2010) A novel mechanism for switching a neural system from one state to another. Front Comput Neurosci 4:2.
Park SJ, Kim IJ, Looger LL, Demb JB, Borghuis BG (2014) Excitatory synaptic inputs to mouse on-off direction-selective retinal ganglion cells lack direction tuning. J Neurosci 34:3976-3981.
Passaglia CL, Enroth-Cugell C, Troy JB (2001) Effects of remote stimulation on the mean firing rate of cat retinal ganglion cells. J Neurosci 21:5794-5803.
Passaglia CL, Freeman DK, Troy JB (2009) Effects of remote stimulation on the modulated activity of cat retinal ganglion cells. J Neurosci 29:2467-2476.
Peichl L, Wassle H (1983) The structural correlate of the receptive field centre of alpha ganglion cells in the cat retina. J Physiol 341:309-324.
Pérez De Sevilla Müller L, Shelley J, Weiler R (2007) Displaced amacrine cells of the mouse retina. The Journal of Comparative Neurology 505:177-189.
Perrone JA, Thiele A (2001) Speed skills: measuring the visual speed analyzing properties of primate MT neurons. Nat Neurosci 4:526-532.
Peters BN, Masland RH (1996) Responses to light of starburst amacrine cells. J Neurophysiol 75:469-480.
Piccolino M, Wade NJ (2008) Galileo's eye: a new vision of the senses in the work of Galileo Galilei. Perception 37:1312-1340.
Poleg-Polsky A, Diamond JS (2011) Imperfect space clamp permits electrotonic interactions between inhibitory and excitatory synaptic conductances, distorting voltage clamp recordings. PLoS One 6:e19463.
Priebe NJ, Cassanello CR, Lisberger SG (2003) The neural representation of speed in macaque area MT/V5. J Neurosci 23:5650-5661.
Priebe NJ, Ferster D (2008) Inhibition, spike threshold, and stimulus selectivity in primary visual cortex. Neuron 57:482-497.
Protti DA, Di Marco S, Huang JY, Vonhoff CR, Nguyen V, Solomon SG (2014) Inner retinal inhibition shapes the receptive field of retinal ganglion cells in primate. J Physiol 592:49-65.
Ratliff F (1965) Mach bands: quantitative studies on neural networks in the retina.
Remtulla S, Hallett PE (1985) A schematic eye for the mouse, and comparisons with the rat. Vision Res 25:21-31.
Rivlin-Etzion M, Wei W, Feller MB (2012) Visual stimulation reverses the directional preference of direction-selective retinal ganglion cells. Neuron 76:518-525.
Roska B, Nemeth E, Orzo L, Werblin FS (2000) Three levels of lateral inhibition: A space-time study of the retina of the tiger salamander. J Neurosci 20:1941-1951.
Roska B, Werblin F (2003) Rapid global shifts in natural scenes block spiking in specific ganglion cell types. Nat Neurosci 6:600-608.
Sanes JR, Masland RH (2015) The types of retinal ganglion cells: current status and implications for neuronal classification. Annu Rev Neurosci 38:221-246.
Schwartz GW, Rieke F (2013) Controlling gain one photon at a time. Elife 2:e00467.

Sethuramanujam S, McLaughlin AJ, deRosenroll G, Hoggarth A, Schwab DJ, Awatramani GB (2016) A Central Role for Mixed Acetylcholine/GABA Transmission in Direction Coding in the Retina. Neuron.

Shields CR, Lukasiewicz PD (2003) Spike-dependent GABA inputs to bipolar cell axon terminals contribute to lateral inhibition of retinal ganglion cells. J Neurophysiol 89:2449-2458.

Simoncelli EP, Heeger DJ (1998) A model of neuronal responses in visual area MT. Vision Res 38:743-761.

Simoncelli EP, Heeger DJ (2001) Representing retinal image speed in visual cortex. Nat Neurosci 4:461-462.

Solomon SG, White AJ, Martin PR (2002) Extraclassical receptive field properties of parvocellular, magnocellular, and koniocellular cells in the primate lateral geniculate nucleus. J Neurosci 22:338-349.

Stasheff SF, Masland RH (2002) Functional inhibition in direction-selective retinal ganglion cells: spatiotemporal extent and intralaminar interactions. J Neurophysiol 88:1026-1039.

Sumbul U, Song S, McCulloch K, Becker M, Lin B, Sanes JR, Masland RH, Seung HS (2014) A genetic and computational approach to structurally classify neuronal types. Nat Commun 5:3512.

Szikra T, Trenholm S, Drinnenberg A, Juttner J, Raics Z, Farrow K, Biel M, Awatramani G, Clark DA, Sahel JA, da Silveira RA, Roska B (2014) Rods in daylight act as relay cells for cone-driven horizontal cell-mediated surround inhibition. Nat Neurosci.

Takeshita D, Gollisch T (2014) Nonlinear spatial integration in the receptive field surround of retinal ganglion cells. J Neurosci 34:7548-7561.

Taylor WR (1999) TTX attenuates surround inhibition in rabbit retinal ganglion cells. Vis Neurosci 16:285-290.

Taylor WR, Vaney DI (2002) Diverse synaptic mechanisms generate direction selectivity in the rabbit retina. J Neurosci 22:7712-7720.

Thorson J (1964) DYNAMICS OF MOTION PERCEPTION IN THE DESERT LOCUST. Science 145:69-71.

Trenholm S, Johnson K, Li X, Smith Robert G, Awatramani Gautam B (2011) Parallel Mechanisms Encode Direction in the Retina. Neuron 71:683-694.

Trenholm S, Schwab DJ, Balasubramanian V, Awatramani GB (2013) Lag normalization in an electrically coupled neural network. Nat Neurosci 16:154-156.

Troy JB, Bohnsack DL, Chen J, Guo X, Passaglia CL (2005) Spatiotemporal integration of light by the cat X-cell center under photopic and scotopic conditions. Vis Neurosci 22:493-500.

Umino Y, Solessio E, Barlow RB (2008) Speed, Spatial, and Temporal Tuning of Rod and Cone Vision in Mouse. Journal of Neuroscience 28:189-198.

van Hateren JH (1990) Directional tuning curves, elementary movement detectors, and the estimation of the direction of visual movement. Vision Res 30:603-614.

Vaney DI, Sivyer B, Taylor WR (2012) Direction selectivity in the retina: symmetry and asymmetry in structure and function. Nat Rev Neurosci 13:194-208.

Venkataramani S, Taylor WR (2016) Synaptic Mechanisms Generating Orientation Selectivity in the ON Pathway of the Rabbit Retina. J Neurosci 36:3336-3349.

Venkataramani S, Van Wyk M, Buldyrev I, Sivyer B, Vaney DI, Taylor WR (2014) Distinct roles for inhibition in spatial and temporal tuning of local edge detectors in the rabbit retina. PLoS One 9:e88560.

Vessey JP, Stratis AK, Daniels BA, Da Silva N, Jonz MG, Lalonde MR, Baldridge WH, Barnes S (2005) Proton-mediated feedback inhibition of presynaptic calcium channels at the cone photoreceptor synapse. J Neurosci 25:4108-4117.

Vickers E, Kim MH, Vigh J, von Gersdorff H (2012) Paired-pulse plasticity in the strength and latency of light-evoked lateral inhibition to retinal bipolar cell terminals. J Neurosci 32:11688-11699.

Vlasits AL, Bos R, Morrie RD, Fortuny C, Flannery JG, Feller MB, Rivlin-Etzion M (2014) Visual stimulation switches the polarity of excitatory input to starburst amacrine cells. Neuron 83:1172-1184.

Volgyi B, Xin D, Amarillo Y, Bloomfield SA (2001) Morphology and physiology of the polyaxonal amacrine cells in the rabbit retina. J Comp Neurol 440:109-125.

Wang YV, Weick M, Demb JB (2011) Spectral and temporal sensitivity of cone-mediated responses in mouse retinal ganglion cells. J Neurosci 31:7670-7681.

Wei W, Hamby AM, Zhou K, Feller MB (2011) Development of asymmetric inhibition underlying direction selectivity in the retina. Nature 469:402-406.

Wiesel TN (1959) Recording inhibition and excitation in the cat's retinal ganglion cells with intracellular electrodes. Nature 183:264-265.

Wyatt HJ, Daw NW (1975) Directionally sensitive ganglion cells in the rabbit retina: specificity for stimulus direction, size, and speed. J Neurophysiol 38:613-626.

Yonehara K, Farrow K, Ghanem A, Hillier D, Balint K, Teixeira M, Juttner J, Noda M, Neve RL, Conzelmann KK, Roska B (2013) The first stage of cardinal direction selectivity is localized to the dendrites of retinal ganglion cells. Neuron 79:1078-1085.

Yoshida K, Watanabe D, Ishikane H, Tachibana M, Pastan I, Nakanishi S (2001) A key role of starburst amacrine cells in originating retinal directional selectivity and optokinetic eye movement. Neuron 30:771-780.

Zaghloul KA, Manookin MB, Borghuis BG, Boahen K, Demb JB (2007) Functional circuitry for peripheral suppression in Mammalian Y-type retinal ganglion cells. J Neurophysiol 97:4327-4340.

Zhang Y, Kim IJ, Sanes JR, Meister M (2012) The most numerous ganglion cell type of the mouse retina is a selective feature detector. Proc Natl Acad Sci U S A 109:E2391-2398.

Zheng J-j, Lee S, Zhou ZJ (2004a) A Developmental Switch in the Excitability and Function of the Starburst Network in the Mammalian Retina. Neuron 44:851-864.

Zheng JJ, Lee S, Zhou ZJ (2004b) A developmental switch in the excitability and function of the starburst network in the mammalian retina. Neuron 44:851-864.

Ackert JM, Wu SH, Lee JC, Abrams J, Hu EH, Perlman I, Bloomfield SA (2006) Light-induced changes in spike synchronization between coupled ON direction selective ganglion cells in the mammalian retina. J Neurosci 26:4206-4215.

Baccus SA, Olveczky BP, Manu M, Meister M (2008) A retinal circuit that computes object motion. J Neurosci 28:6807-6817.

Badea TC, Nathans J (2004) Quantitative analysis of neuronal morphologies in the mouse retina visualized by using a genetically directed reporter. The Journal of Comparative Neurology 480:331-351.

Baden T, Berens P, Bethge M, Euler T (2013) Spikes in mammalian bipolar cells support temporal layering of the inner retina. Curr Biol 23:48-52.

Barlow HB (1961) The coding of sensory messages. In: Current Problems in Animal Behaviour, vol. 331-360 (W.H. Thorpe, O. L. Z., ed), pp 331-360: Cambridge Univ. Press.

Barlow HB, Fitzhugh R, Kuffler SW (1957) Change of organization in the receptive fields of the cat's retina during dark adaptation. J Physiol 137:338-354.

Barlow HB, Levick WR (1965) The mechanism of directionally selective units in rabbit's retina. J Physiol 178:477-504.

Bloomfield SA (1992) Relationship between receptive and dendritic field size of amacrine cells in the rabbit retina. J Neurophysiol 68:711-725.

Borst A, Euler T (2011) Seeing Things in Motion: Models, Circuits, and Mechanisms. Neuron 71:974-994.

Brainard DH (1997) The Psychophysics Toolbox. Spat Vis 10:433-436.

Breton JD, Stuart GJ (2012) Somatic and dendritic GABA(B) receptors regulate neuronal excitability via different mechanisms. J Neurophysiol 108:2810-2818.

Briggman KL, Helmstaedter M, Denk W (2011) Wiring specificity in the direction-selectivity circuit of the retina. Nature 471:183-188.

Cafaro J, Rieke F (2010) Noise correlations improve response fidelity and stimulus encoding. Nature 468:964-967.

Caldwell JH, Daw NW, Wyatt HJ (1978) Effects of picrotoxin and strychnine on rabbit retinal ganglion cells: lateral interactions for cells with more complex receptive fields. J Physiol 276:277-298.

Chen M, Lee S, Park SJ, Looger LL, Zhou ZJ (2014) Receptive field properties of bipolar cell axon terminals in the direction-selective sublaminas of the mouse retina. J Neurophysiol.

Chiao CC, Masland RH (2003) Contextual tuning of direction-selective retinal ganglion cells. Nat Neurosci 6:1251-1252.

Chiovini B, Turi GF, Katona G, Kaszas A, Palfi D, Maak P, Szalay G, Szabo MF, Szabo G, Szadai Z, Kali S, Rozsa B (2014) Dendritic spikes induce ripples in parvalbumin interneurons during hippocampal sharp waves. Neuron 82:908-924.

Cook PB, McReynolds JS (1998) Lateral inhibition in the inner retina is important for spatial tuning of ganglion cells. Nat Neurosci 1:714-719.

Cui J, Pan ZH (2008) Two types of cone bipolar cells express voltage-gated Na+ channels in the rat retina. Vis Neurosci 25:635-645.

Dacheux RF, Chimento MF, Amthor FR (2003) Synaptic input to the on-off directionally selective ganglion cell in the rabbit retina. The Journal of Comparative Neurology 456:267-278.

Dedek K, Pandarinath C, Alam NM, Wellershaus K, Schubert T, Willecke K, Prusky GT, Weiler R, Nirenberg S (2008) Ganglion cell adaptability: does the coupling of horizontal cells play a role? PLoS One 3:e1714.

Demb JB, Haarsma L, Freed MA, Sterling P (1999) Functional circuitry of the retinal ganglion cell's nonlinear receptive field. J Neurosci 19:9756-9767.

Demb JB, Singer JH (2015) Functional Circuitry of the Retina. Annual Review of Vision Science 1:263-289.

Demb JB, Zaghloul K, Haarsma L, Sterling P (2001) Bipolar cells contribute to nonlinear spatial summation in the brisk-transient (Y) ganglion cell in mammalian retina. J Neurosci 21:7447-7454.

Deniz S, Wersinger E, Schwab Y, Mura C, Erdelyi F, Szabo G, Rendon A, Sahel JA, Picaud S, Roux MJ (2011) Mammalian retinal horizontal cells are unconventional GABAergic neurons. J Neurochem 116:350-362.

Deschenes M, Paradis M, Roy JP, Steriade M (1984) Electrophysiology of neurons of lateral thalamic nuclei in cat: resting properties and burst discharges. J Neurophysiol 51:1196-1219.

Dhande OS, Estevez ME, Quattrochi LE, El-Danaf RN, Nguyen PL, Berson DM, Huberman AD (2013) Genetic dissection of retinal inputs to brainstem nuclei controlling image stabilization. J Neurosci 33:17797-17813.

Duffy KR, Hubel DH (2007) Receptive field properties of neurons in the primary visual cortex under photopic and scotopic lighting conditions. Vision Res 47:2569-2574.

Enroth-Cugell C, Jakiela HG (1980) Suppression of cat retinal ganglion cell responses by moving patterns. J Physiol 302:49-72.

Enroth-Cugell C, Robson J (1966) The contrast sensitivity of retinal ganglion cells of the cat. J Physiol 187:517-552.

Enroth-Cugell C, Robson JG, Schweitzer-Tong DE, Watson AB (1983) Spatio-temporal interactions in cat retinal ganglion cells showing linear spatial summation. J Physiol 341:279-307.

Euler T, Detwiler PB, Denk W (2002) Directionally selective calcium signals in dendrites of starburst amacrine cells. Nature 418:845-852.

Famiglietti EV (2005) Synaptic organization of complex ganglion cells in rabbit retina: type and arrangement of inputs to directionally selective and local-edge-detector cells. J Comp Neurol 484:357-391.

Famiglietti EV, Jr. (1983) On and off pathways through amacrine cells in mammalian retina: the synaptic connections of "starburst" amacrine cells. Vision Res 23:1265-1279.

Famiglietti EV, Jr., Kolb H (1975) A bistratified amacrine cell and synaptic cirucitry in the inner plexiform layer of the retina. Brain Res 84:293-300.

Famiglietti EV, Jr., Kolb H (1976) Structural basis for ON-and OFF-center responses in retinal ganglion cells. Science 194:193-195.

Farrow K, Teixeira M, Szikra T, Viney TJ, Balint K, Yonehara K, Roska B (2013) Ambient illumination toggles a neuronal circuit switch in the retina and visual perception at cone threshold. Neuron 78:325-338.

Flores-Herr N, Protti DA, Wassle H (2001) Synaptic currents generating the inhibitory surround of ganglion cells in the mammalian retina. J Neurosci 21:4852-4863.

Fried SI, Mu¨nch TA, Werblin FS (2005) Directional Selectivity Is Formed at Multiple Levels by Laterally Offset Inhibition in the Rabbit Retina. Neuron 46:117-127.

Frishman LJ, Freeman AW, Troy JB, Schweitzer-Tong DE, Enroth-Cugell C (1987) Spatiotemporal frequency responses of cat retinal ganglion cells. J Gen Physiol 89:599-628.

Gale SD, Murphy GJ (2014) Distinct representation and distribution of visual information by specific cell types in mouse superficial superior colliculus. J Neurosci 34:13458-13471.

Gollisch T, Meister M (2010) Eye smarter than scientists believed: neural computations in circuits of the retina. Neuron 65:150-164.

Grimes WN, Schwartz GW, Rieke F (2014) The synaptic and circuit mechanisms underlying a change in spatial encoding in the retina. Neuron 82:460-473.

Grimes WN, Seal RP, Oesch N, Edwards RH, Diamond JS (2011) Genetic targeting and physiological features of VGLUT3+ amacrine cells. Vis Neurosci 28:381-392.

Grzywacz NM, Amthor FR (2007) Robust directional computation in on-off directionally selective ganglion cells of rabbit retina. Vis Neurosci 24:647-661.

Grzywacz NM, Amthor FR, Merwine DK (1994) Directional hyperacuity in ganglion cells of the rabbit retina. Vis Neurosci 11:1019-1025.

Hartline HK, Ratliff F (1957) Inhibitory interaction of receptor units in the eye of Limulus. J Gen Physiol 40:357-376.

He S, Levick WR (2000) Spatial-temporal response characteristics of the ON-OFF direction selective ganglion cells in the rabbit retina. Neurosci Lett 285:25-28.

Hecht S, Shlaer S, Pirenne MH (1942) ENERGY, QUANTA, AND VISION. J Gen Physiol 25:819-840.

Helmstaedter M, Briggman KL, Turaga SC, Jain V, Seung HS, Denk W (2013) Connectomic reconstruction of the inner plexiform layer in the mouse retina. Nature 500:168-174.

Hirasawa H (2003) pH Changes in the Invaginating Synaptic Cleft Mediate Feedback from Horizontal Cells to Cone Photoreceptors by Modulating Ca2+ Channels. The Journal of General Physiology 122:657-671.

Hochstein S, Shapley RM (1976a) Linear and nonlinear spatial subunits in Y cat retinal ganglion cells. J Physiol 262:265-284.

Hochstein S, Shapley RM (1976b) Quantitative analysis of retinal ganglion cell classifications. J Physiol 262:237-264.

Hoggarth A, McLaughlin AJ, Ronellenfitch K, Trenholm S, Vasandani R, Sethuramanujam S, Schwab D, Briggman KL, Awatramani GB (2015) Specific wiring of distinct amacrine cells in the directionally selective retinal circuit permits independent coding of direction and size. Neuron 86:276-291.

Hu EH, Pan F, Volgyi B, Bloomfield SA (2010) Light increases the gap junctional coupling of retinal ganglion cells. J Physiol 588:4145-4163.

Hubel DH, Wiesel TN (1962) Receptive fields, binocular interaction and functional architecture in the cat's visual cortex. J Physiol 160:106-154.

Kay JN, De la Huerta I, Kim IJ, Zhang Y, Yamagata M, Chu MW, Meister M, Sanes JR (2011) Retinal ganglion cells with distinct directional preferences differ in molecular identity, structure, and central projections. J Neurosci 31:7753-7762.

Kim JS, Greene MJ, Zlateski A, Lee K, Richardson M, Turaga SC, Purcaro M, Balkam M, Robinson A, Behabadi BF, Campos M, Denk W, Seung HS (2014) Space-time wiring specificity supports direction selectivity in the retina. Nature 509:331-336.

Kolb H (1974) The connections between horizontal cells and photoreceptors in the retina of the cat: electron microscopy of Golgi preparations. J Comp Neurol 155:1-14.
Kolb H (2003) How the retina works. American scientist 91:28-35.
Krekelberg B, van Wezel RJ (2013) Neural mechanisms of speed perception: transparent motion. J Neurophysiol 110:2007-2018.
Kuffler SW (1953) Discharge patterns and functional organization of mammalian retina. J Neurophysiol 16:37-68.
Lee S, Chen L, Chen M, Ye M, Seal RP, Zhou ZJ (2014) An Unconventional Glutamatergic Circuit in the Retina Formed by vGluT3 Amacrine Cells. Neuron 84:708-715.
Lee S, Zhou ZJ (2006) The synaptic mechanism of direction selectivity in distal processes of starburst amacrine cells. Neuron 51:787-799.
Li PH, Gauthier JL, Schiff M, Sher A, Ahn D, Field GD, Greschner M, Callaway EM, Litke AM, Chichilnisky EJ (2015) Anatomical identification of extracellularly recorded cells in large-scale multielectrode recordings. J Neurosci 35:4663-4675.
Lin B, Masland RH (2006) Populations of wide-field amacrine cells in the mouse retina. The Journal of Comparative Neurology 499:797-809.
Mach E (1865) Über die Wirkung der räumlichen Vertheilung des Lichtreizes auf die Netzhaut. Sitzungsberichte der mathematisch-naturwissenschaftlichen Classe der kaiserlichen Akademie der Wissenschaften 52:303-322.
MacNeil MA, Masland RH (1998) Extreme diversity among amacrine cells: implications for function. Neuron 20:971-982.
Mangel SC (1991) Analysis of the horizontal cell contribution to the receptive field surround of ganglion cells in the rabbit retina. J Physiol 442:211-234.
Masland RH (2001) The fundamental plan of the retina. Nat Neurosci 4:877-886.
Masland RH (2012) The tasks of amacrine cells. Vis Neurosci 29:3-9.
McMahon MJ, Packer OS, Dacey DM (2004) The classical receptive field surround of primate parasol ganglion cells is mediated primarily by a non-GABAergic pathway. J Neurosci 24:3736-3745.
Miller RF, Bloomfield SA (1983) Electroanatomy of a unique amacrine cell in the rabbit retina. Proc Natl Acad Sci U S A 80:3069-3073.
Mitchell SJ, Silver RA (2003) Shunting inhibition modulates neuronal gain during synaptic excitation. Neuron 38:433-445.
Morgan IG, Boelen MK (1996) A retinal dark-light switch: a review of the evidence. Vis Neurosci 13:399-409.
Murphy-Baum BL, Taylor WR (2015) The Synaptic and Morphological Basis of Orientation Selectivity in a Polyaxonal Amacrine Cell of the Rabbit Retina. J Neurosci 35:13336-13350.
Nath A, Schwartz GW (2016) Cardinal Orientation Selectivity Is Represented by Two Distinct Ganglion Cell Types in Mouse Retina. J Neurosci 36:3208-3221.
Nelson R, Kolb H (1983) Synaptic patterns and response properties of bipolar and ganglion cells in the cat retina. Vision Res 23:1183-1195.
Nowak P, Dobbins AC, Gawne TJ, Grzywacz NM, Amthor FR (2011) Separability of stimulus parameter encoding by on-off directionally selective rabbit retinal ganglion cells. J Neurophysiol 105:2083-2099.

O'Malley DM, Sandell JH, Masland RH (1992) Co-release of acetylcholine and GABA by the starburst amacrine cells. J Neurosci 12:1394-1408.
Oesch N, Euler T, Taylor WR (2005) Direction-selective dendritic action potentials in rabbit retina. Neuron 47:739-750.
Oesch NW, Taylor WR (2010) Tetrodotoxin-resistant sodium channels contribute to directional responses in starburst amacrine cells. PLoS One 5:e12447.
Olveczky BP, Baccus SA, Meister M (2003) Segregation of object and background motion in the retina. Nature 423:401-408.
Oyster CW, Barlow HB (1967) Direction-selective units in rabbit retina: distribution of preferred directions. Science 155:841-842.
Oyster CW, Simpson JI, Takahashi ES, Soodak RE (1980) Retinal ganglion cells projecting to the rabbit accessory optic system. J Comp Neurol 190:49-61.
Oyster CW, Takahashi E, Collewijn H (1972) Direction-selective retinal ganglion cells and control of optokinetic nystagmus in the rabbit. Vision Res 12:183-193.
Pandarinath C, Bomash I, Victor JD, Prusky GT, Tschetter WW, Nirenberg S (2010) A novel mechanism for switching a neural system from one state to another. Front Comput Neurosci 4:2.
Park SJ, Kim IJ, Looger LL, Demb JB, Borghuis BG (2014) Excitatory synaptic inputs to mouse on-off direction-selective retinal ganglion cells lack direction tuning. J Neurosci 34:3976-3981.
Passaglia CL, Enroth-Cugell C, Troy JB (2001) Effects of remote stimulation on the mean firing rate of cat retinal ganglion cells. J Neurosci 21:5794-5803.
Passaglia CL, Freeman DK, Troy JB (2009) Effects of remote stimulation on the modulated activity of cat retinal ganglion cells. J Neurosci 29:2467-2476.
Peichl L, Wassle H (1983) The structural correlate of the receptive field centre of alpha ganglion cells in the cat retina. J Physiol 341:309-324.
Pérez De Sevilla Müller L, Shelley J, Weiler R (2007) Displaced amacrine cells of the mouse retina. The Journal of Comparative Neurology 505:177-189.
Perrone JA, Thiele A (2001) Speed skills: measuring the visual speed analyzing properties of primate MT neurons. Nat Neurosci 4:526-532.
Peters BN, Masland RH (1996) Responses to light of starburst amacrine cells. J Neurophysiol 75:469-480.
Piccolino M, Wade NJ (2008) Galileo's eye: a new vision of the senses in the work of Galileo Galilei. Perception 37:1312-1340.
Poleg-Polsky A, Diamond JS (2011) Imperfect space clamp permits electrotonic interactions between inhibitory and excitatory synaptic conductances, distorting voltage clamp recordings. PLoS One 6:e19463.
Priebe NJ, Cassanello CR, Lisberger SG (2003) The neural representation of speed in macaque area MT/V5. J Neurosci 23:5650-5661.
Priebe NJ, Ferster D (2008) Inhibition, spike threshold, and stimulus selectivity in primary visual cortex. Neuron 57:482-497.
Protti DA, Di Marco S, Huang JY, Vonhoff CR, Nguyen V, Solomon SG (2014) Inner retinal inhibition shapes the receptive field of retinal ganglion cells in primate. J Physiol 592:49-65.
Ratliff F (1965) Mach bands: quantitative studies on neural networks in the retina.

Remtulla S, Hallett PE (1985) A schematic eye for the mouse, and comparisons with the rat. Vision Res 25:21-31.

Rivlin-Etzion M, Wei W, Feller MB (2012) Visual stimulation reverses the directional preference of direction-selective retinal ganglion cells. Neuron 76:518-525.

Roska B, Nemeth E, Orzo L, Werblin FS (2000) Three levels of lateral inhibition: A space-time study of the retina of the tiger salamander. J Neurosci 20:1941-1951.

Roska B, Werblin F (2003) Rapid global shifts in natural scenes block spiking in specific ganglion cell types. Nat Neurosci 6:600-608.

Ryan SJ, Ehrlich DE, Jasnow AM, Daftary S, Madsen TE, Rainnie DG (2012) Spike-timing precision and neuronal synchrony are enhanced by an interaction between synaptic inhibition and membrane oscillations in the amygdala. PLoS One 7:e35320.

Sanes JR, Masland RH (2015) The types of retinal ganglion cells: current status and implications for neuronal classification. Annu Rev Neurosci 38:221-246.

Schwartz GW, Rieke F (2013) Controlling gain one photon at a time. Elife 2:e00467.

Sethuramanujam S, McLaughlin AJ, deRosenroll G, Hoggarth A, Schwab DJ, Awatramani GB (2016) A Central Role for Mixed Acetylcholine/GABA Transmission in Direction Coding in the Retina. Neuron.

Shields CR, Lukasiewicz PD (2003) Spike-dependent GABA inputs to bipolar cell axon terminals contribute to lateral inhibition of retinal ganglion cells. J Neurophysiol 89:2449-2458.

Silver RA (2010) Neuronal arithmetic. Nat Rev Neurosci 11:474-489.

Simoncelli EP, Heeger DJ (1998) A model of neuronal responses in visual area MT. Vision Res 38:743-761.

Simoncelli EP, Heeger DJ (2001) Representing retinal image speed in visual cortex. Nat Neurosci 4:461-462.

Solomon SG, White AJ, Martin PR (2002) Extraclassical receptive field properties of parvocellular, magnocellular, and koniocellular cells in the primate lateral geniculate nucleus. J Neurosci 22:338-349.

Stasheff SF, Masland RH (2002) Functional inhibition in direction-selective retinal ganglion cells: spatiotemporal extent and intralaminar interactions. J Neurophysiol 88:1026-1039.

Sumbul U, Song S, McCulloch K, Becker M, Lin B, Sanes JR, Masland RH, Seung HS (2014) A genetic and computational approach to structurally classify neuronal types. Nat Commun 5:3512.

Szikra T, Trenholm S, Drinnenberg A, Juttner J, Raics Z, Farrow K, Biel M, Awatramani G, Clark DA, Sahel JA, da Silveira RA, Roska B (2014) Rods in daylight act as relay cells for cone-driven horizontal cell-mediated surround inhibition. Nat Neurosci.

Takeshita D, Gollisch T (2014) Nonlinear spatial integration in the receptive field surround of retinal ganglion cells. J Neurosci 34:7548-7561.

Taylor WR (1999) TTX attenuates surround inhibition in rabbit retinal ganglion cells. Vis Neurosci 16:285-290.

Taylor WR, Smith RG (2012) The role of starburst amacrine cells in visual signal processing. Visual neuroscience 29:73-81.

Taylor WR, Vaney DI (2002) Diverse synaptic mechanisms generate direction selectivity in the rabbit retina. J Neurosci 22:7712-7720.
Thorson J (1964) DYNAMICS OF MOTION PERCEPTION IN THE DESERT LOCUST. Science 145:69-71.
Trenholm S, Johnson K, Li X, Smith Robert G, Awatramani Gautam B (2011) Parallel Mechanisms Encode Direction in the Retina. Neuron 71:683-694.
Trenholm S, Schwab DJ, Balasubramanian V, Awatramani GB (2013) Lag normalization in an electrically coupled neural network. Nat Neurosci 16:154-156.
Troy JB, Bohnsack DL, Chen J, Guo X, Passaglia CL (2005) Spatiotemporal integration of light by the cat X-cell center under photopic and scotopic conditions. Vis Neurosci 22:493-500.
Umino Y, Solessio E, Barlow RB (2008) Speed, Spatial, and Temporal Tuning of Rod and Cone Vision in Mouse. Journal of Neuroscience 28:189-198.
van Hateren JH (1990) Directional tuning curves, elementary movement detectors, and the estimation of the direction of visual movement. Vision Res 30:603-614.
van Nes FL, Koenderink JJ, Nas H, Bouman MA (1967) Spatiotemporal modulation transfer in the human eye. J Opt Soc Am 57:1082-1088.
Vaney DI, Sivyer B, Taylor WR (2012) Direction selectivity in the retina: symmetry and asymmetry in structure and function. Nat Rev Neurosci 13:194-208.
Venkataramani S, Taylor WR (2016) Synaptic Mechanisms Generating Orientation Selectivity in the ON Pathway of the Rabbit Retina. J Neurosci 36:3336-3349.
Venkataramani S, Van Wyk M, Buldyrev I, Sivyer B, Vaney DI, Taylor WR (2014) Distinct roles for inhibition in spatial and temporal tuning of local edge detectors in the rabbit retina. PLoS One 9:e88560.
Vessey JP, Stratis AK, Daniels BA, Da Silva N, Jonz MG, Lalonde MR, Baldridge WH, Barnes S (2005) Proton-mediated feedback inhibition of presynaptic calcium channels at the cone photoreceptor synapse. J Neurosci 25:4108-4117.
Vickers E, Kim MH, Vigh J, von Gersdorff H (2012) Paired-pulse plasticity in the strength and latency of light-evoked lateral inhibition to retinal bipolar cell terminals. J Neurosci 32:11688-11699.
Vlasits AL, Bos R, Morrie RD, Fortuny C, Flannery JG, Feller MB, Rivlin-Etzion M (2014) Visual stimulation switches the polarity of excitatory input to starburst amacrine cells. Neuron 83:1172-1184.
Volgyi B, Xin D, Amarillo Y, Bloomfield SA (2001) Morphology and physiology of the polyaxonal amacrine cells in the rabbit retina. J Comp Neurol 440:109-125.
Wang YV, Weick M, Demb JB (2011) Spectral and temporal sensitivity of cone-mediated responses in mouse retinal ganglion cells. J Neurosci 31:7670-7681.
Wiesel TN (1959) Recording inhibition and excitation in the cat's retinal ganglion cells with intracellular electrodes. Nature 183:264-265.
Wyatt HJ, Daw NW (1975) Directionally sensitive ganglion cells in the rabbit retina: specificity for stimulus direction, size, and speed. J Neurophysiol 38:613-626.
Yonehara K, Farrow K, Ghanem A, Hillier D, Balint K, Teixeira M, Juttner J, Noda M, Neve RL, Conzelmann KK, Roska B (2013) The first stage of cardinal direction selectivity is localized to the dendrites of retinal ganglion cells. Neuron 79:1078-1085.

Yonehara K, Ishikane H, Sakuta H, Shintani T, Nakamura-Yonehara K, Kamiji NL, Usui S, Noda M (2009) Identification of retinal ganglion cells and their projections involved in central transmission of information about upward and downward image motion. PLoS One 4:e4320.

Yoshida K, Watanabe D, Ishikane H, Tachibana M, Pastan I, Nakanishi S (2001) A key role of starburst amacrine cells in originating retinal directional selectivity and optokinetic eye movement. Neuron 30:771-780.

Zaghloul KA, Manookin MB, Borghuis BG, Boahen K, Demb JB (2007) Functional circuitry for peripheral suppression in Mammalian Y-type retinal ganglion cells. J Neurophysiol 97:4327-4340.

Zhang Y, Kim IJ, Sanes JR, Meister M (2012) The most numerous ganglion cell type of the mouse retina is a selective feature detector. Proc Natl Acad Sci U S A 109:E2391-2398.